Iodonium Salts as Efficient Iodine(III)-based Noncovalent Organocatalysts for Knorr-type Reactions

Sevilya N. Yunusova,[a] Alexander S. Novikov,[a] Natalia S. Soldatova,[a] Mikhail A. Vovk,[b] Dmitrii S. Bolotin*,[a]

[a] Institute of Chemistry, Saint Petersburg State University, Universitetskaya Nab. 7/9, Saint Petersburg, 199034 Russian Federation

[b] Center for Magnetic Resonance, Saint Petersburg State University, Universitetskii Pr., 26, Saint Petersburg, 198504 Russian Federation

Table of Contents

Characterization of 1–15

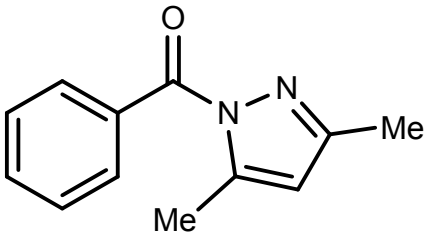

1 (3,5-dimethyl-1H-pyrazol-1-yl)(phenyl)methanone. Yield: 99% (198 mg). HRESI$^+$-MS (MeOH, *m*/*z*): 201.1006 ([M+H]$^+$, calcd 201.1022), 223.0831 ([M + Na]$^+$, calcd 223.0841). IR (KBr, selected bonds, cm^{-1}): 3061 (m), 2986 (m), 2929 (m), 2867 (s) ν(C−H); 1696(s) ν(C=O). ^{1}H NMR (400 MHz, $(CD_3)_2SO$, δ): 7.87 (d, J = 7.1 Hz, 2H, Ar), 7.63 (t, J = 7.4 Hz, 1H, Ar), 7.52 (t, J = 7.6 Hz, 2H, Ar), 6.28 (s, 1H, CH), 2.57 (s, 3H, CH_3), 2.16 (s, 3H, CH_3). ^{13}C{^{1}H} NMR (100 MHz, $(CD_3)_2SO$, δ) 168.40, 152.12, 144.91, 133.78, 132.73, 131.15, 129.72, 129.01, 128.29, 111.77, 14.35, 13.92.

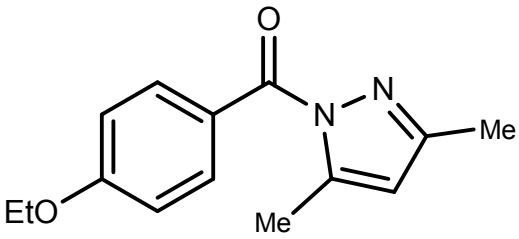

2 (3,5-dimethyl-1H-pyrazol-1-yl)(4-ethoxyphenyl)methanone. Yield: 95% (232 mg). Mp: 91–93 °C. HRESI$^+$-MS (MeOH, *m*/*z*): 267.1113 ([M + Na]$^+$, calcd 267.1104). IR (KBr, selected bonds, cm^{-1}): 3334 (m) ν(N–H); 3107 (m), 3071 (m), 2980 (m), 2932 (m), 2898 (m), 2866 (m) ν(C−H); 1676 (vs) ν(C=O). ^{1}H NMR (400 MHz, $(CD_3)_2SO$, δ): 7.95 (d, J = 9.0 Hz, 2H, Ar), 7.00 (d, J = 9.0 Hz, 2H, Ar), 6.17 (s, 1H, CH), 4.17–4.12 (q, J = 7.0 Hz, 2H, CH_2), 2.57 (s, 3H, CH_3), 2.23 (s, 3H, CH_3), 1.44 (t, J = 7.0 Hz, 3H, CH_3). ^{13}C{^{1}H} NMR (100 MHz, $(CD_3)_2SO$, δ) 167.26, 162.53, 151.53, 144.77, 134.07, 125.15, 114.11, 111.31, 64.00, 14.94, 14.27, 13.92.

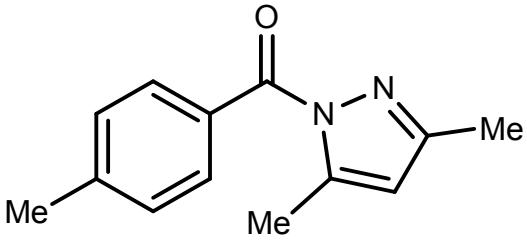

3 (3,5-dimethyl-1H-pyrazol-1-yl)(p-tolyl)methanone. Yield: 99% (212 mg). HRESI$^+$-MS (MeOH, *m*/*z*): 215.1192 ([M+H]$^+$, calcd 215.1179), 237.1013 ([M + Na]$^+$, calcd 237.0998). IR (KBr, selected bonds, cm^{-1}): 3396 (m) ν(N–H); 3034 (m), 2980 (m), 2928 (m), 2866 (m) ν(C−H); 1694 (vs) ν(C=O). ^{1}H NMR (400 MHz, $(CD_3)_2SO$, δ):): 7.80 (d, J = 8.2 Hz, 2H, Ar), 7.32 (d, J = 7.8 Hz, 1H, Ar), 6.26 (s, 1H, CH), 2.55 (s, 3H, CH_3), 2.40 (s, 3H, CH_3), 2.16 (s, 3H, CH_3). ^{13}C{^{1}H} NMR (100 MHz,

$(CD_3)_2SO$, δ) 168.16, 151.85, 144.81, 143.20, 131.47, 130.80, 129.78, 129.56, 128.86, 111.58, 21.59, 14.31, 13.91.

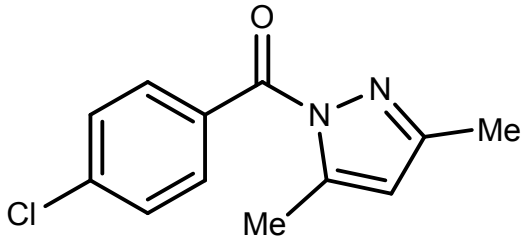

4 (4-chlorophenyl)(3,5-dimethyl-1H-pyrazol-1-yl)methanone. Yield: 84% (197 mg). HRESI$^+$-MS (MeOH, *m*/*z*): 257.0460 ([M + Na]$^+$, calcd 257.0452). IR (KBr, selected bonds, cm^{-1}): 3076 (m), 2984 (m), 2930 (m), 2854 (m) ν(C−H); 1694 (vs) ν(C=O). ^{1}H NMR (400 MHz, $(CD_3)_2SO$, δ): 7.90 (d, J = 8.5 Hz, 2H, Ar), 7.59 (d, J = 8.5 Hz, 2H, Ar), 6.30 (s, 1H, CH), 2.56 (s, 3H, CH_3), 2.16 (s, 3H, CH_3). ^{13}C{^{1}H} NMR (100 MHz, $(CD_3)_2SO$, δ) 167.26, 152.39, 145.03, 137.66, 133.06, 132.49, 128.43, 111.94, 14.35, 13.92.

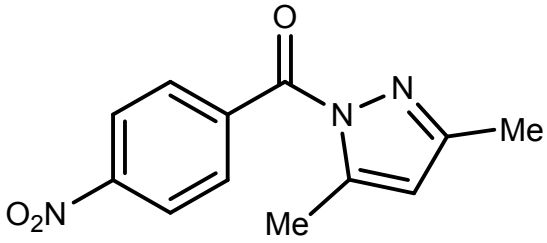

5 (3,5-dimethyl-1H-pyrazol-1-yl)(4-nitrophenyl)methanone. Yield: 46% (113mg). Mp: 123–124 °C. HRESI$^+$-MS (MeOH, *m*/*z*): 268.0701 ([M + Na]$^+$, calcd 2268.0693). IR (KBr, selected bonds, cm^{-1}): 3478 (w), 3377 (w) ν(N–H); 3115 (m), 2980 (m), 2930 (m), 2848 (m) ν(C−H); 1701 (vs) ν(C=O). ^{1}H NMR (400 MHz, $(CD_3)_2SO$, δ): 8.34 (d, J = 8.8 Hz, 2H, Ar), 8.06 (d, J = 8.8 Hz, 2H, Ar), 6.35 (s, 1H, CH), 2.60 (s, 3H, CH_3), 2.15 (s, 3H, CH_3). ^{13}C{^{1}H} NMR (100 MHz, $(CD_3)_2SO$, δ) 167.04, 153.05, 149.55, 145.18, 139.99, 131.96, 123.35, 14.36, 13.93.

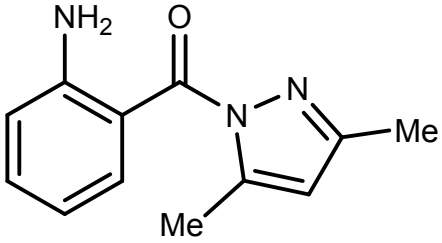

6 (2-aminophenyl)(3,5-dimethyl-1H-pyrazol-1-yl)methanone. Yield: 67% (159 mg). HRESI$^+$-MS (MeOH, *m*/*z*): 238.0955 ([M + Na]$^+$, calcd 238.0951). IR (KBr, selected bonds, cm^{-1}): 3478 (s), 3375 (s) ν(N–H); 2983 (m), 2927 (m), 2866 (m) ν(C−H); 1675 (vs) ν(C=O). ^{1}H NMR (400 MHz, $(CD_3)_2SO$, δ): 7.46 (d, J = 8.1 Hz, 1H, Ar), 7.25 (t, J = 7.7 Hz, 1H, Ar), 6.81 (d, J = 8.3 Hz, 1H, Ar), 6.53 (s, 2H, NH_2), 6.22 (s, 1H, CH), 2.49 (s, 3H, CH_3), 2.15 (s, 3H, CH_3). ^{13}C{^{1}H} NMR (100 MHz, $(CD_3)_2SO$, δ) 169.29, 151.95, 150.87, 144.19, 134.09, 13.01, 116.74, 114.56, 113.30, 110.81, 13.88, 13.79.

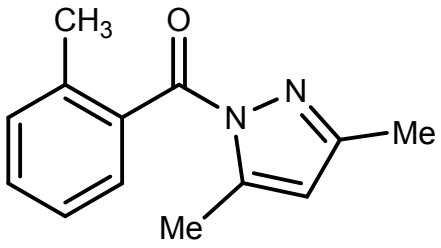

7 (3,5-dimethyl-1H-pyrazol-1-yl)(o-tolyl)methanone. Yield: 74% (196 mg). HRESI$^+$-MS (MeOH, *m*/*z*): 288.1115 ([M + Na]$^+$, calcd 288.1107). IR (KBr, selected bonds, cm^{-1}): 3407 (m) ν(N–H); 3103 (m), 3064 (m), 2967 (m), 2927 (m) ν(C−H); 1711 (vs) ν(C=O). ^{1}H NMR (400 MHz, $(CD_3)_2SO$, *δ*): 7.68–7.57 (m, 2H, Ar), 7.51–7.46 (m, 2H, Ar), 6.18 (s, 2H, Ar), 6.14 (s, 1H, CH), 6.08 (s, 2H, Ar), 2.47 (s, 3H, CH_3), 1.99 (s, 3H, CH_3).^{13}C{^{1}H} NMR (100 MHz, $(CD_3)_2SO$, *δ*) 168.28, 152.65, 143.81, 138.64, 131.90, 131.19, 129.52, 126.79, 125.27, 121.47, 112.02, 110.25, 14.10, 13.74.

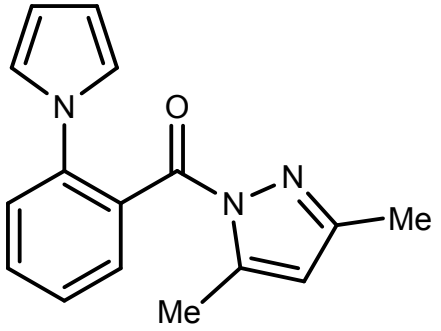

8 (2-(1H-pyrrol-1-yl)phenyl)(3,5-dimethyl-1H-pyrazol-1-yl)methanone. Yield: 90% (193 mg). HRESI$^+$-MS (MeOH, *m*/*z*): 237.1005 ([M + Na]$^+$, calcd 237.0998). IR (KBr, selected bonds, cm^{-1}): 3396 (m) ν(N–H); 3065 (m), 2968 (m), 2929 (m), 2866 (m) ν(C−H); 1709 (vs) ν(C=O). ^{1}H NMR (400 MHz, $(CD_3)_2SO$, *δ*): 7.44–7.33 (m, 2H, Ar), 7.31–7.26 (m, 2H, Ar), 6.27 (s, 1H, CH), 2.59 (s, 3H, CH_3), 2.18 (s, 3H, CH_3), 2.09 (s, 3H, CH_3). ^{13}C{^{1}H} NMR (100 MHz, $(CD_3)_2SO$, *δ*) 170.07, 152.67, 144.32, 135.80, 135.58, 130.60, 135.55, 128.58, 125.61, 19.58, 14.34, 13.86.

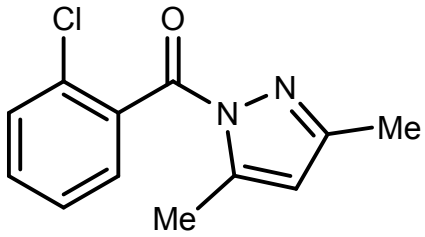

9 (2-chlorophenyl)(3,5-dimethyl-1H-pyrazol-1-yl)methanone. Yield: 70% (164 mg). HRESI$^+$-MS (MeOH, *m*/*z*): 257.0471 ([M + Na]$^+$, calcd 257.0452). IR (KBr, selected bonds, cm^{-1}): 3411 (m) ν(N–H); 3065 (m), 2968 (m), 2929 (m), 2861 (m) ν(C−H); 1714 (vs) ν(C=O). ^{1}H NMR (400 MHz, $(CD_3)_2SO$, *δ*): 7.61–7.52 (m, 3H, Ar), 7.49–7.44 (m, 1H, Ar), 6.30 (s, 1H, CH), 2.60 (s, 3H, CH_3), 2.08 (s, 3H, CH_3). ^{13}C{^{1}H} NMR (100 MHz, $(CD_3)_2SO$, *δ*) 167.27, 167.21, 153.28, 144.29, 135.64, 131.92, 130.23, 129.67, 127.35, 112.53, 14.24, 13.89.

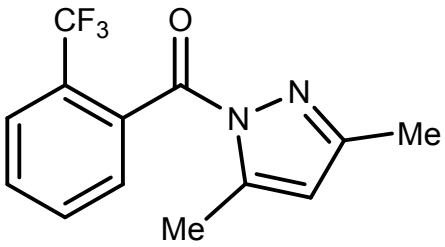

10 (3,5-dimethyl-1H-pyrazol-1-yl)(2-(trifluoromethyl)phenyl)methanone. Yield: 75% (201 mg). HRESI$^+$-MS (MeOH, *m*/*z*): 291.0734 ([M + Na]$^+$, calcd 291.0716).). IR (KBr, selected bonds, cm^{-1}): 3417 (m) ν(N–H); 3079 (m), 2995 (m), 2931 (m) ν(C−H); 1721 (vs) ν(C=O). ^{1}H NMR (400 MHz, $(CD_3)_2SO$, *δ*): 7.86 (d, *J* = 7.3 Hz, 1H, Ar), 7.80–7.72 (m, 2H, Ar), 7.66 (d, *J* = 7.0 Hz, 1H, Ar), 6.31 (s, 1H, CH), 2.60 (s, 3H, CH_3), 2.06 (s, 3H, CH_3). ^{13}C{^{1}H} NMR (100 MHz, $(CD_3)_2SO$, *δ*) 167.79, 153.14, 144.55, 134.16 (q, *J* = 2.5 Hz), 132.56, 130.87, 129.04, 126.65 (q, *J* = 4.3 Hz), 126.17 (q, *J* = 31.5 Hz), 124.10 (q, *J* = 272 Hz), 14.17, 13.81. ^{19}F NMR (($CD_3)_2SO$, *δ*) –58.21.

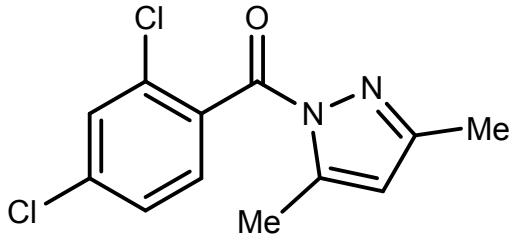

11 (2,4-dichlorophenyl)(3,5-dimethyl-1H-pyrazol-1-yl)methanone. Yield: 78% (209 mg). HRESI$^+$-MS (MeOH, *m*/*z*): 291.0070 ([M + Na]$^+$, calcd 291.0062).). IR (KBr, selected bonds, cm^{-1}): 3410 (m) ν(N–H); 3092 (m), 2988 (m), 2929 (m), 2862 (m) ν(C−H); 1711 (vs) ν(C=O). ^{1}H NMR (400 MHz, $(CD_3)_2SO$, *δ*): 7.76 (d, *J* = 1.8 Hz, 1H, Ar), 7.64 (d, *J* = 8.3 Hz, 1H, Ar), 7.57–7.54 (m, 1H, Ar), 6.31 (s, 1H, CH), 2.59 (s, 3H, CH_3), 2.09 (s, 3H, CH_3). ^{13}C{^{1}H} NMR (100 MHz, $(CD_3)_2SO$, *δ*) 166.35, 153.65, 144.43, 135.84, 134.48, 131.49, 130.85, 129.33, 127.69, 112.71, 14.15, 13.85.

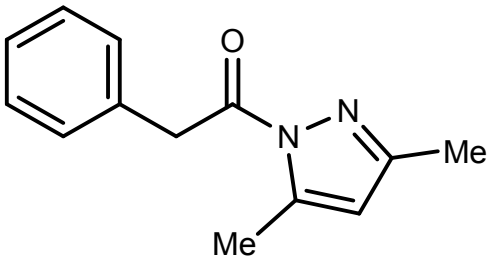

12 1-(3,5-dimethyl-1H-pyrazol-1-yl)-2-phenylethanone. Yield: 60% (128 mg). HRESI$^+$-MS (MeOH, *m*/*z*): 237.1024 ([M + Na]$^+$, calcd 237.0998). IR (KBr, selected bonds, cm^{-1}): 3448 (m) ν(N–H); 3110 (m), 3071 (m), 3064 (m), 3031 (m), 2828 (m) ν(C−H); 1732 (vs) ν(C=O). ^{1}H NMR (400 MHz, $(CD_3)_2SO$, *δ*):): 7.35–7.24 (m, 5H, Ar), 6.22 (s, 1H, CH), 4.41 (s, 2H, CH_2), 2.46 (s, 3H, CH_3), 2.22 (s, 3H, CH_3). ^{13}C{^{1}H} NMR (100 MHz, $(CD_3)_2SO$, *δ*) 171.82, 151.94, 143.96, 134.84, 130.32, 128.70, 127.21, 111.94, 41.46, 14.58, 13.99.

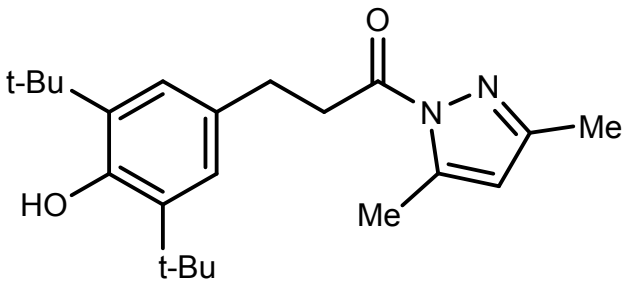

13 3-(3,5-di-tert-butyl-4-hydroxyphenyl)-1-(3,5-dimethyl-1H-pyrazol-1-yl)propan-1-one. Yield: 52% (185 mg). Mp: 88–90 °C. HRESI$^+$-MS (MeOH, *m*/*z*): 379.2559 ([M + Na]$^+$, calcd 379.2356). IR (KBr, selected bonds, cm^{-1}): 3610 (s), 3435 (m) ν(N–H); 2961 (s), 2930 (s), 2872 (s) ν(C−H); 1728 (vs) ν(C=O). ^{1}H NMR (400 MHz, $(CD_3)_2SO$, *δ*): 7.9 (s, 1H, Ar), 6.71 (s, 1H, Ar), 6.17 (s, 1H, CH), 3.34–3.29 (m, 2H, CH_2), 2.85 (t, *J* = 7.6 Hz, 2H, CH_2), 2.46 (s, 3H, CH_3), 2.16 (s, 3H, CH_3), 1.35 (s, 18H, t-Bu). ^{13}C{^{1}H} NMR (100 MHz, $(CD_3)_2SO$, *δ*) 173.36, 152.45, 151.63, 143.53, 139.63, 131.92, 124.71, 111.53, 37.20, 34.89, 30.39, 14.57, 13.92.

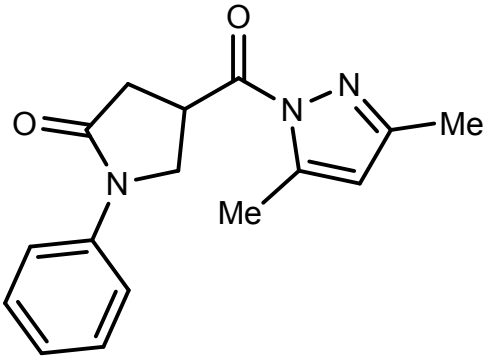

14 4-(3,5-dimethyl-1H-pyrazole-1-carbonyl)-1-phenylpyrrolidin-2-one. Yield: 60% (170 mg). Mp: 133–134 °C. HRESI$^+$-MS (MeOH, *m*/*z*): 306.1226 ([M + Na]$^+$, calcd 306.1213). IR (KBr, selected bonds, cm^{-1}): 3418 (m), 3379 (m) ν(N–H); 3066 (m), 3031 (m), 2978 (m), 2925 (m), 2898 (m), 2888 (m), 2854 (m) ν(C−H); 1720 (vs), 1703 (sh) ν(C=O). ^{1}H NMR (400 MHz, $(CD_3)_2SO$, *δ*): 7.65 (d, *J* = 7.8 Hz, 2H, Ar), 7.38 (t, *J* = 8.0 Hz, 1H, Ar), 7.15 (t, *J* = 7.4 Hz, 1H, Ar), 6.24 (s, 1H, CH), 4.56–4.44 (m, 1H, CH), 4.22 (t, *J* = 9.4 Hz, 1H, CH), 4.06–4.02 (m, 1H, CH), 2.50 (s, 3H, CH_3), 2.22 (s, 3H, CH_3). ^{13}C{^{1}H} NMR (100 MHz, $(CD_3)_2SO$, *δ*) 173.06, 17.98, 152.62, 144.35, 139.51, 129.14, 124.62, 120.04, 112.04, 50.60, 35.38, 35.61, 14.49, 14.02.

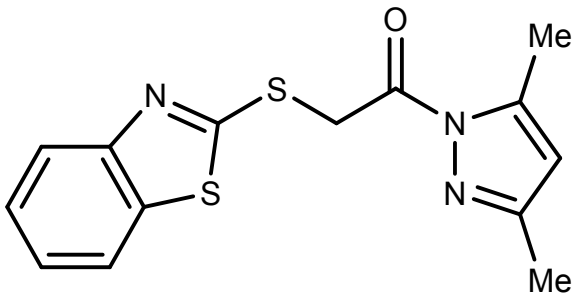

15 2-(benzo[d]thiazol-2-ylthio)-1-(3,5-dimethyl-1H-pyrazol-1-yl)ethanone. Yield: 64% (194 mg). Mp: 113–114 °C. HRESI$^+$-MS (MeOH, *m*/*z*): 326.0395 ([M + Na]$^+$, calcd 326.0392). IR (KBr,

selected bonds, cm^{-1}): 3410 (m) ν(N–H); 3116 (m), 3059 (m), 2981 (m), 2930 (m) ν(C−H); 1714 (vs) ν(C=O). ^{1}H NMR (400 MHz, $(CD_3)_2SO$, δ): 8.02 (d, J = 7.9 Hz, 1H, Ar), 8.81 (d, J = 8.0 Hz, 1H, Ar), 7.46 (t, J = 7.4 Hz, 1H, Ar), 7.37 (t, J = 7.4 Hz, 1H, Ar), 6.28 (s, 1H, CH), 5.08 (s, 1H, CH_2), 2.47 (s, 3H, CH_3), 2.24 (s, 3H, CH_3). $^{13}C\{^{1}H\}$ NMR (100 MHz, $(CD_3)_2SO$, δ)167.60, 166.02, 152.87, 152.79, 144.24, 135.24, 126.86, 125.04, 122.35, 121.61, 112.14, 37.77, 14.29, 13.98.

Spectra of 1–15

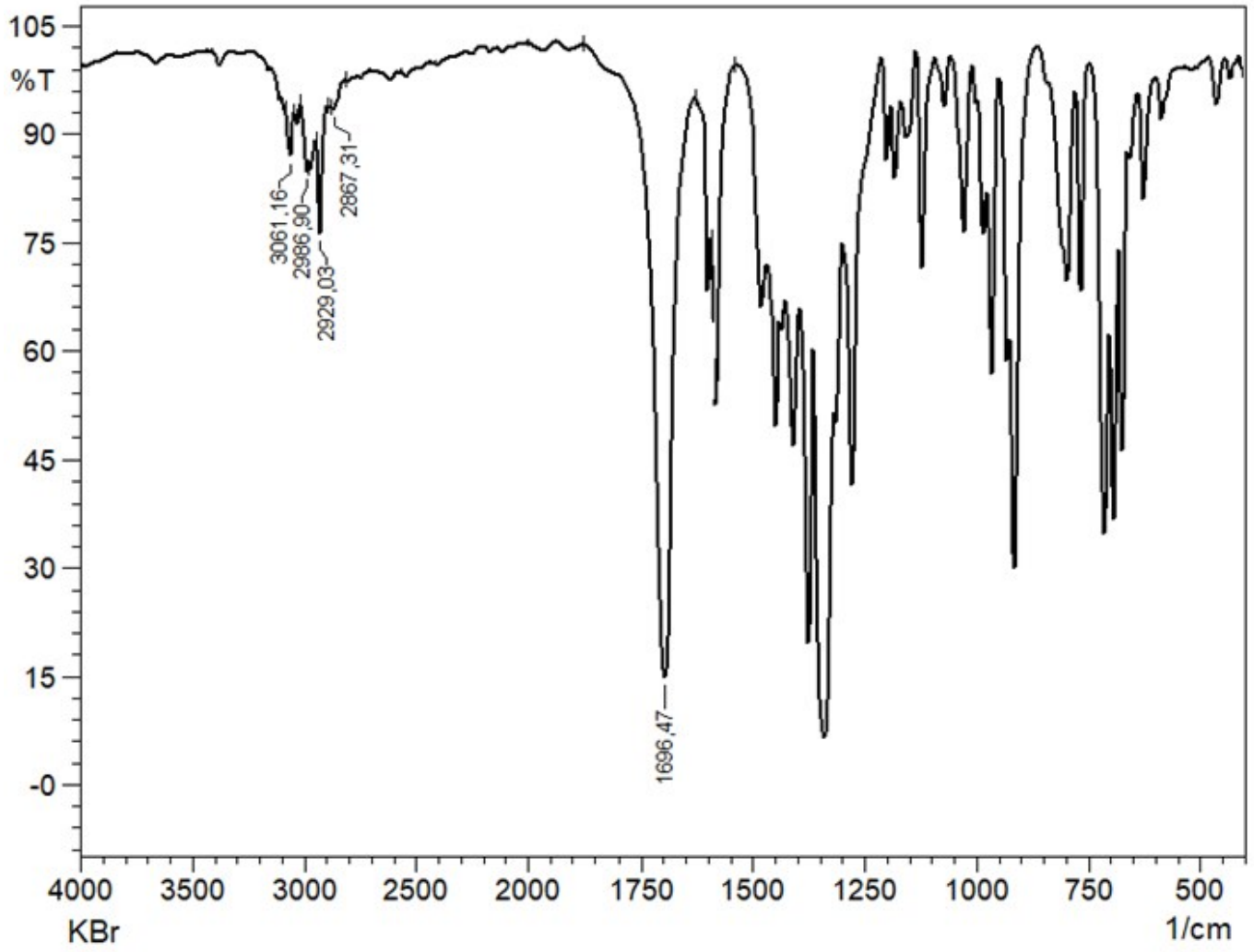

Figure 1S. IR spectrum of **1**.

Acquisition Parameter

Source Type	ESI	Ion Polarity	Positive	Set Nebulizer	0.4 Bar
Focus	Not active			Set Dry Heater	180 °C
Scan Begin	50 m/z	Set Capillary	4500 V	Set Dry Gas	4.0 l/min
Scan End	3000 m/z	Set End Plate Offset	-500 V	Set Divert Valve	Source

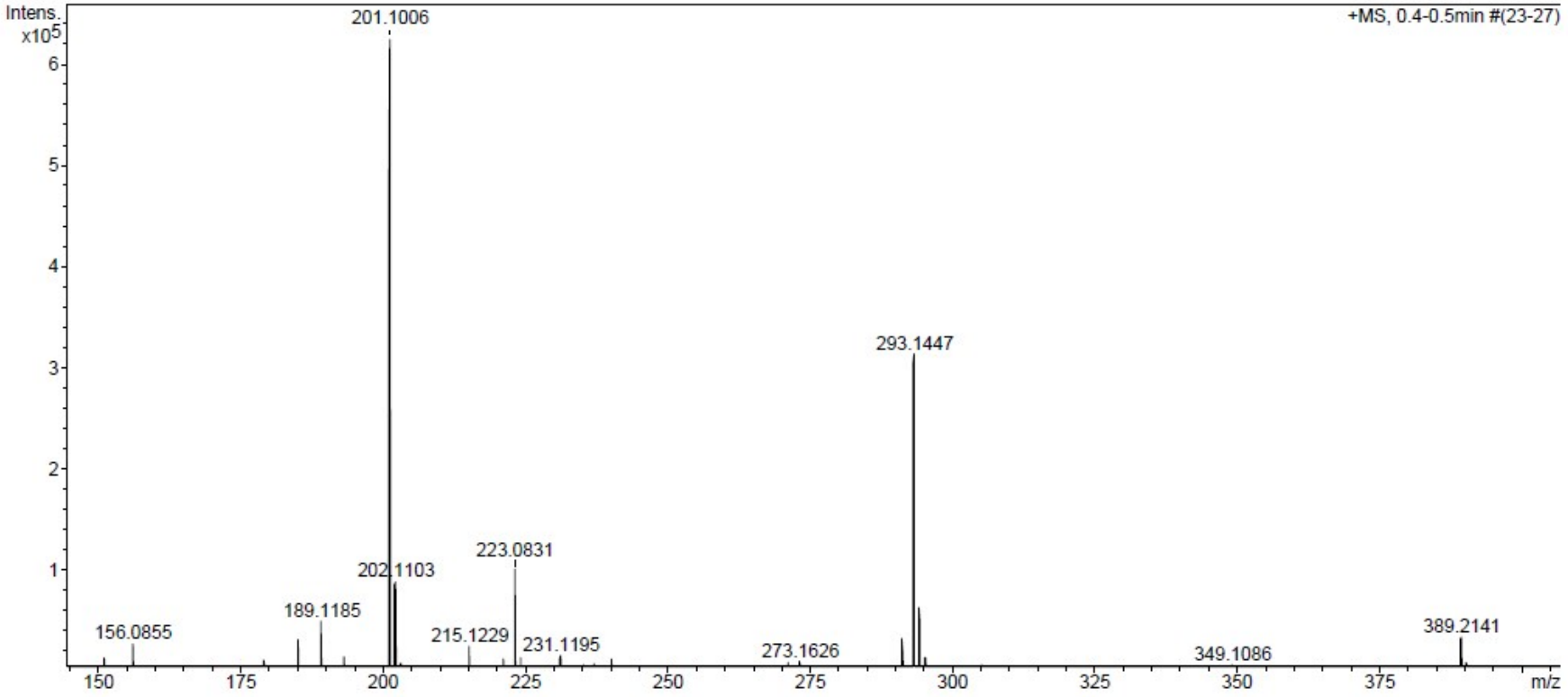

Figu

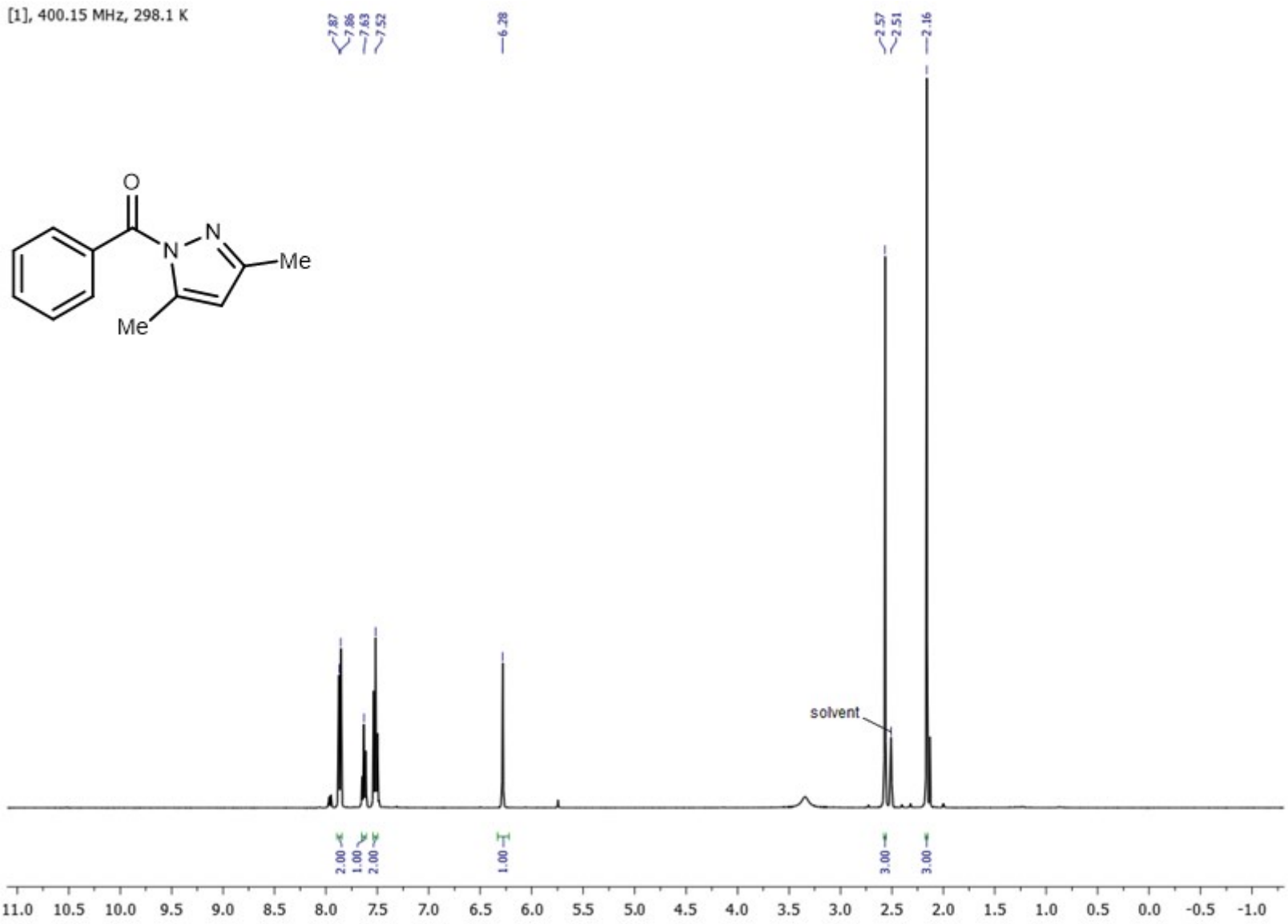

re 2S. HRESI MS of **1**.

Figure 3S. ^{1}H NMR spectrum of **1**.

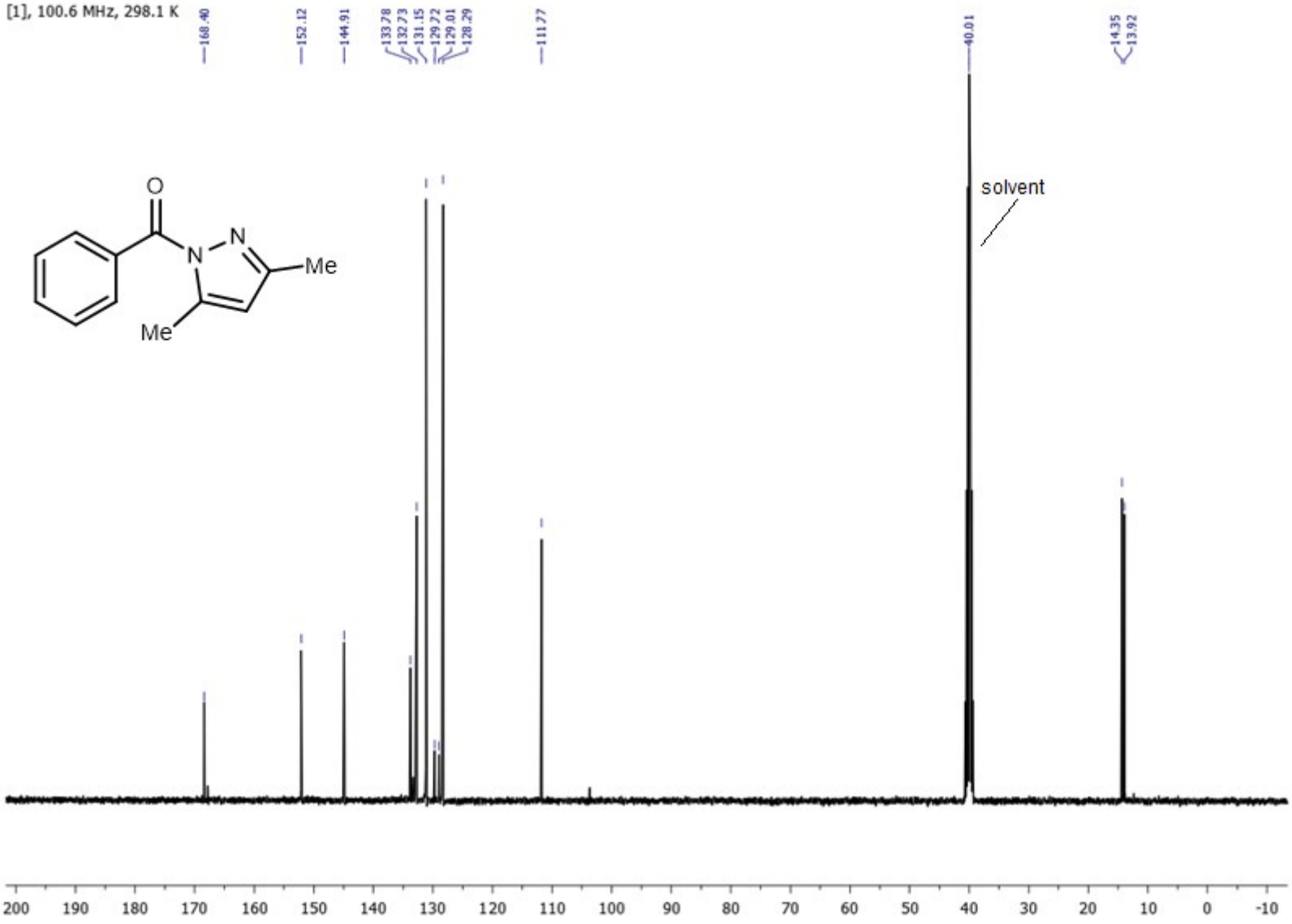

Figure 4S. $^{13}C\{^{1}H\}$ NMR spectrum of **1**.

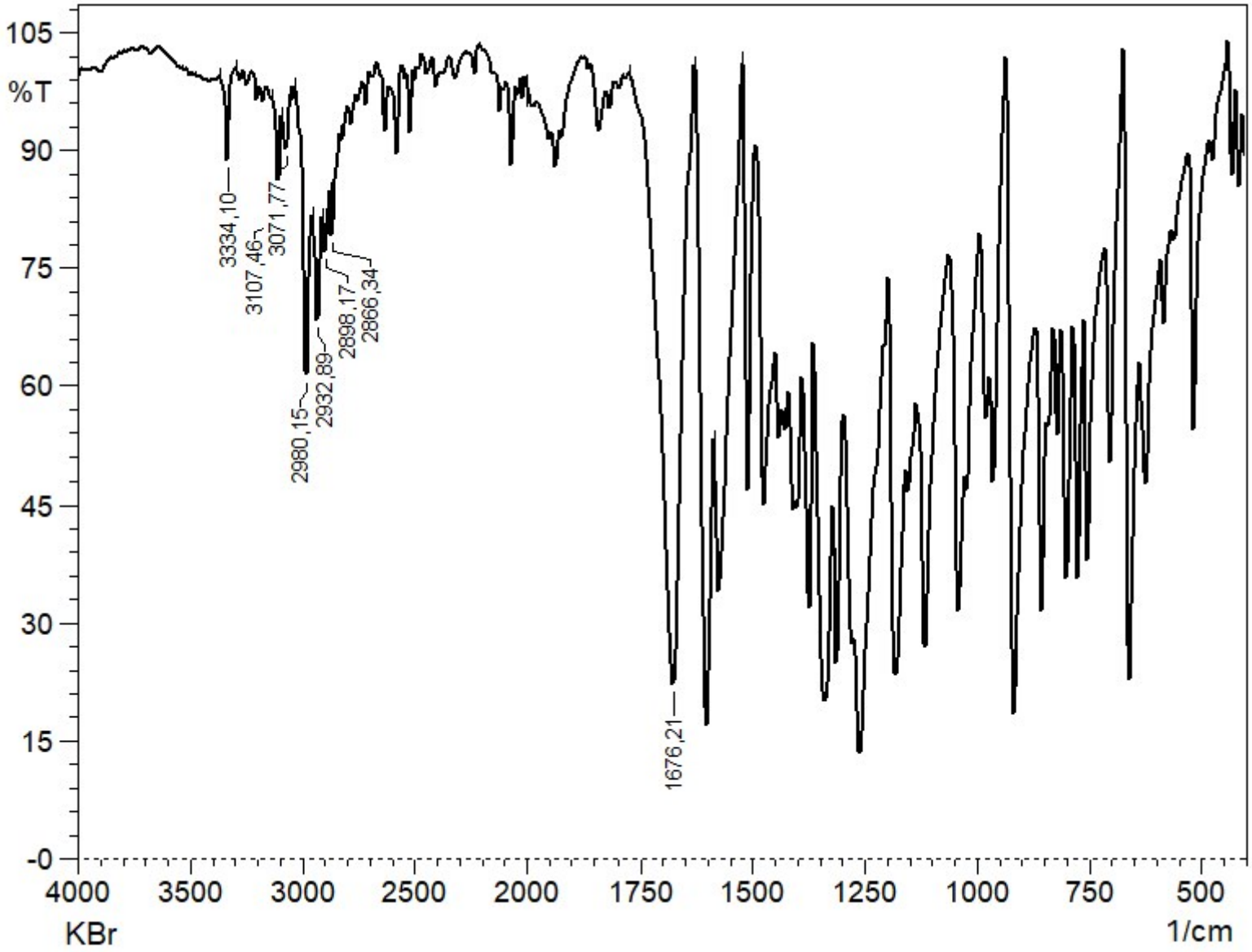

Figure 5S. IR spectrum of **2**.

Acquisition Parameter

Source Type	ESI	Ion Polarity	Positive	Set Nebulizer	0.4 Bar
Focus	Not active			Set Dry Heater	180 °C
Scan Begin	50 m/z	Set Capillary	4500 V	Set Dry Gas	4.0 l/min
Scan End	3000 m/z	Set End Plate Offset	-500 V	Set Divert Valve	Source

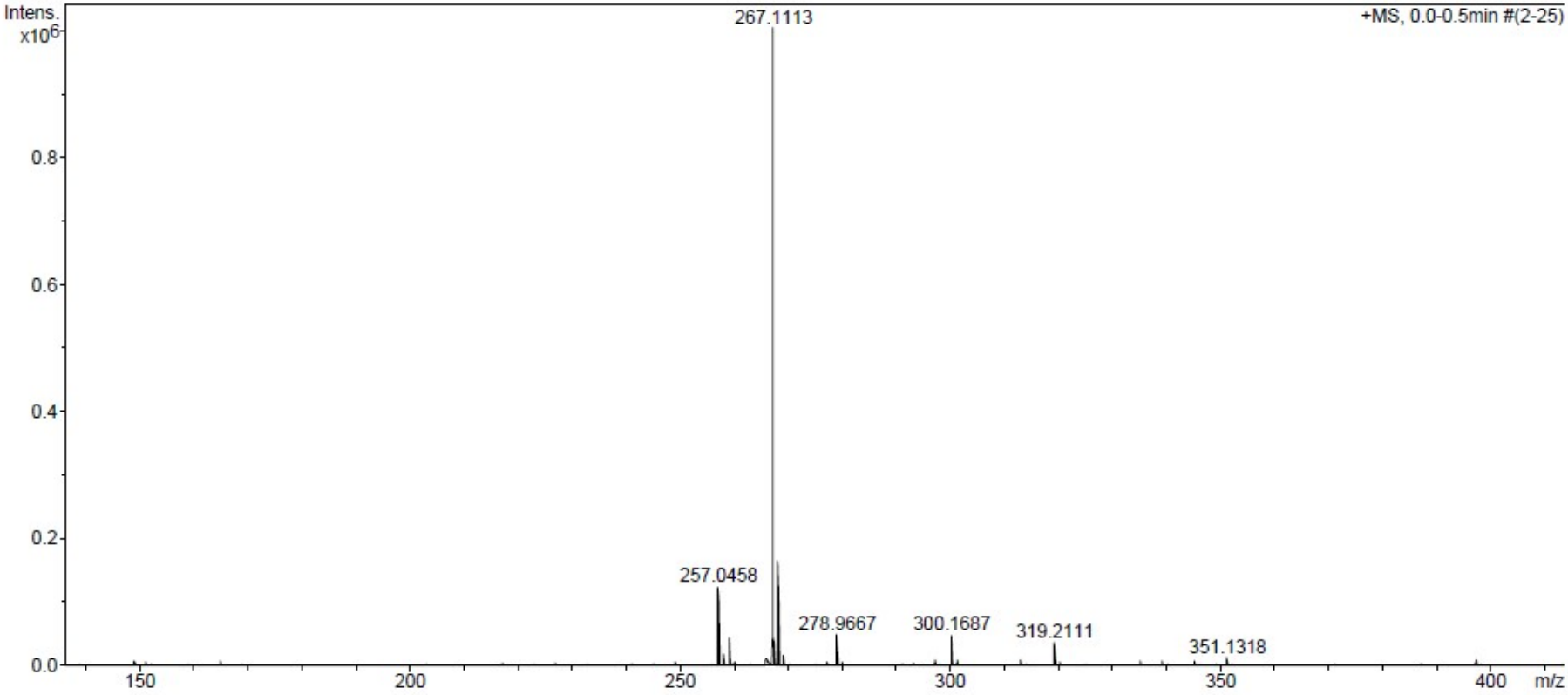

Figure 6S. HRESI^{+}-MS of **2**.

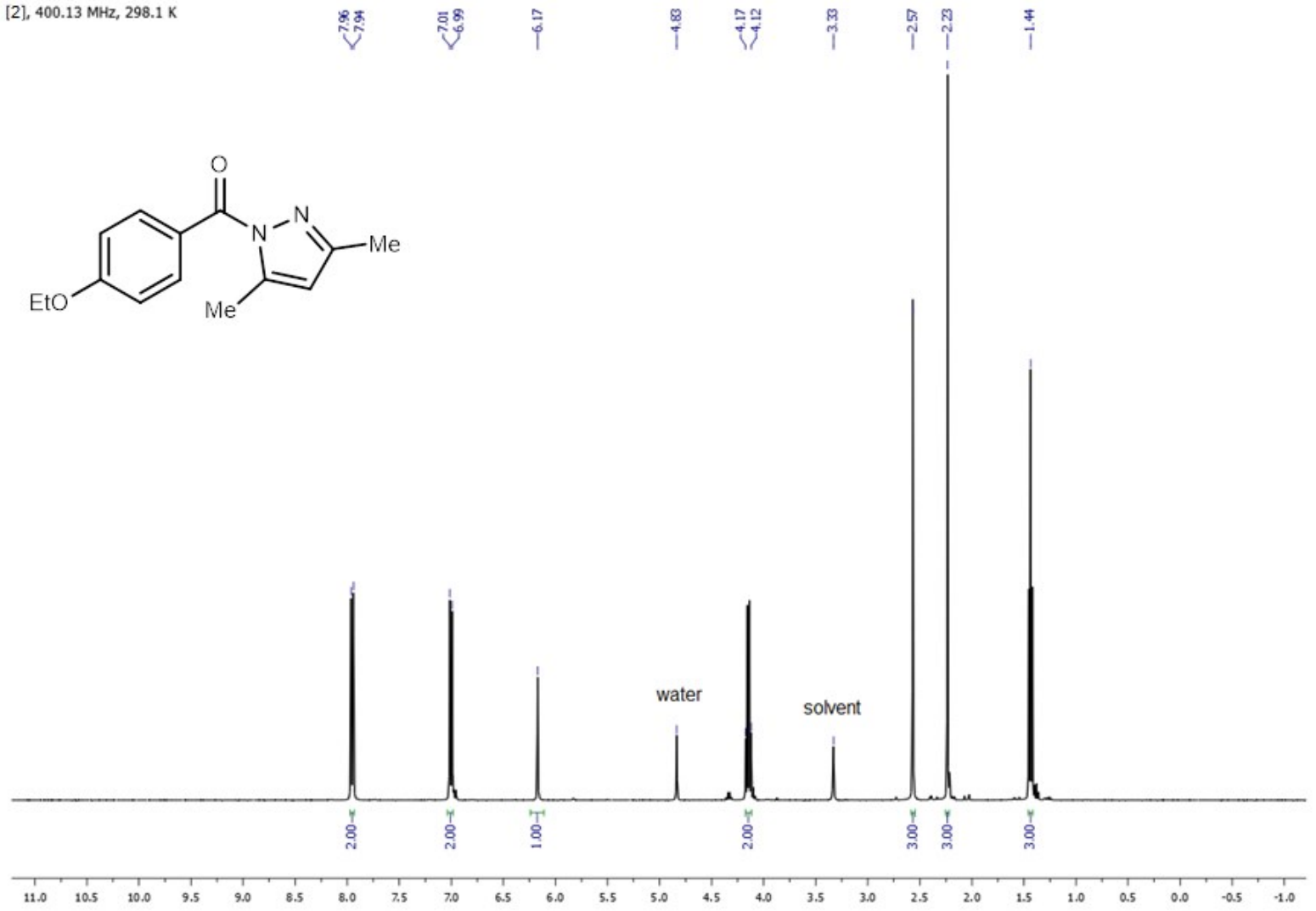

Figure 7S. ^{1}H NMR spectrum of **2**.

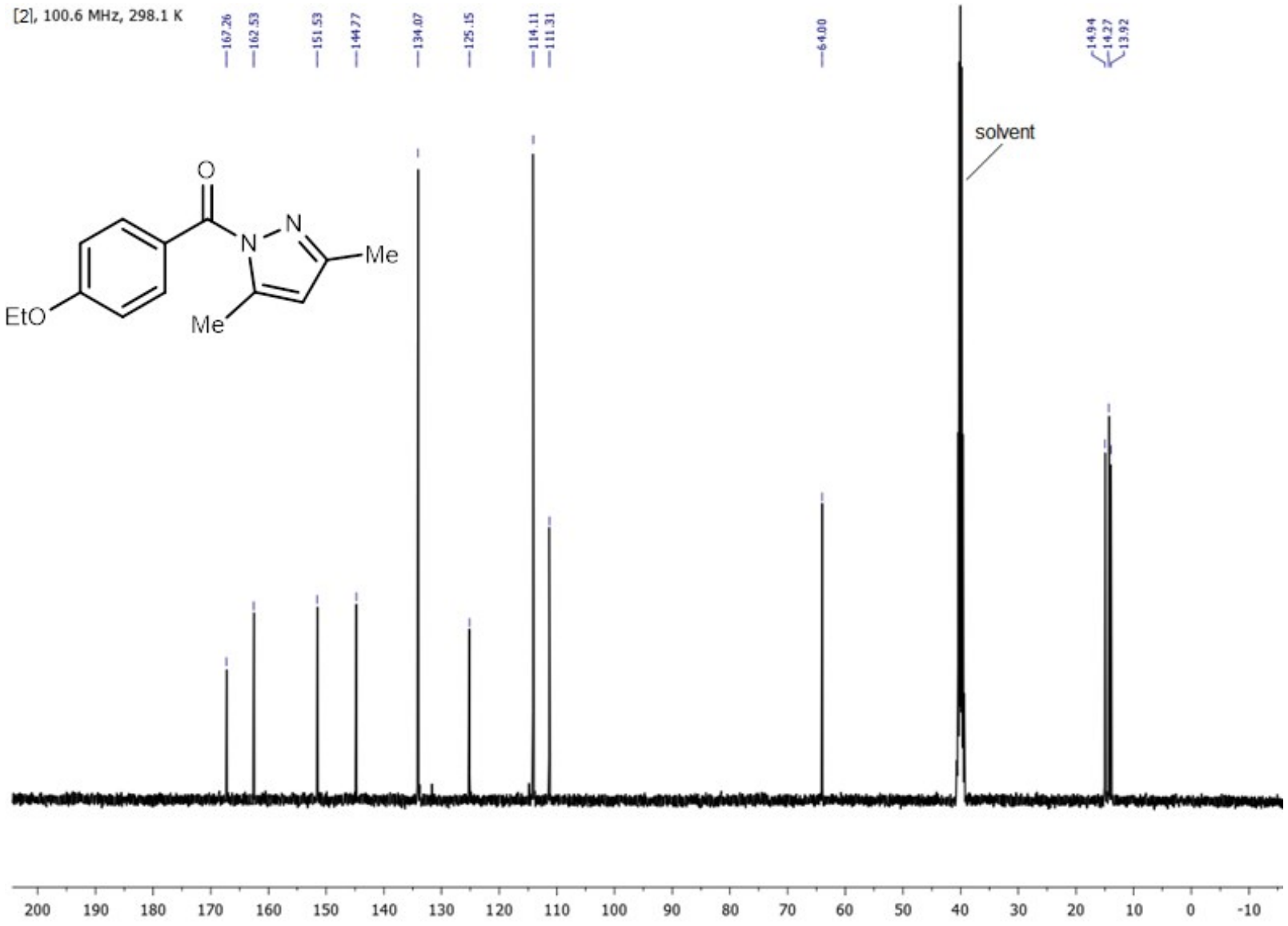

Figure 8S. $^{13}C\{^{1}H\}$ NMR spectrum of **2**.

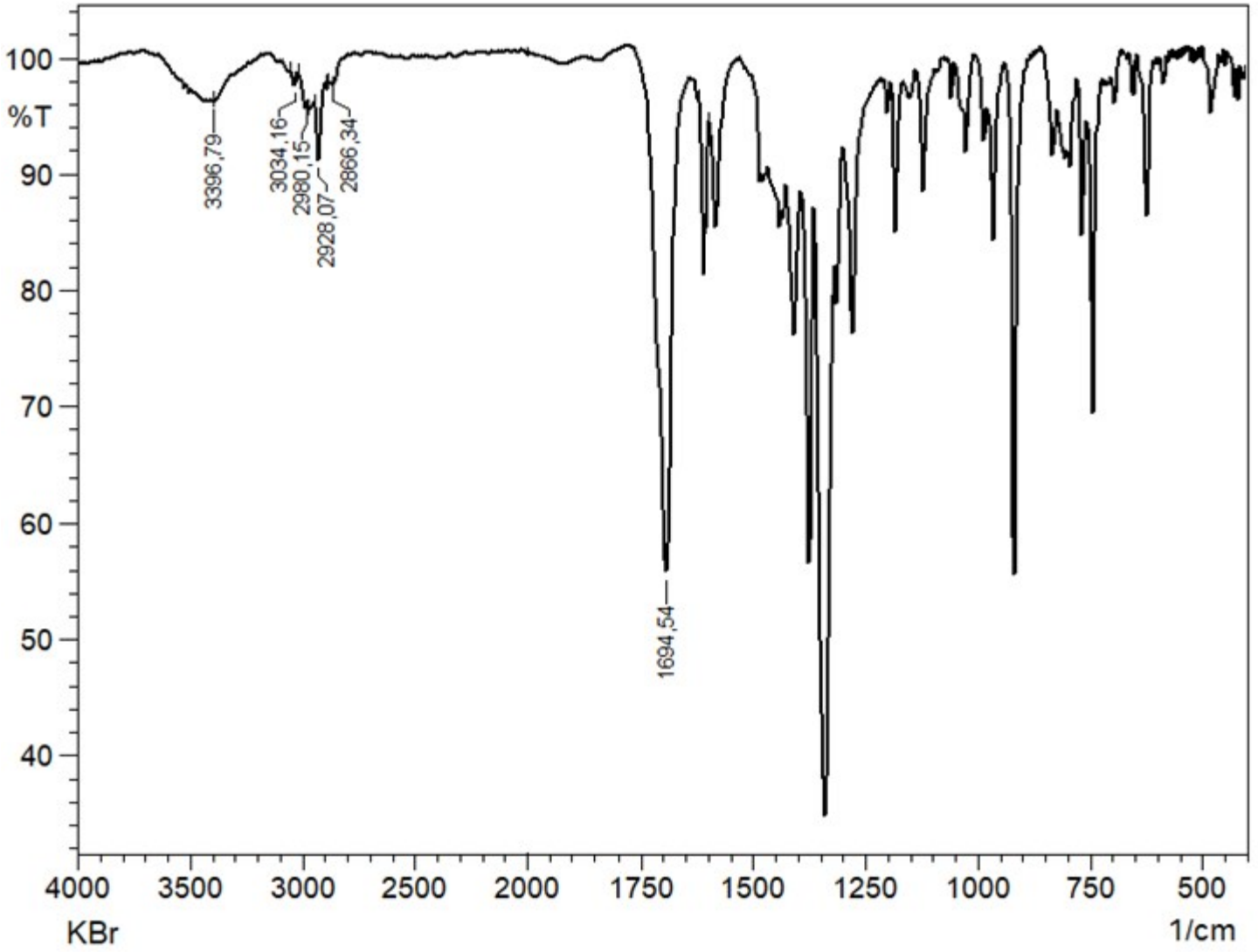

Figure 9S. IR spectrum of **3**.

Acquisition Parameter

Source Type	ESI	Ion Polarity	Positive	Set Nebulizer	0.4 Bar
Focus	Not active			Set Dry Heater	180 °C
Scan Begin	50 m/z	Set Capillary	4500 V	Set Dry Gas	4.0 l/min
Scan End	3000 m/z	Set End Plate Offset	-500 V	Set Divert Valve	Source

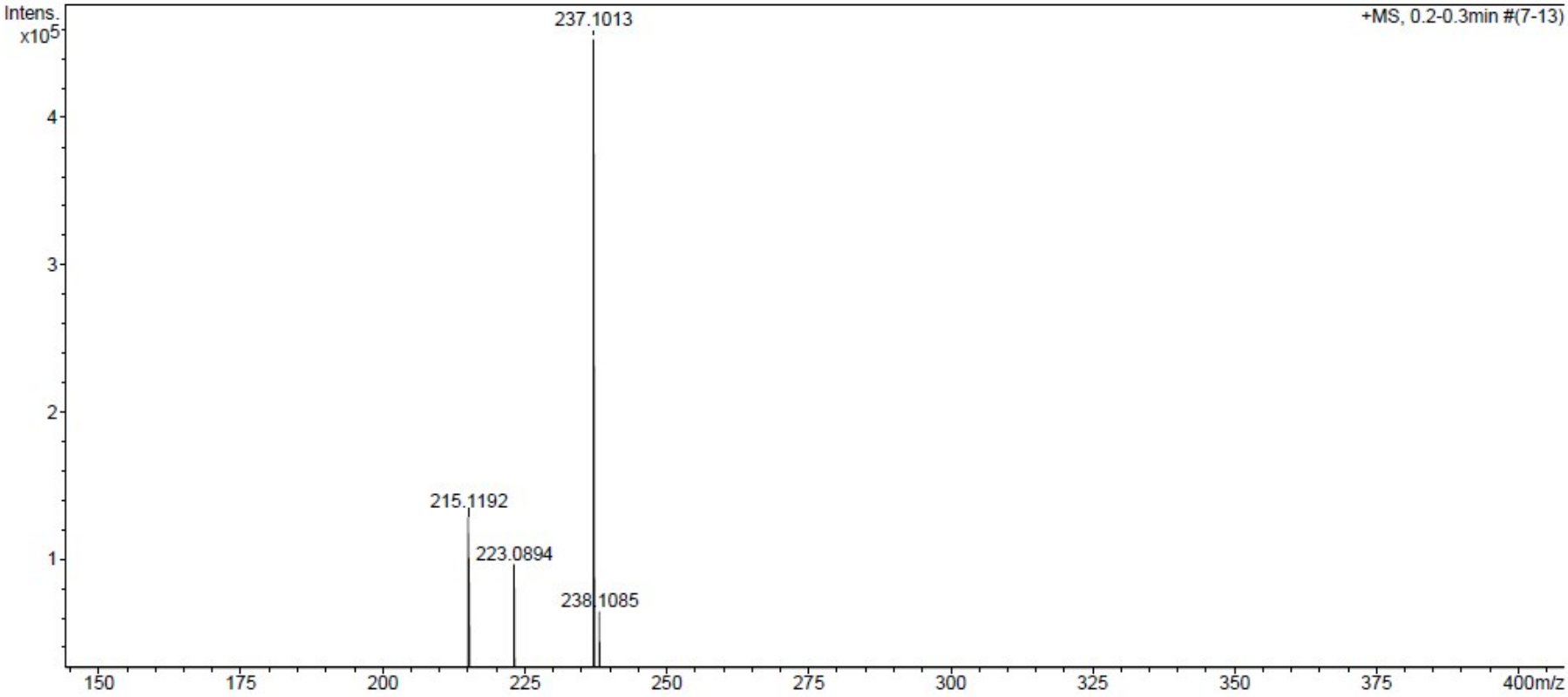

Figure 10S. HRESI^{+}-MS of **3**.

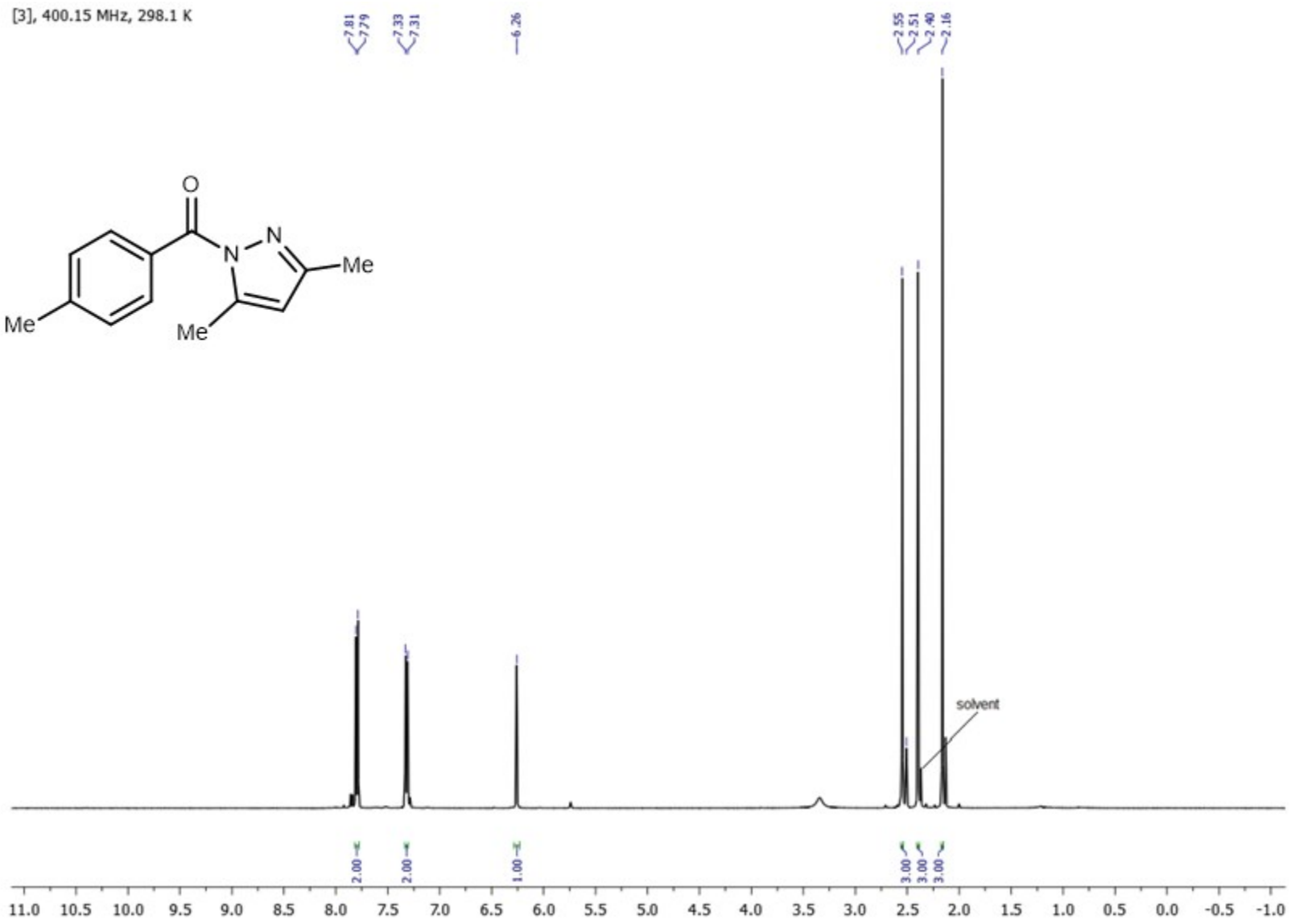

Figure 11S. ^{1}H NMR spectrum of **3**.

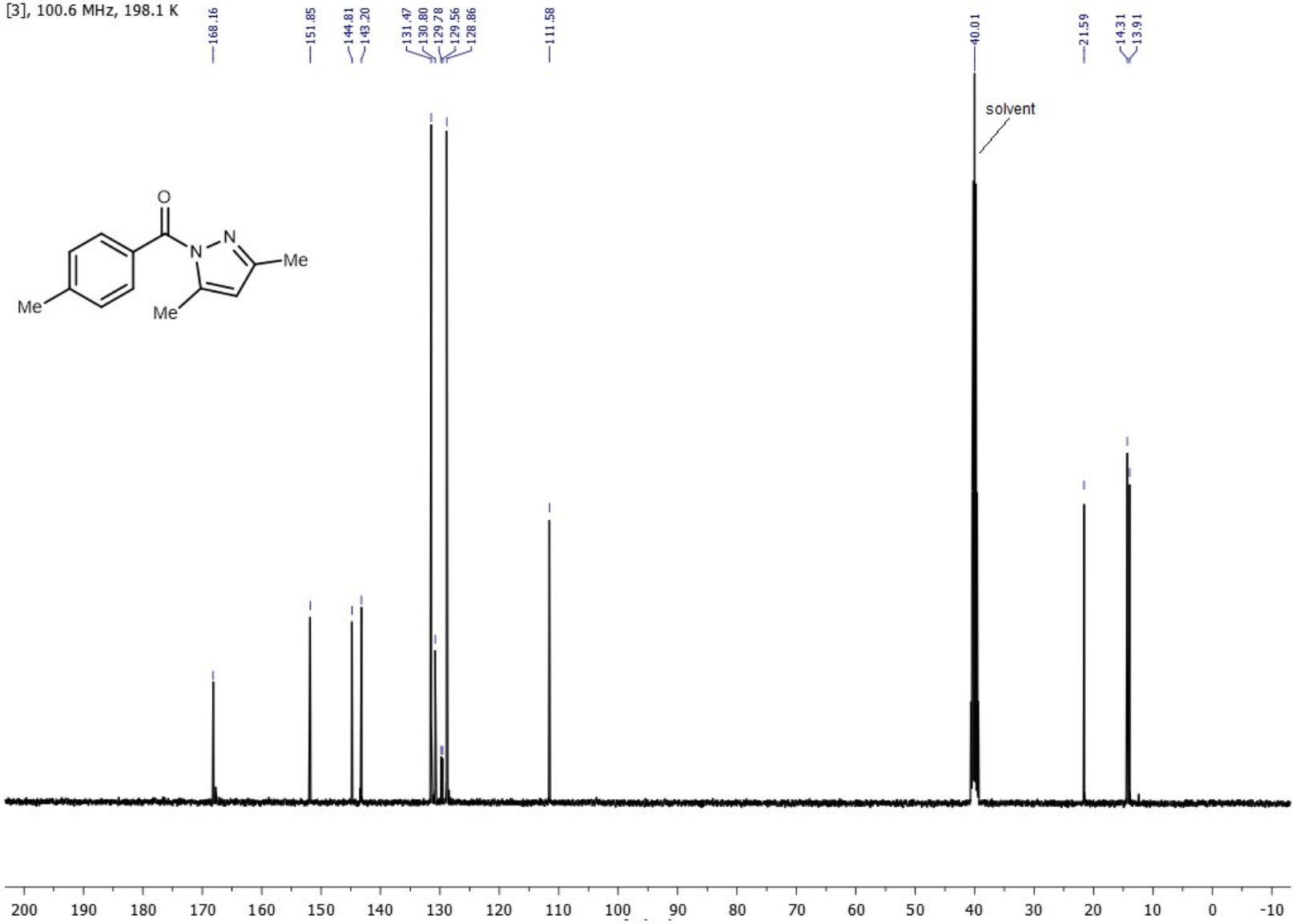

Figure 12S. $^{13}C\{^{1}H\}$ NMR spectrum of **3**.

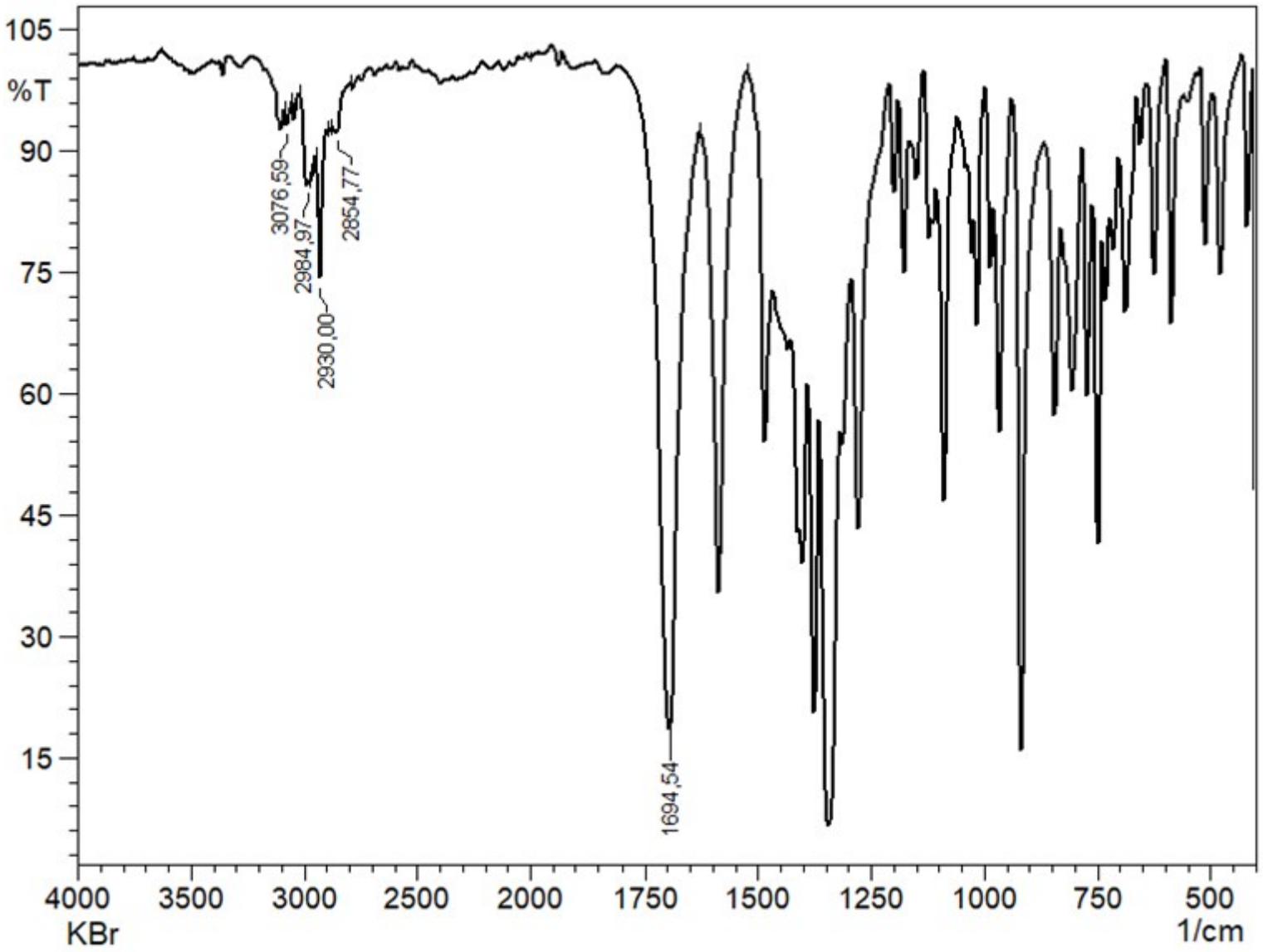

Figure 13S. IR spectrum of **4**.

Acquisition Parameter

Source Type	ESI	Ion Polarity	Positive	Set Nebulizer	0.4 Bar
Focus	Not active			Set Dry Heater	180 °C
Scan Begin	50 m/z	Set Capillary	4500 V	Set Dry Gas	4.0 l/min
Scan End	3000 m/z	Set End Plate Offset	-500 V	Set Divert Valve	Source

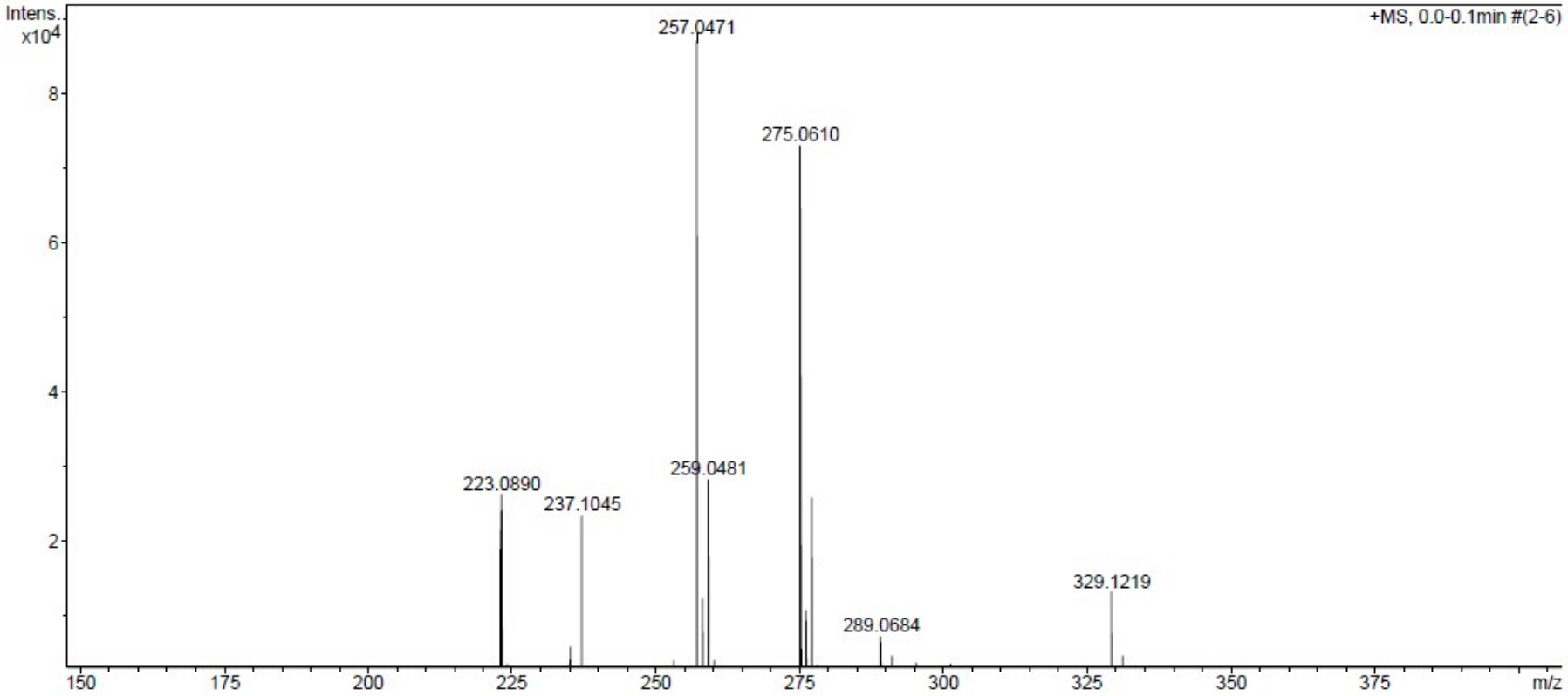

Figure 14. HRESI^{+}-MS of **4**.

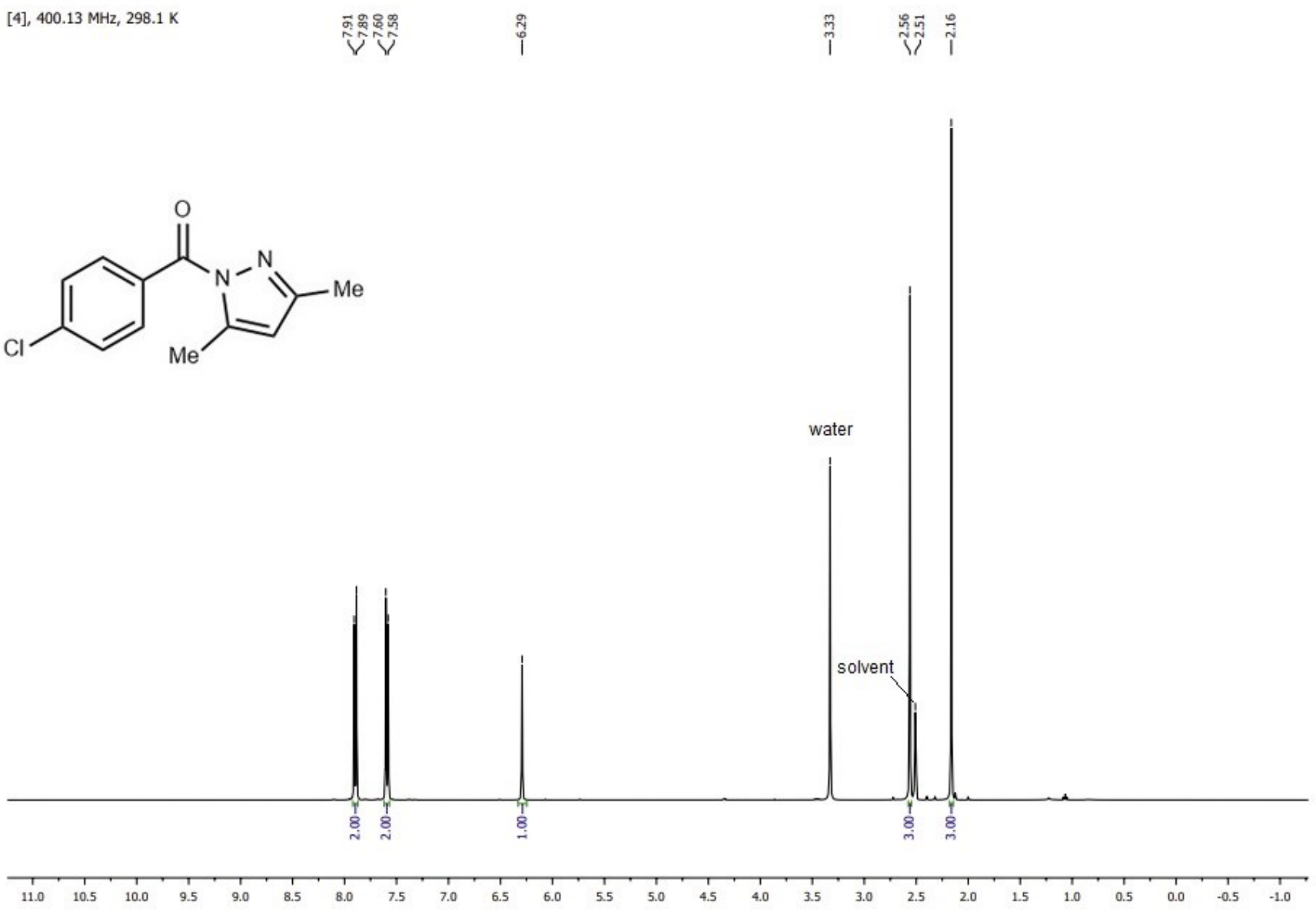

Figure 15S. ^{1}H NMR spectrum of **4**.

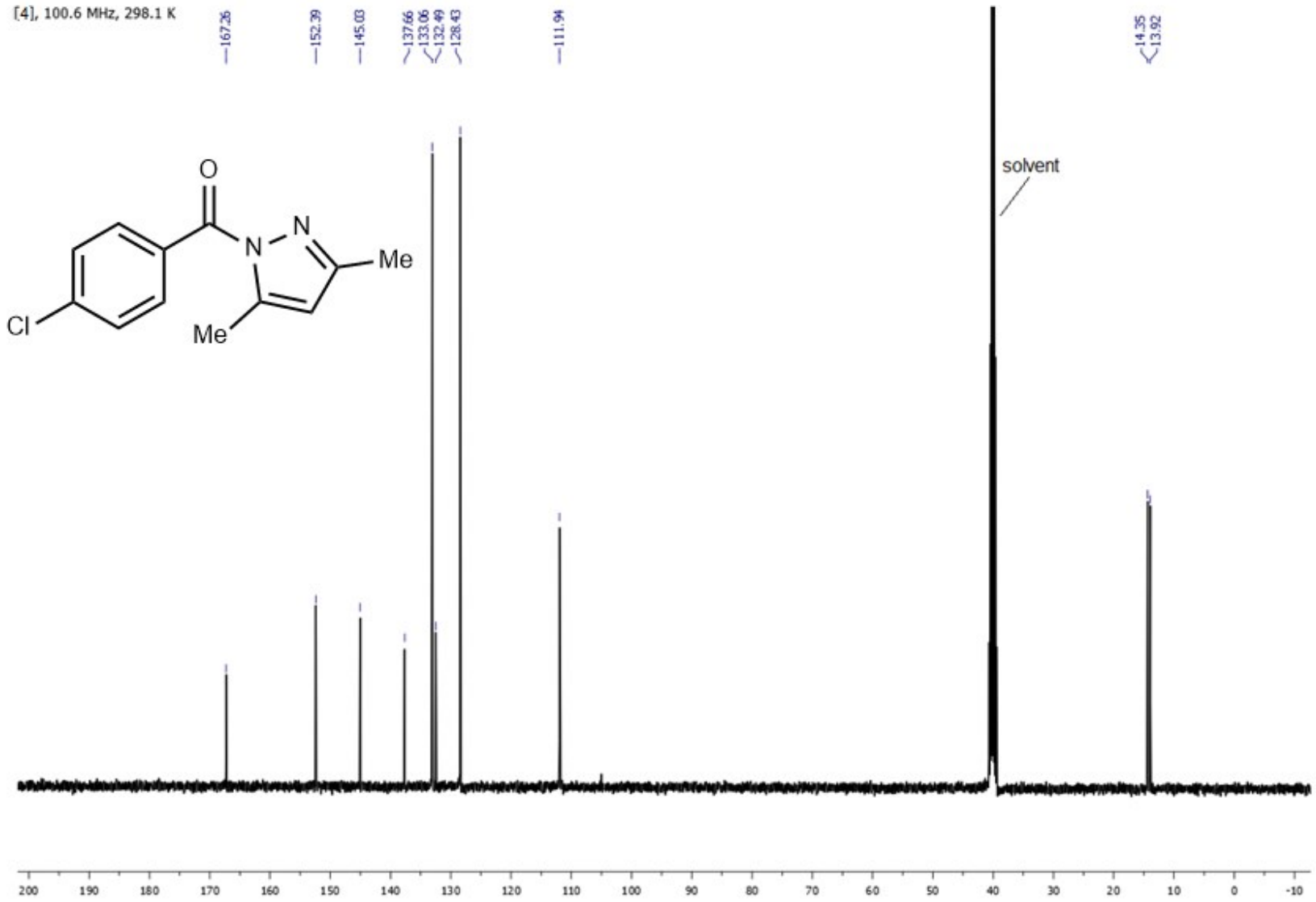

Figure 16S. $^{13}C\{^{1}H\}$ NMR spectrum of **4**.

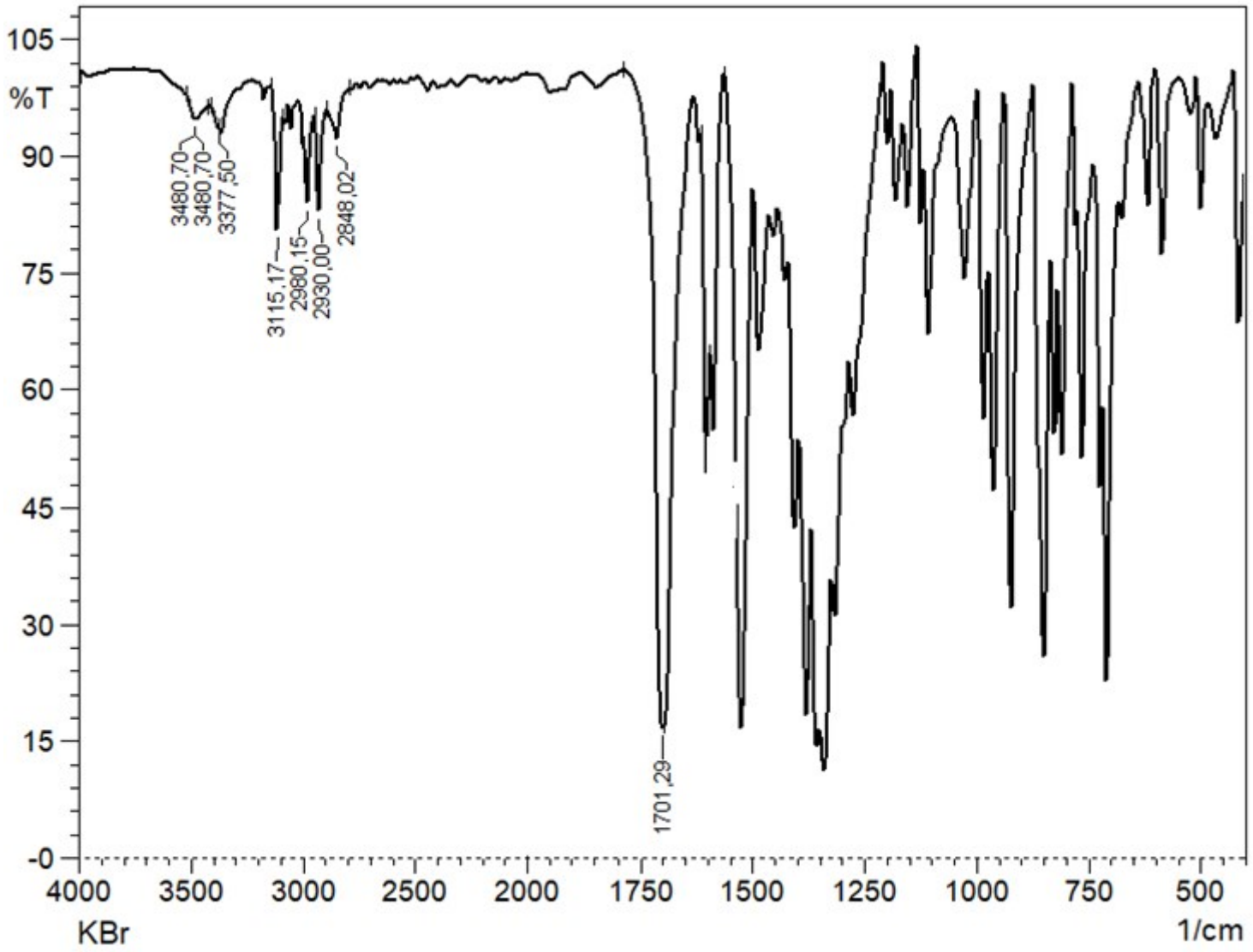

Figure 17S. IR spectrum of **5**.

Acquisition Parameter

Source Type	ESI	Ion Polarity	Positive	Set Nebulizer	0.4 Bar
Focus	Not active			Set Dry Heater	180 °C
Scan Begin	50 m/z	Set Capillary	4500 V	Set Dry Gas	4.0 l/min
Scan End	3000 m/z	Set End Plate Offset	-500 V	Set Divert Valve	Source

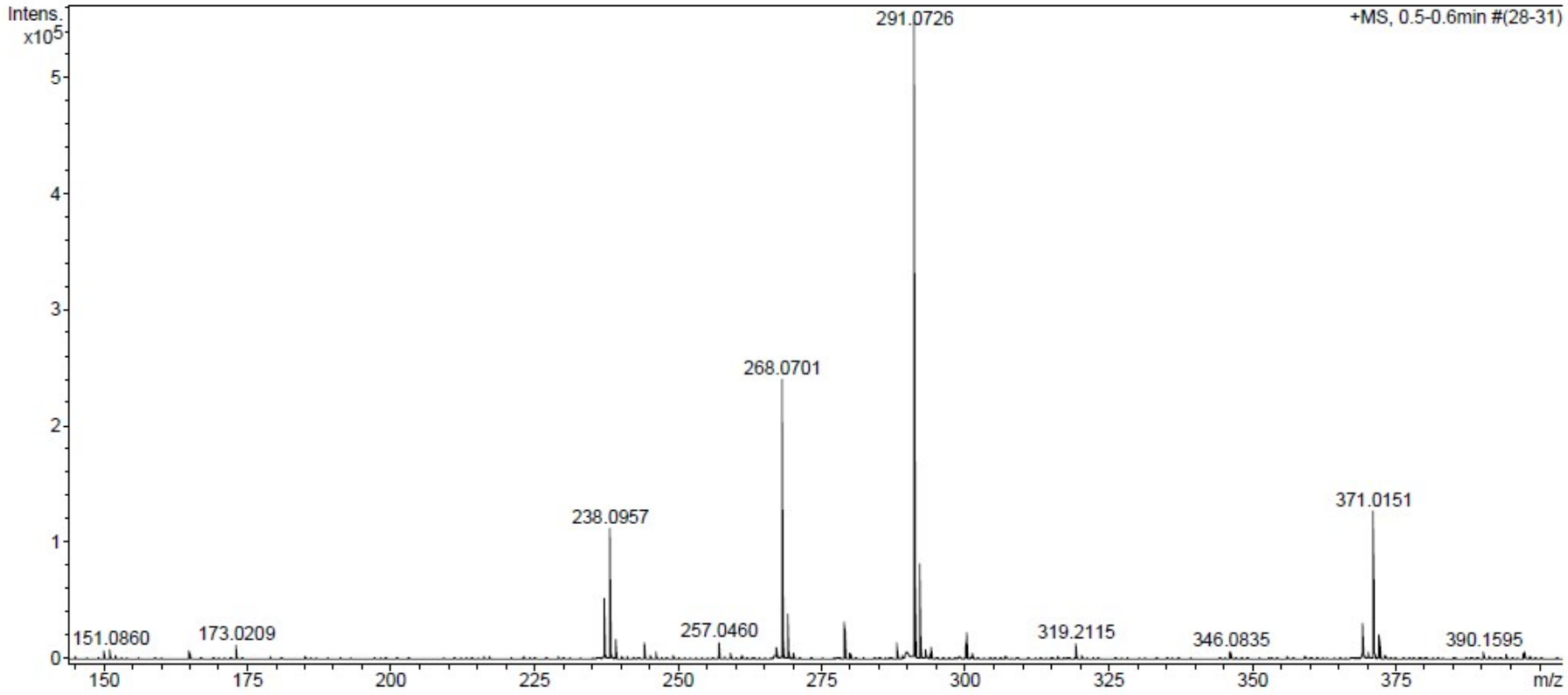

Figure 18S. HRESI^{+}-MS of **5**.

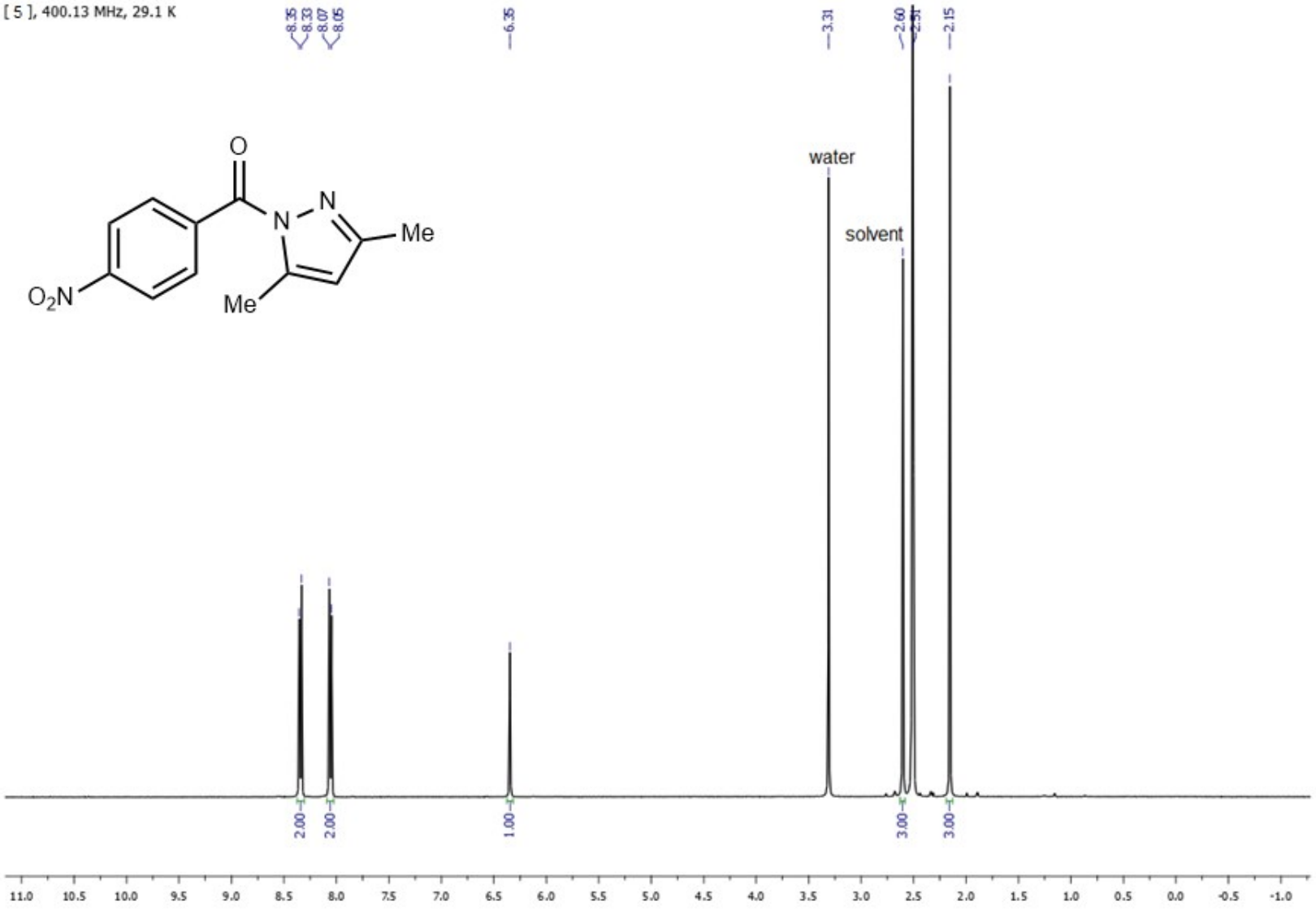

Figure 19S. ^{1}H NMR spectrum of **5**.

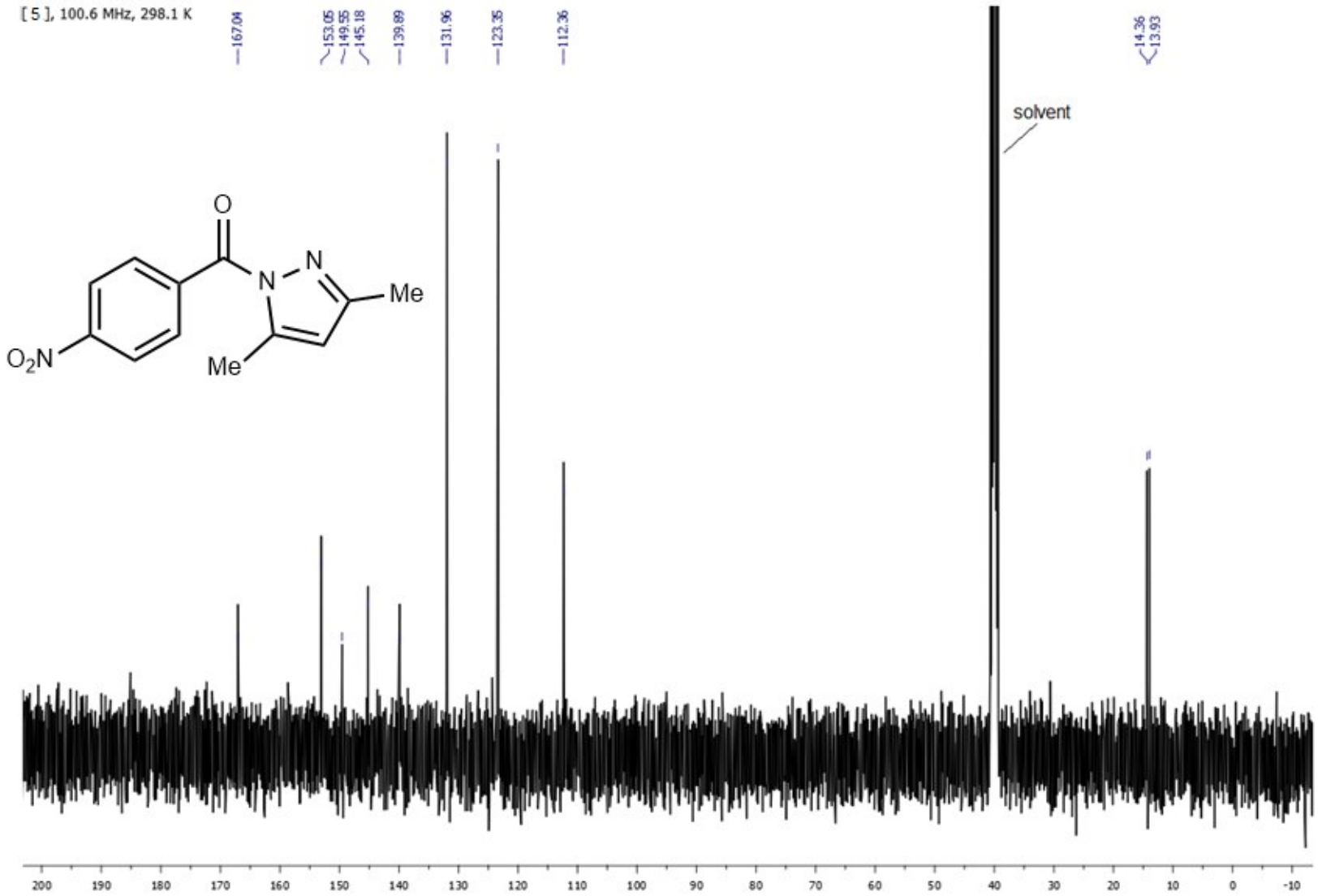

Figure 20S. $^{13}C\{^{1}H\}$ NMR spectrum of **5**.

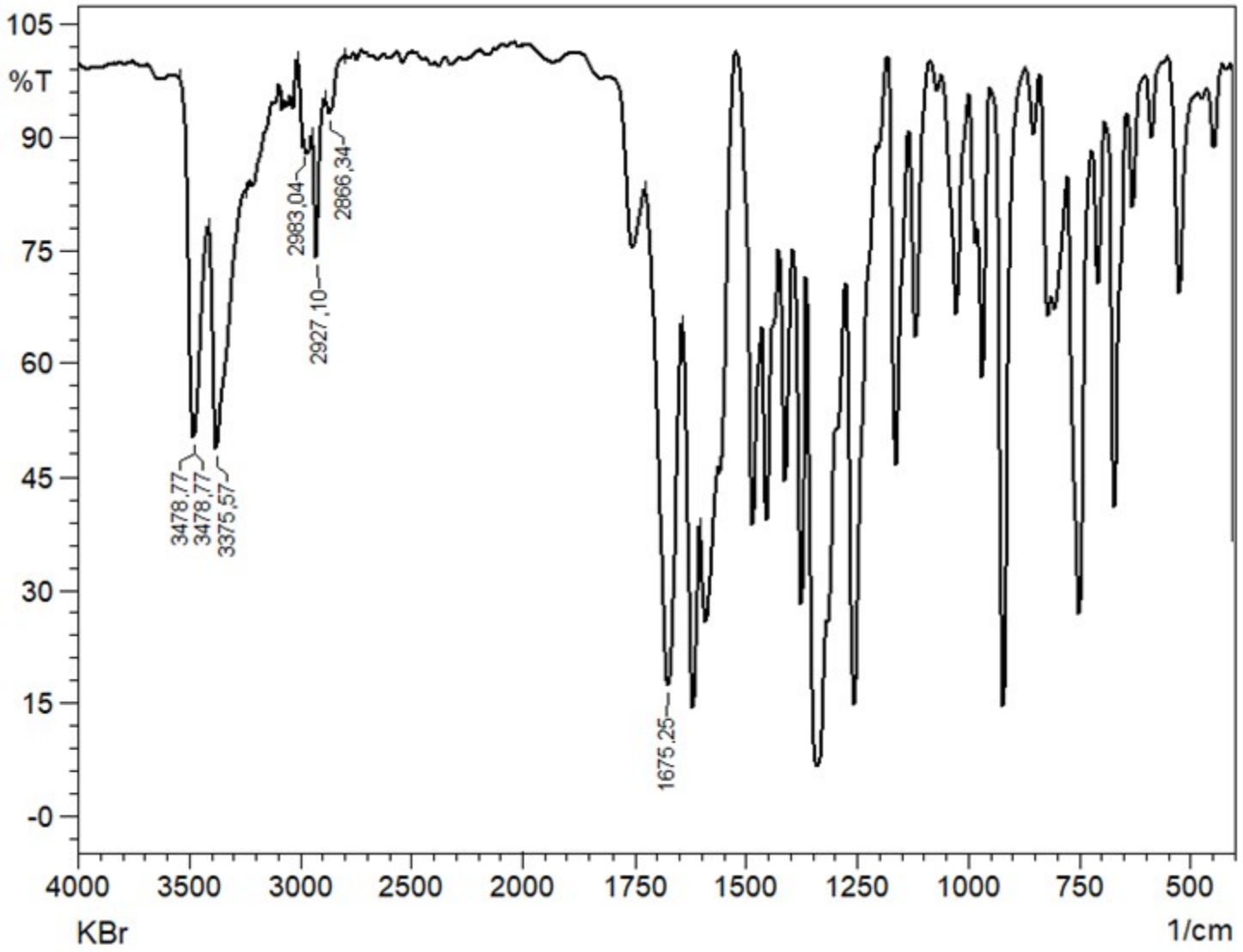

Figure 21S. IR spectrum of **6**.

Acquisition Parameter

Source Type	ESI	Ion Polarity	Positive	Set Nebulizer	0.4 Bar
Focus	Not active			Set Dry Heater	180 °C
Scan Begin	50 m/z	Set Capillary	4500 V	Set Dry Gas	4.0 l/min
Scan End	3000 m/z	Set End Plate Offset	-500 V	Set Divert Valve	Source

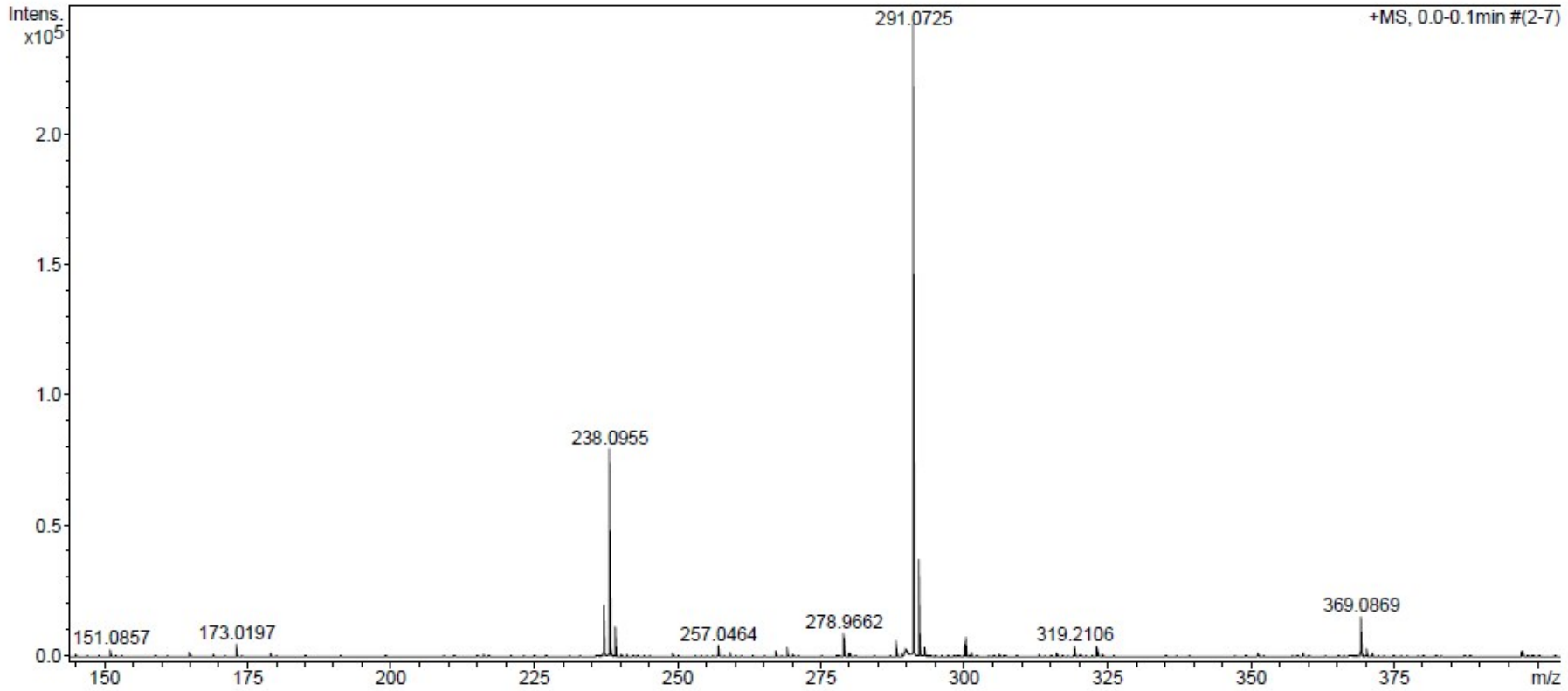

Figure 22S. HRESI^{+}-MS of **6**.

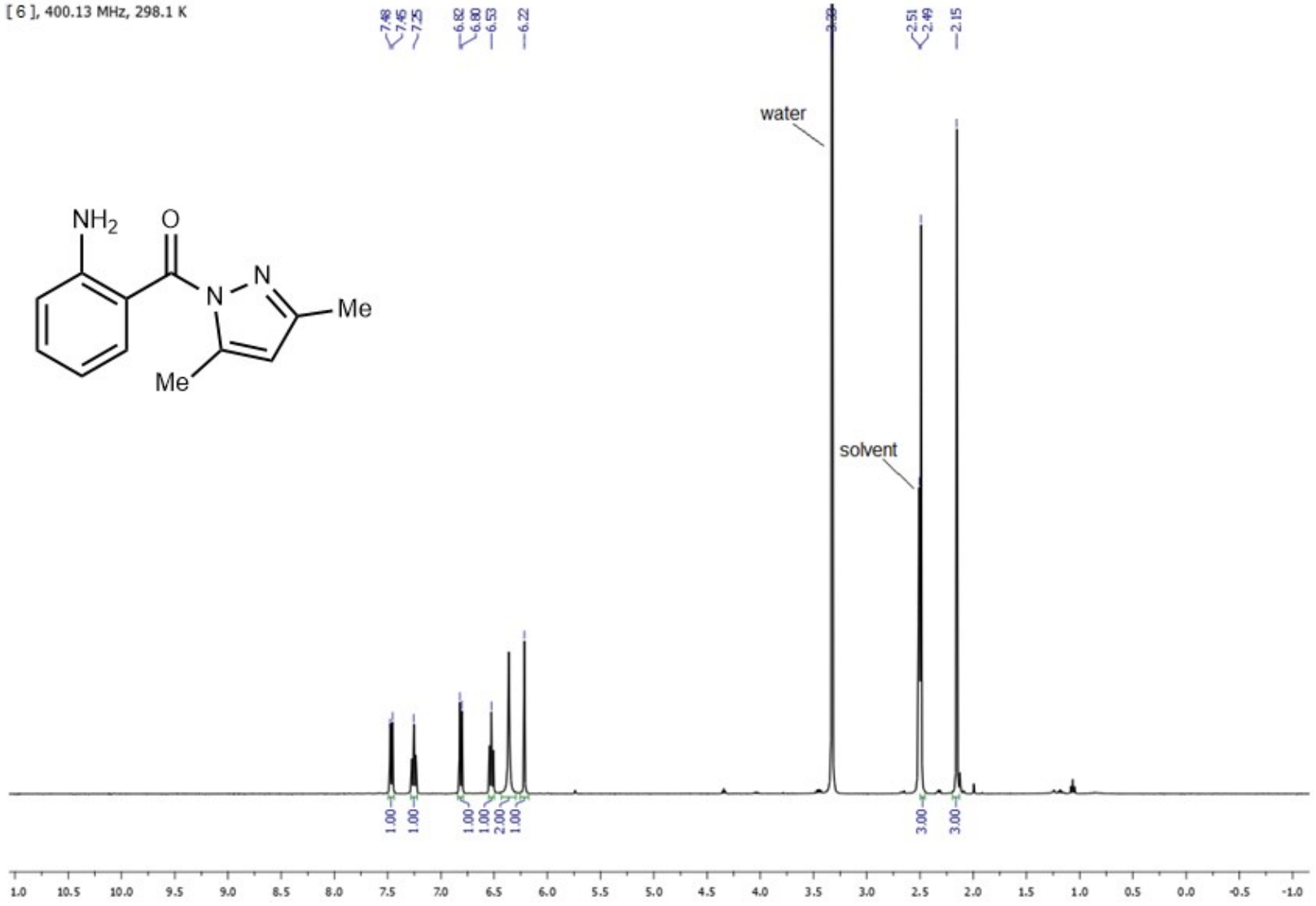

Figure 23S. ^{1}H NMR spectrum of **6**.

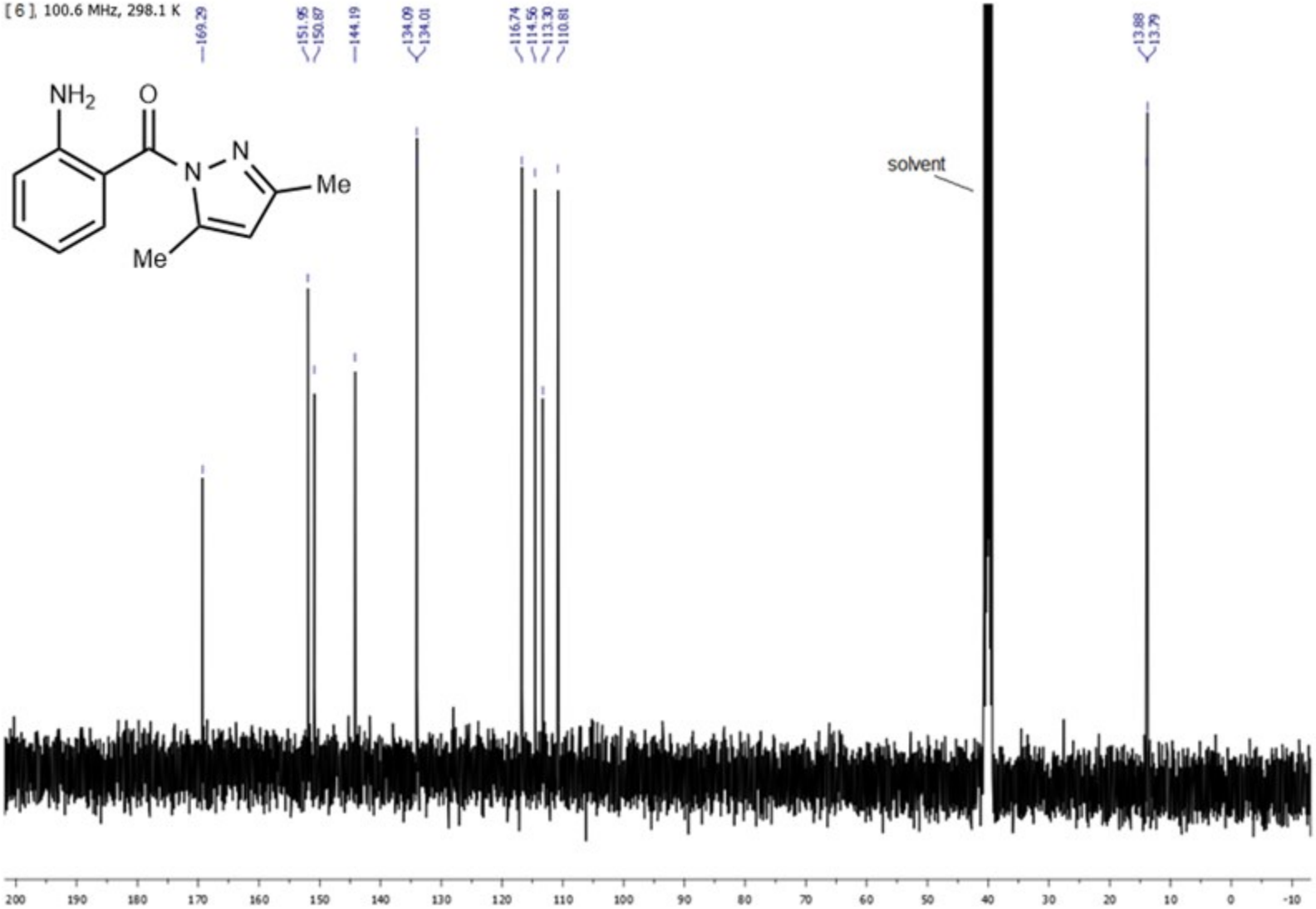

Figure 24S. $^{13}C\{^{1}H\}$ NMR spectrum of **6**.

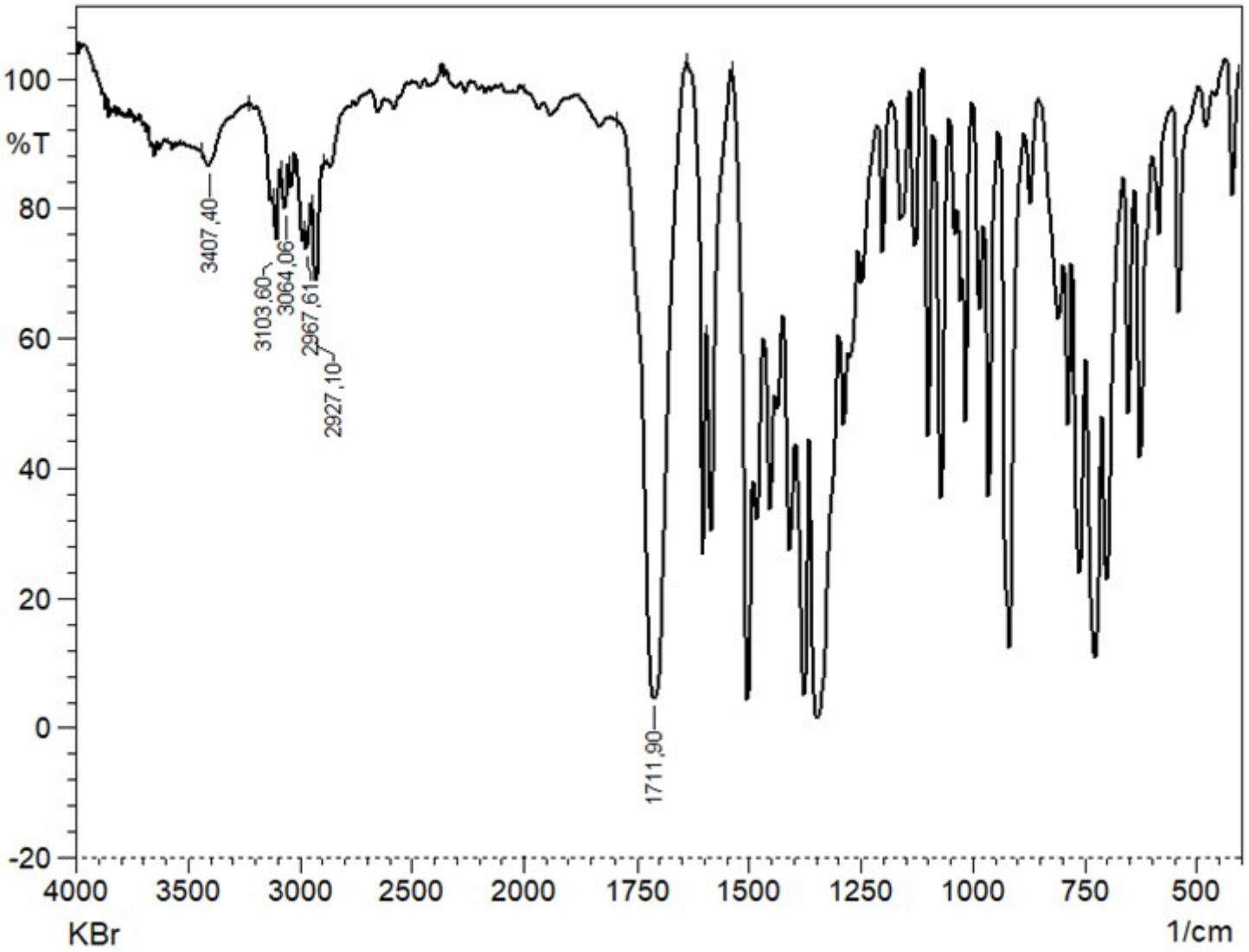

Figure 25S. IR spectrum of **7**.

Acquisition Parameter

Source Type	ESI	Ion Polarity	Positive	Set Nebulizer	0.4 Bar
Focus	Not active			Set Dry Heater	180 °C
Scan Begin	50 m/z	Set Capillary	4500 V	Set Dry Gas	4.0 l/min
Scan End	3000 m/z	Set End Plate Offset	-500 V	Set Divert Valve	Source

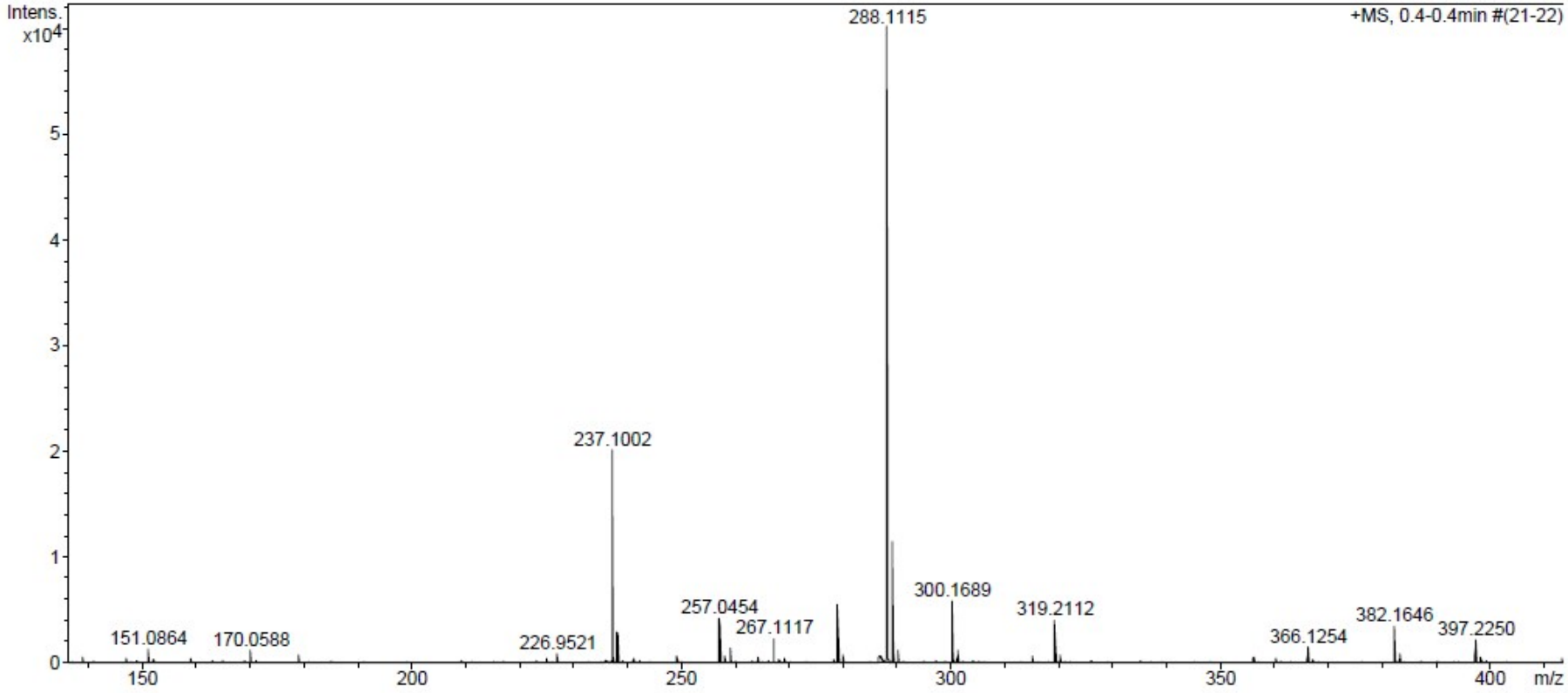

Figure 26S. HRESI^{+}-MS of **7**.

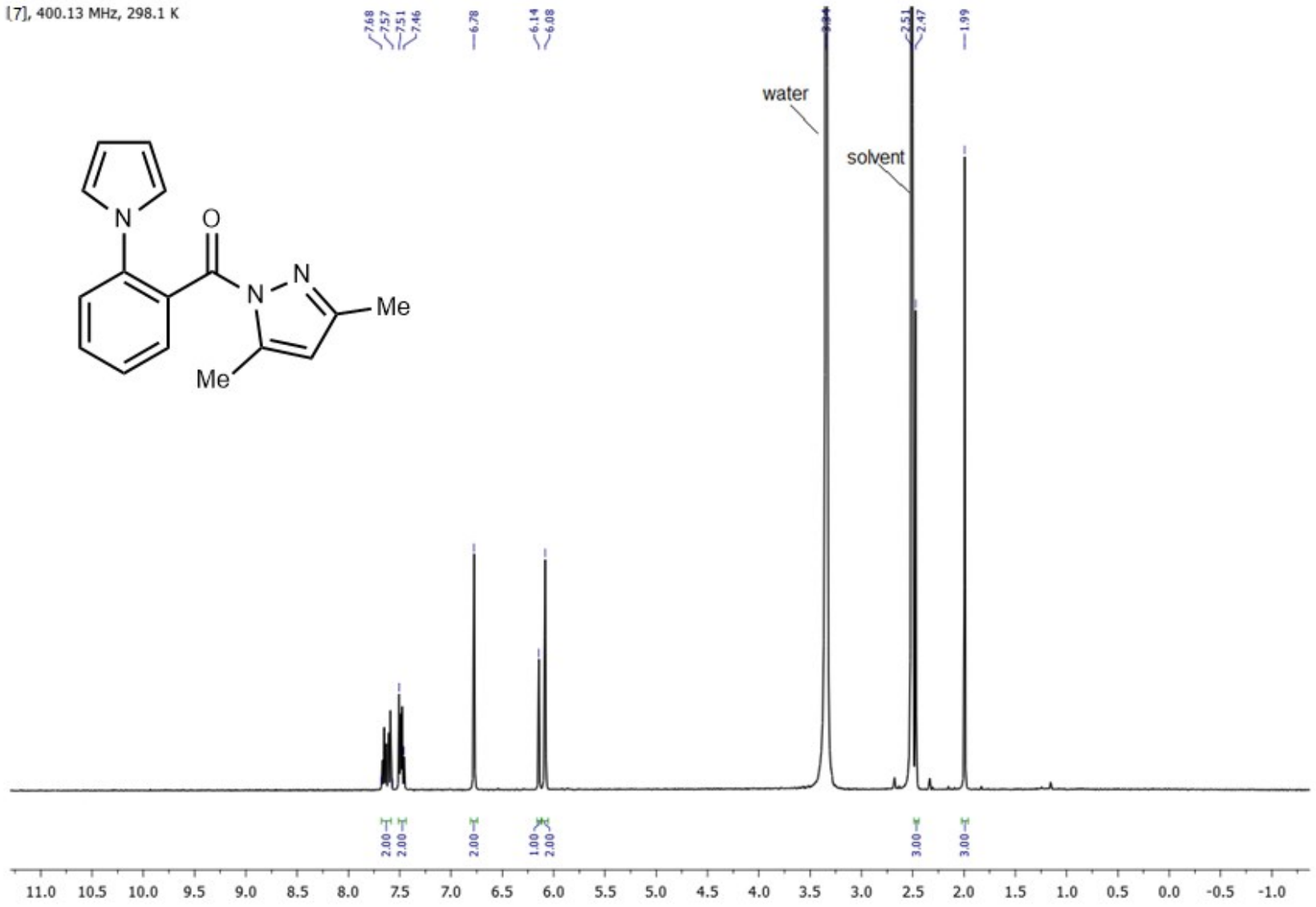

Figure 27S. ^{1}H NMR spectrum of **7**.

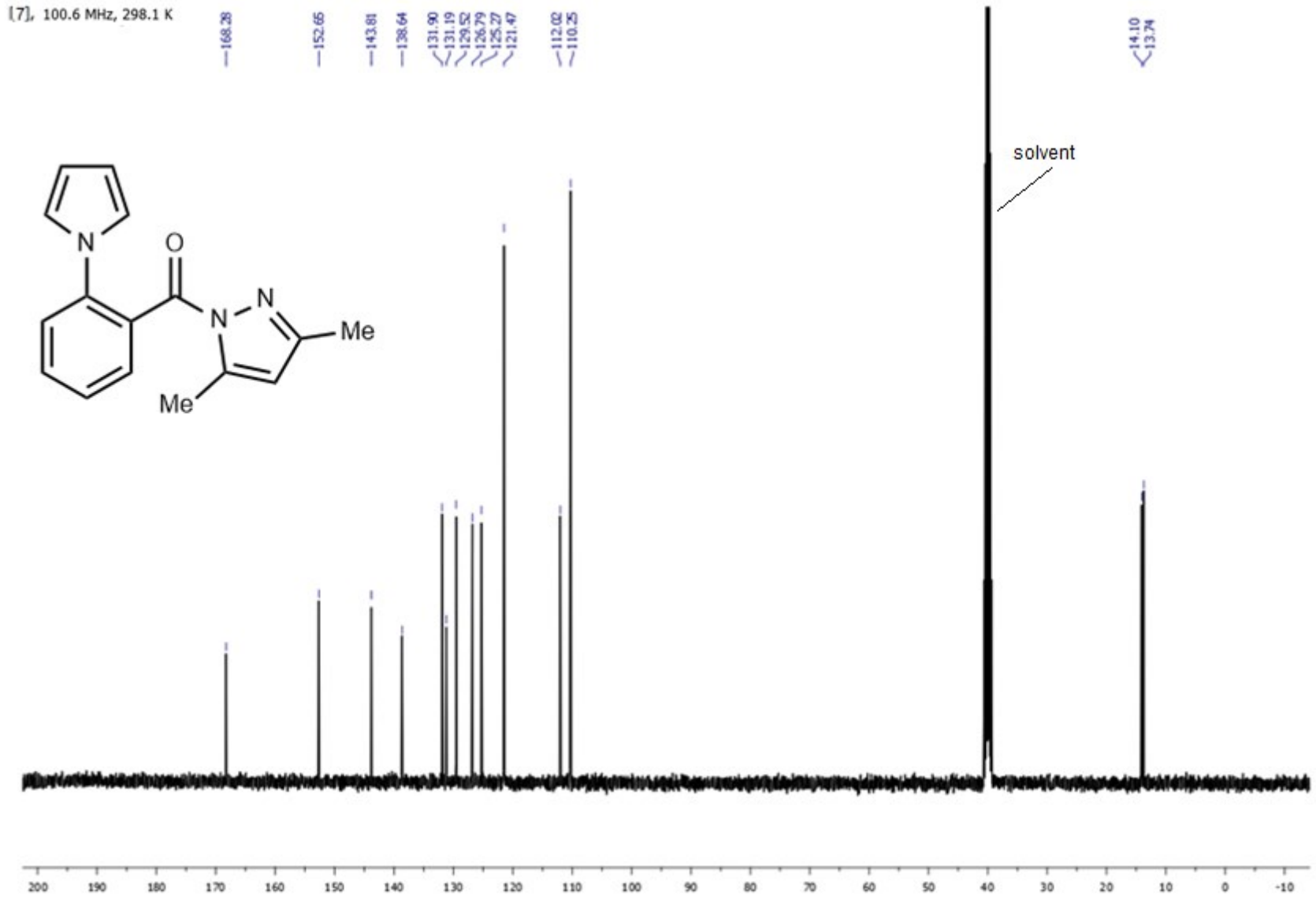

Figure 28S. $^{13}C\{^{1}H\}$ NMR spectrum of **7**.

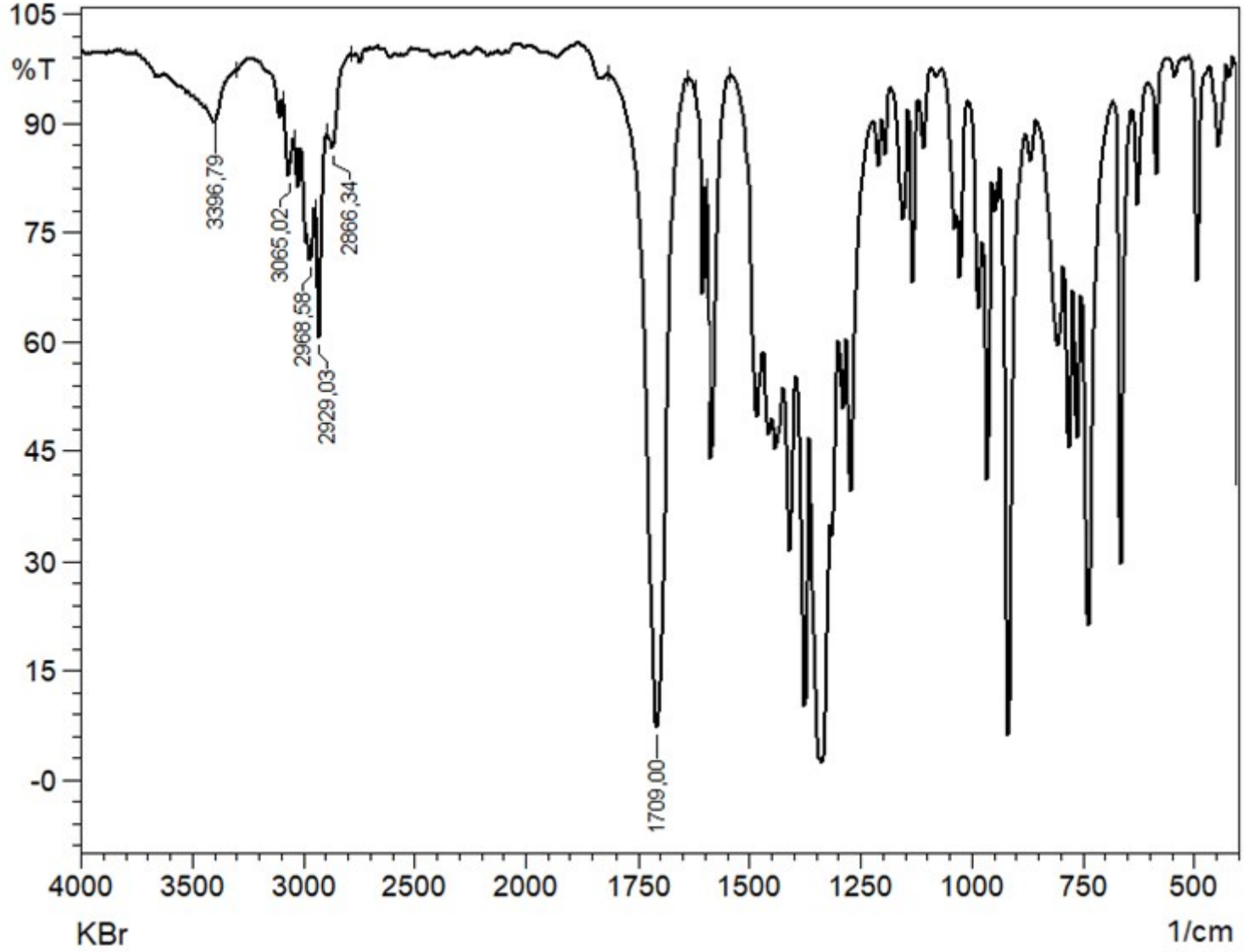

Figure 29S. IR spectrum of **8**.

Acquisition Parameter

Source Type	ESI	Ion Polarity	Positive	Set Nebulizer	0.4 Bar
Focus	Not active			Set Dry Heater	180 °C
Scan Begin	50 m/z	Set Capillary	4500 V	Set Dry Gas	4.0 l/min
Scan End	3000 m/z	Set End Plate Offset	-500 V	Set Divert Valve	Source

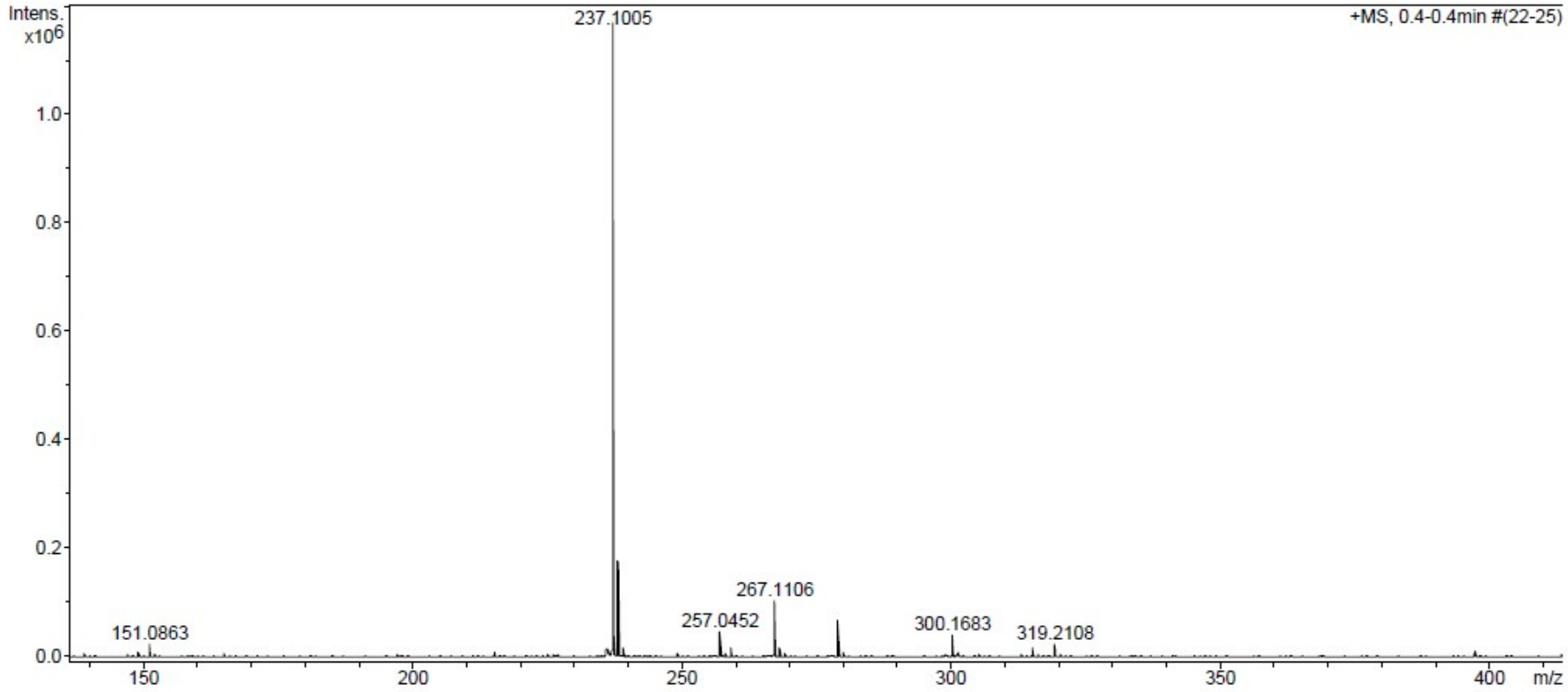

Figure 30S. HRESI^{+}-MS of **8**.

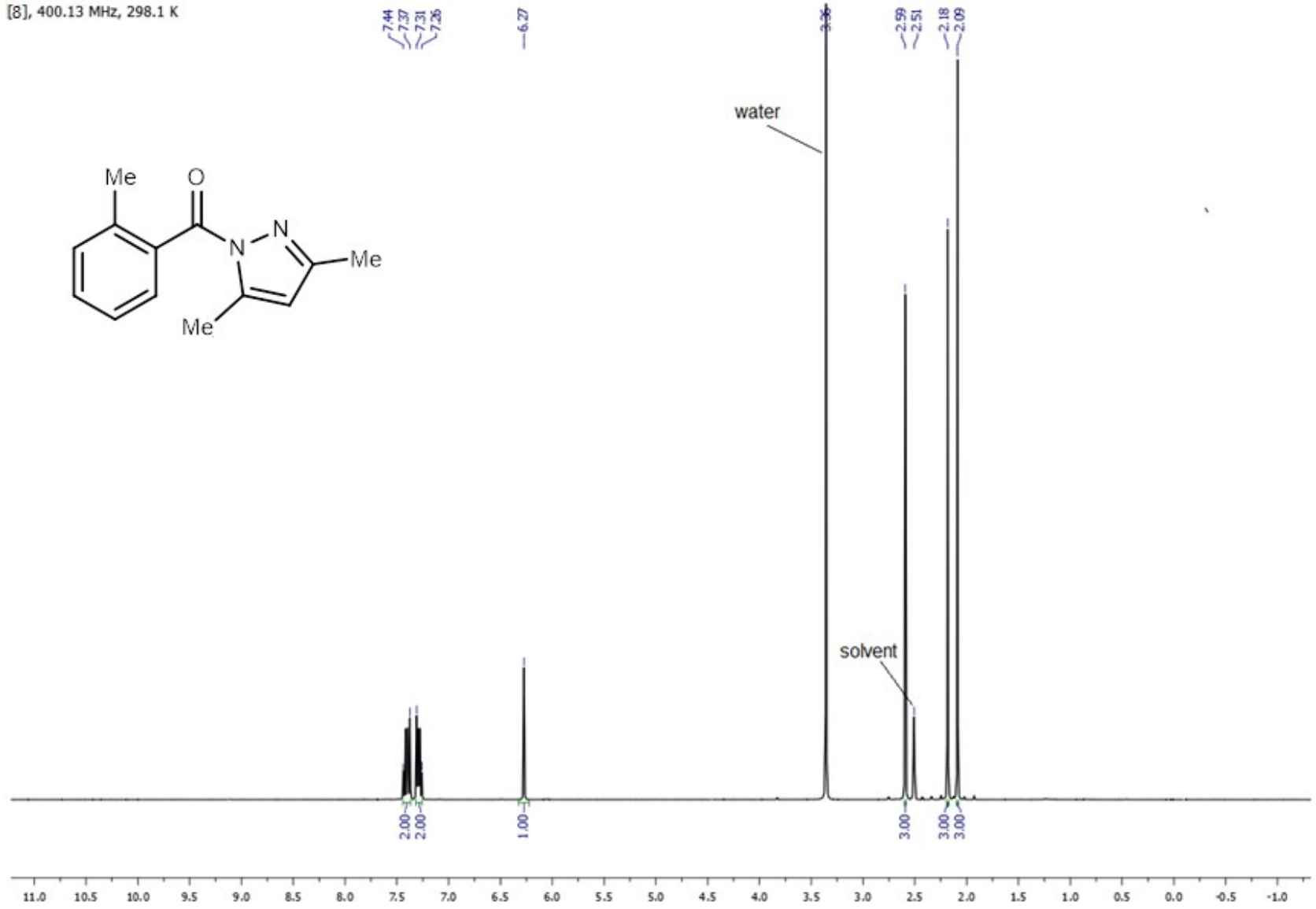

Figure 31S. ^{1}H NMR spectrum of **8**.

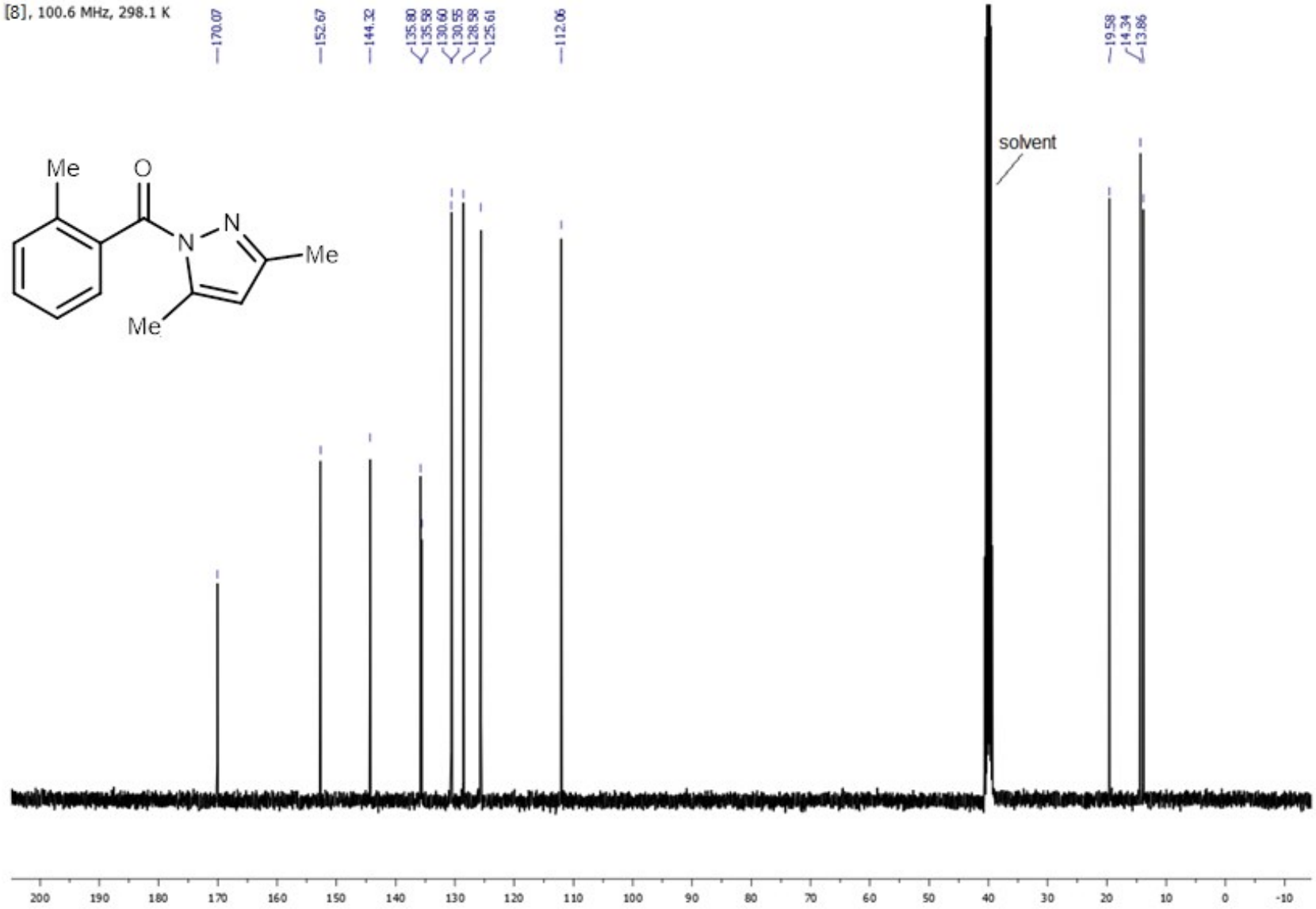

Figure 32S. $^{13}C\{^{1}H\}$ NMR spectrum of **8**.

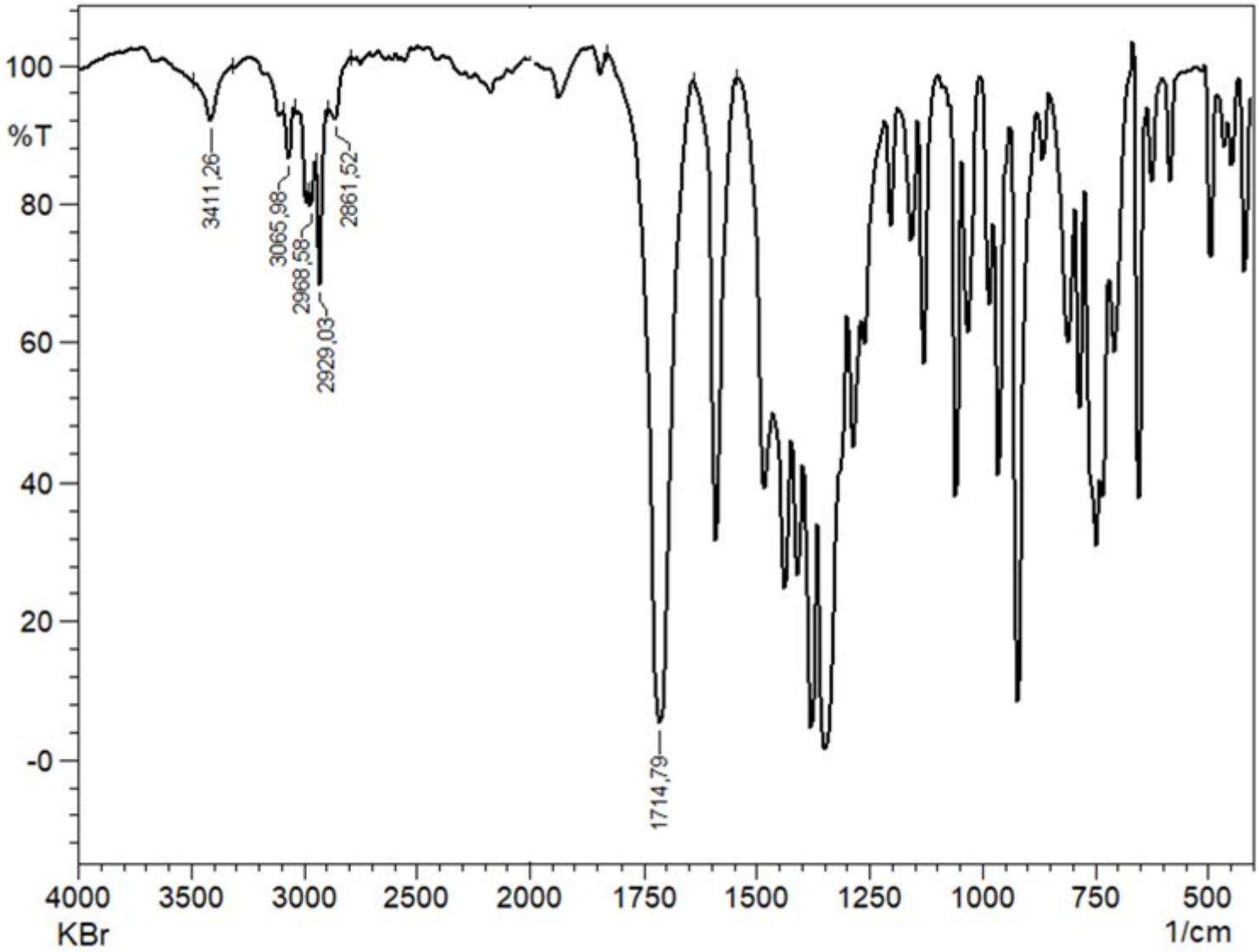

Figure 33S. IR spectrum of **9**.

Acquisition Parameter

Source Type	ESI	Ion Polarity	Positive	Set Nebulizer	0.4 Bar
Focus	Not active			Set Dry Heater	180 °C
Scan Begin	50 m/z	Set Capillary	4500 V	Set Dry Gas	4.0 l/min
Scan End	3000 m/z	Set End Plate Offset	-500 V	Set Divert Valve	Source

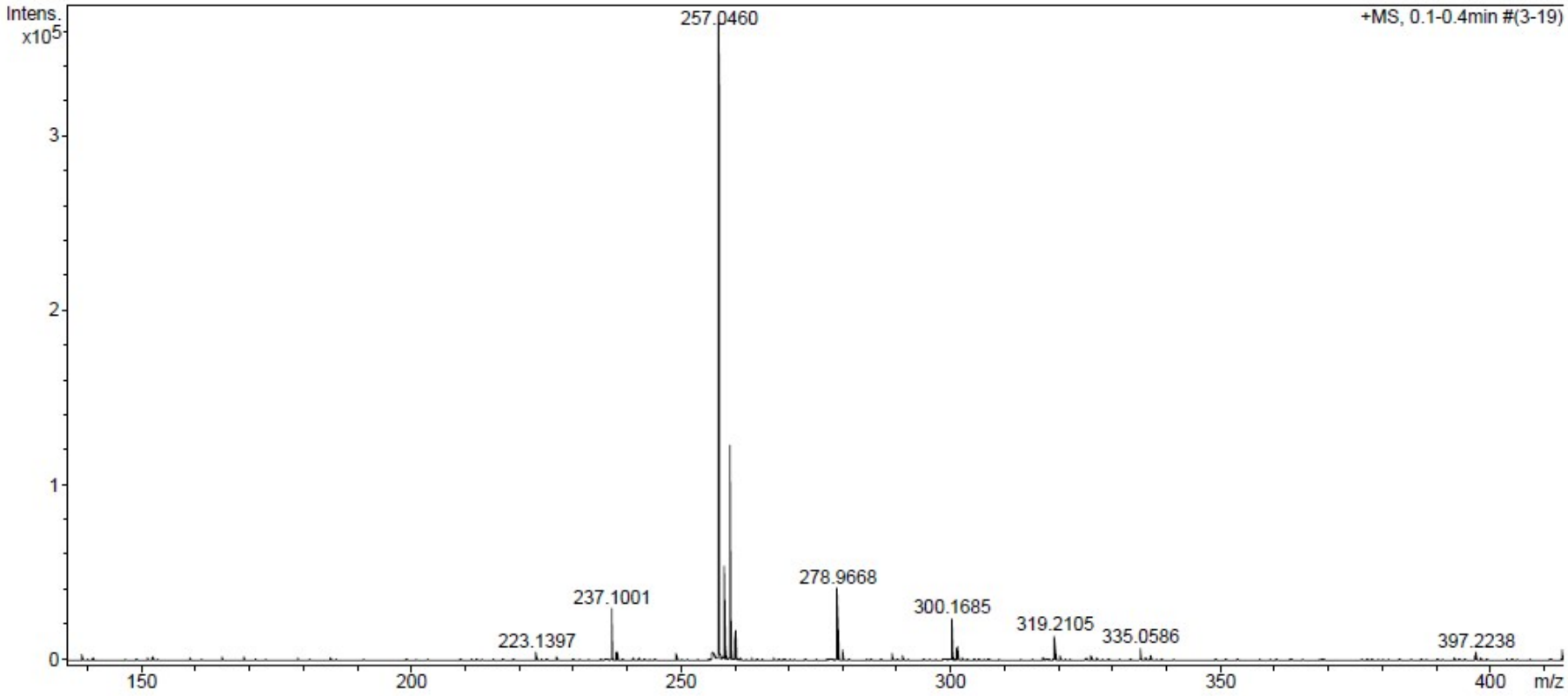

Figure 34S. HRESI^{+}-MS of **9**.

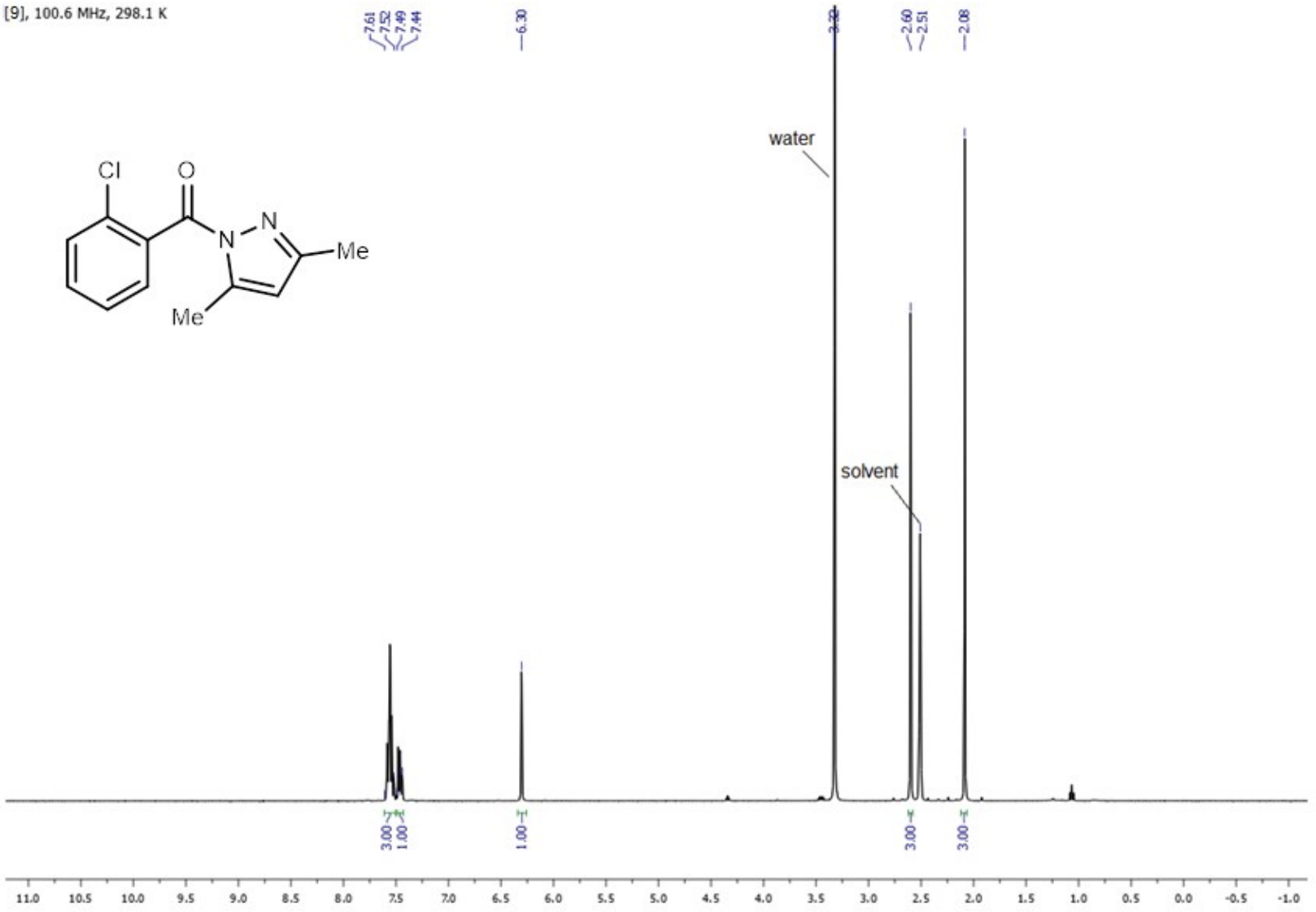

Figure 35S. ^{1}H NMR spectrum of **9**.

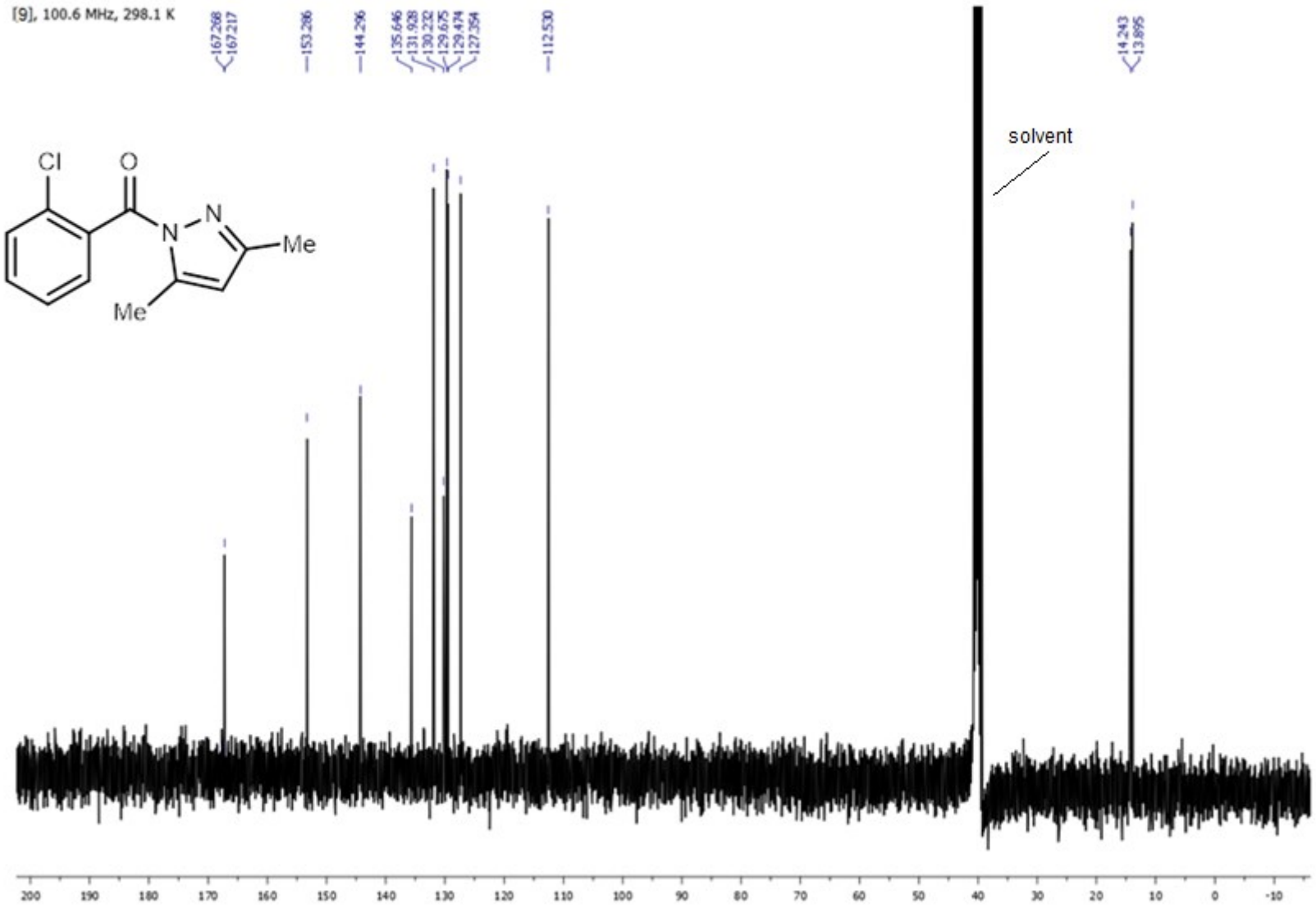

Figure 36S. $^{13}C\{^{1}H\}$ NMR spectrum of **9**.

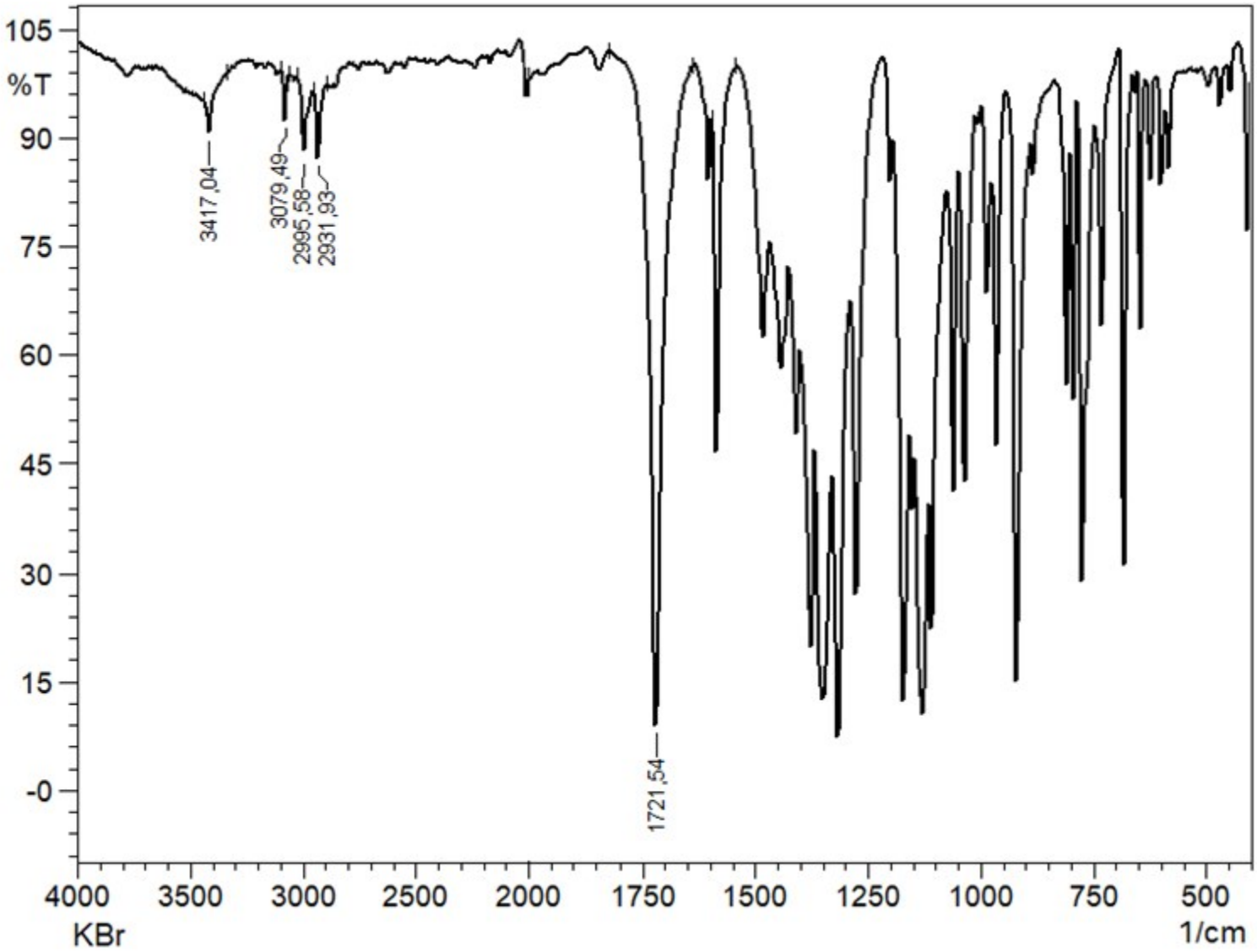

Figure 37S. IR spectrum of **10**.

Figure 38S. HRESI^{+}-MS of **10**.

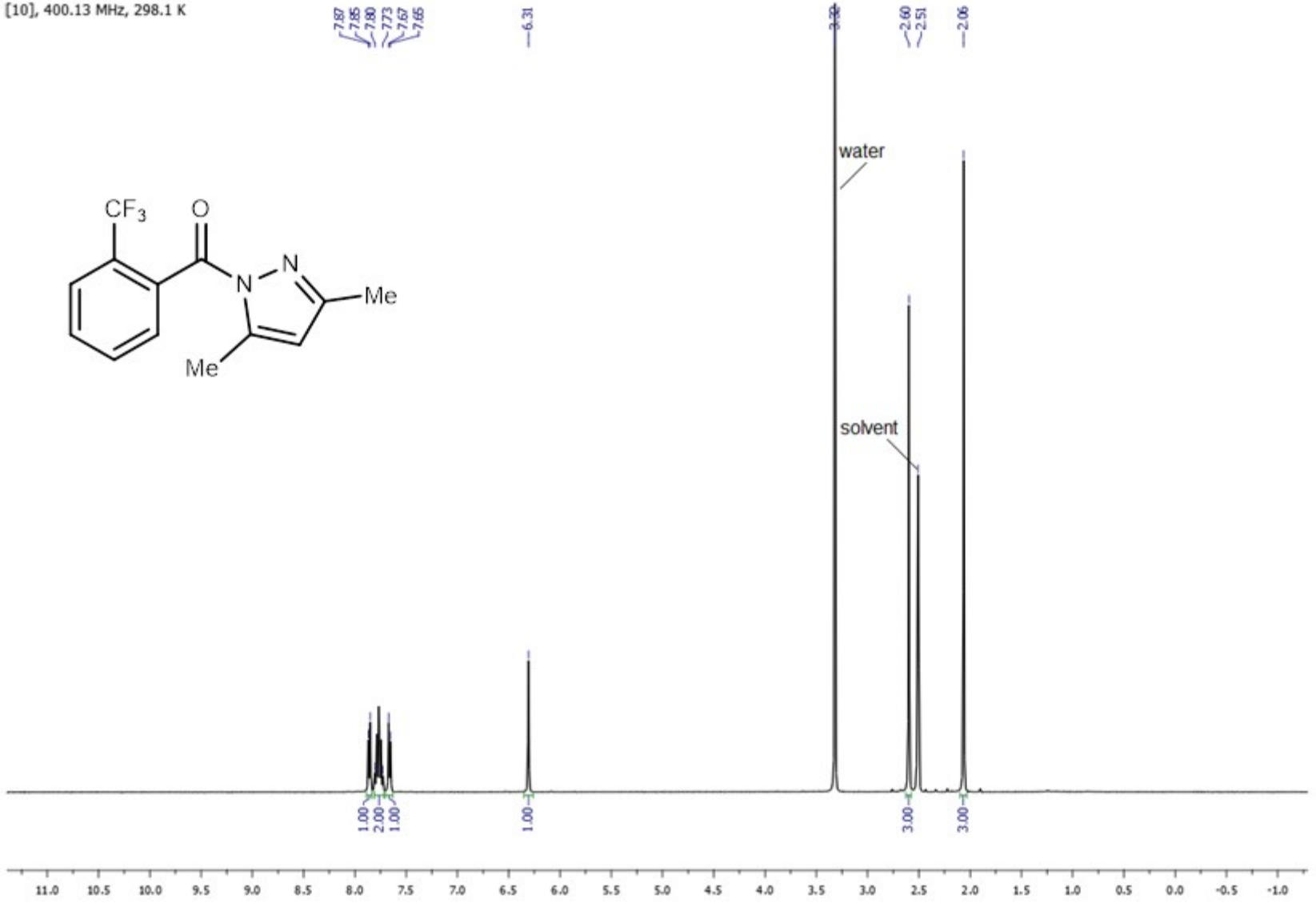

Figure 39S. ^{1}H NMR spectrum of **10**.

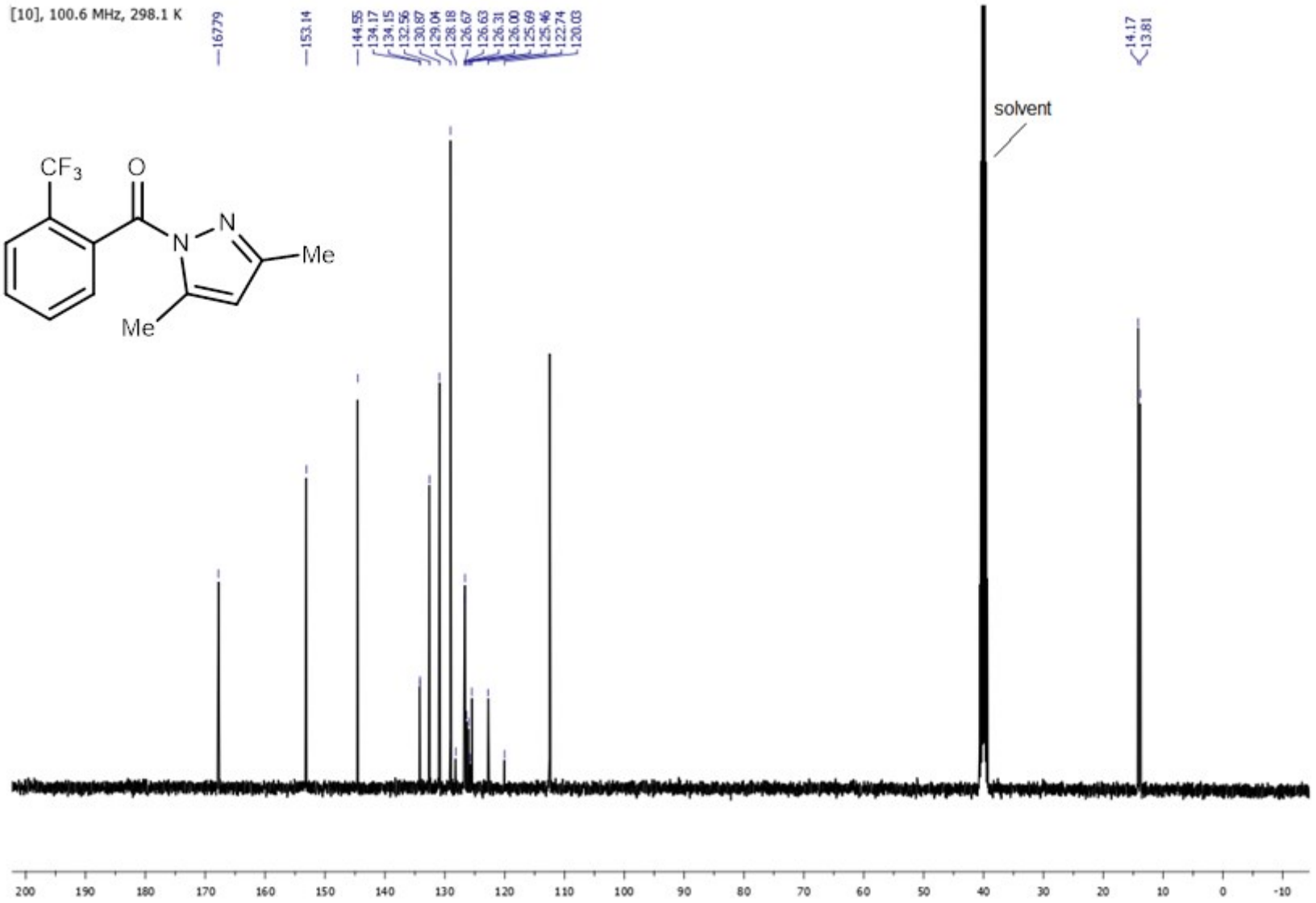

Figure 40S. $^{13}C\{^{1}H\}$ NMR spectrum of **10**.

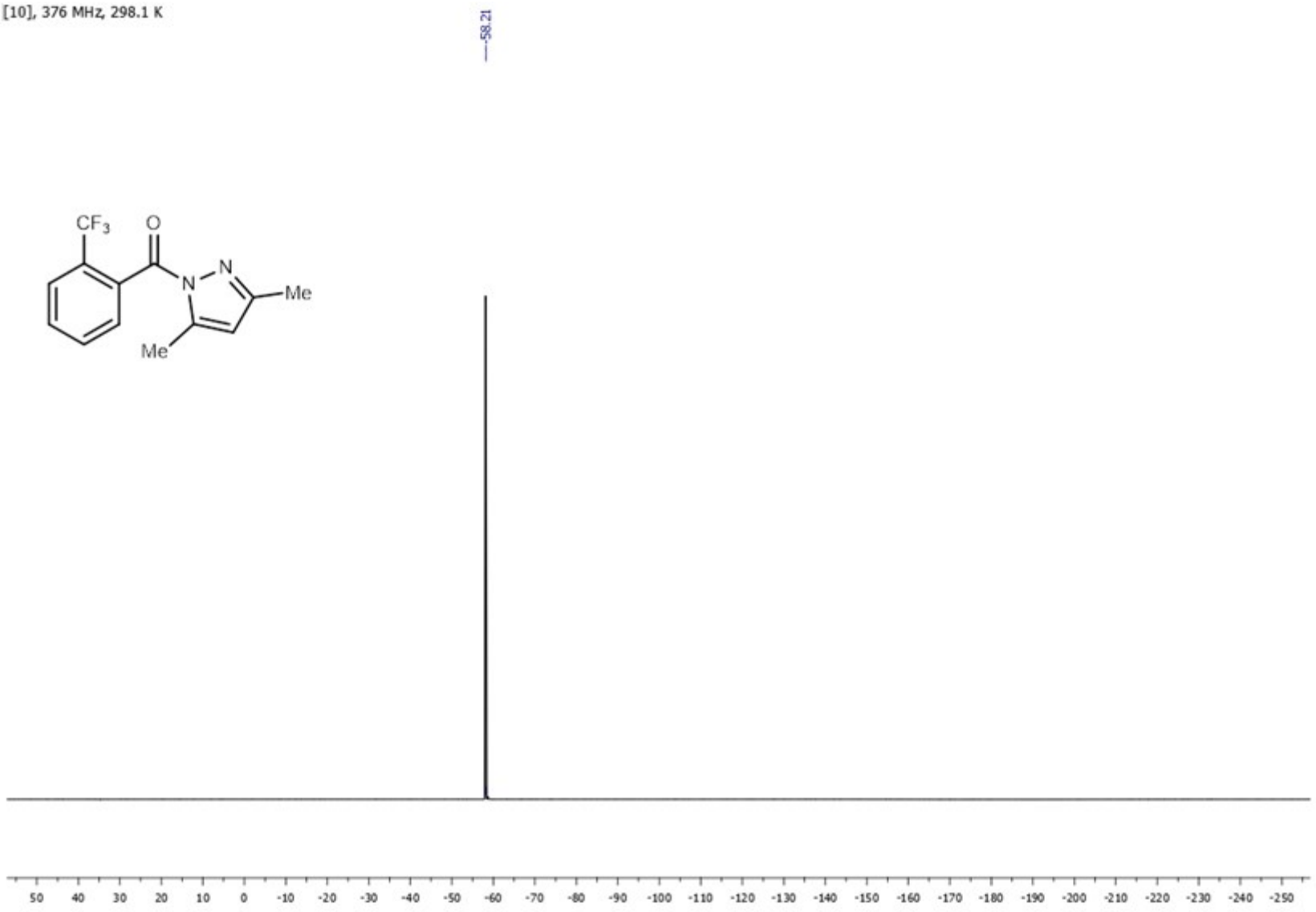

Figure 41S. ^{19}F NMR spectrum of **10**.

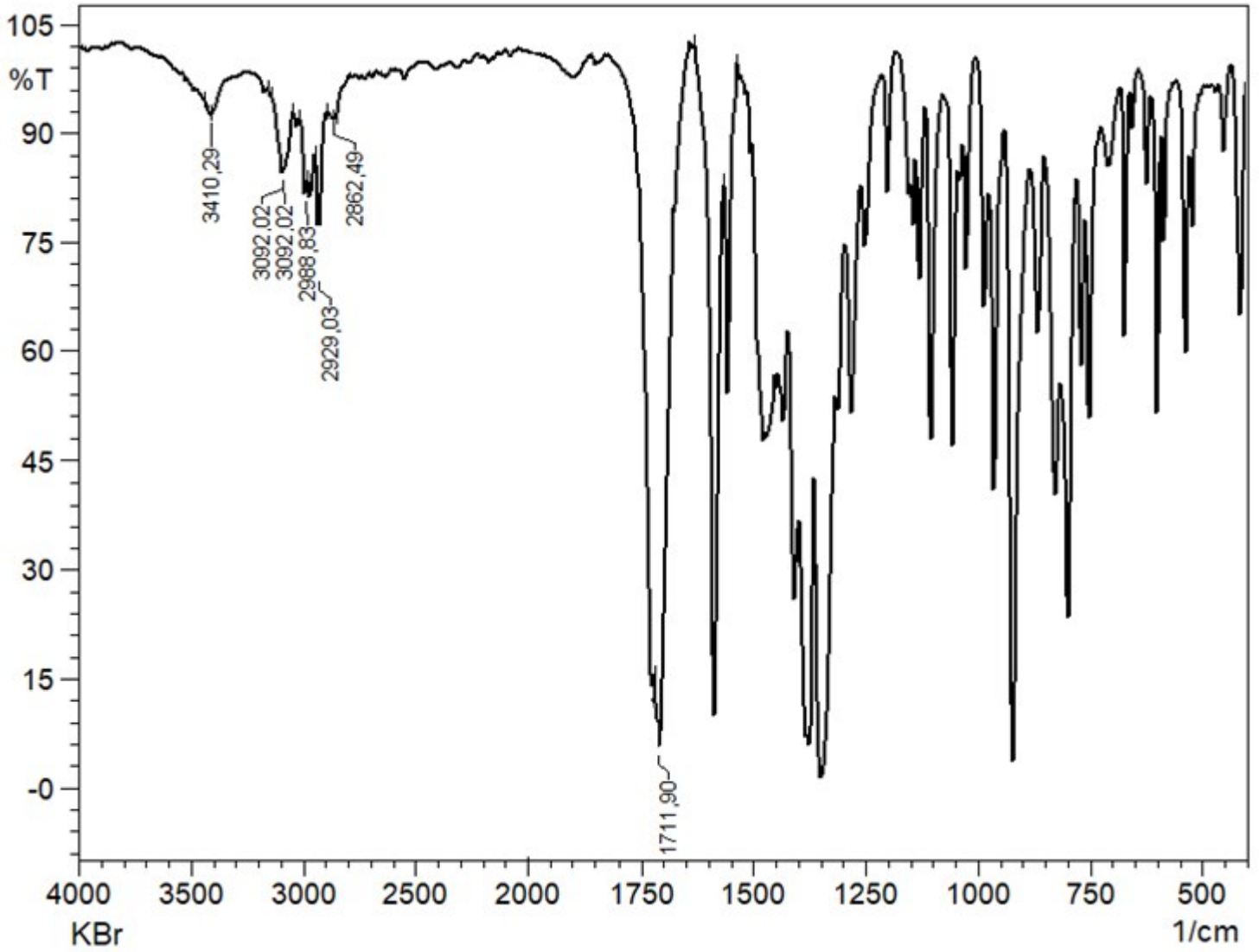

Figure 42S. IR spectrum of **11**.

Acquisition Parameter

Source Type	ESI	Ion Polarity	Positive	Set Nebulizer	0.4 Bar
Focus	Not active			Set Dry Heater	180 °C
Scan Begin	50 m/z	Set Capillary	4500 V	Set Dry Gas	4.0 l/min
Scan End	3000 m/z	Set End Plate Offset	-500 V	Set Divert Valve	Source

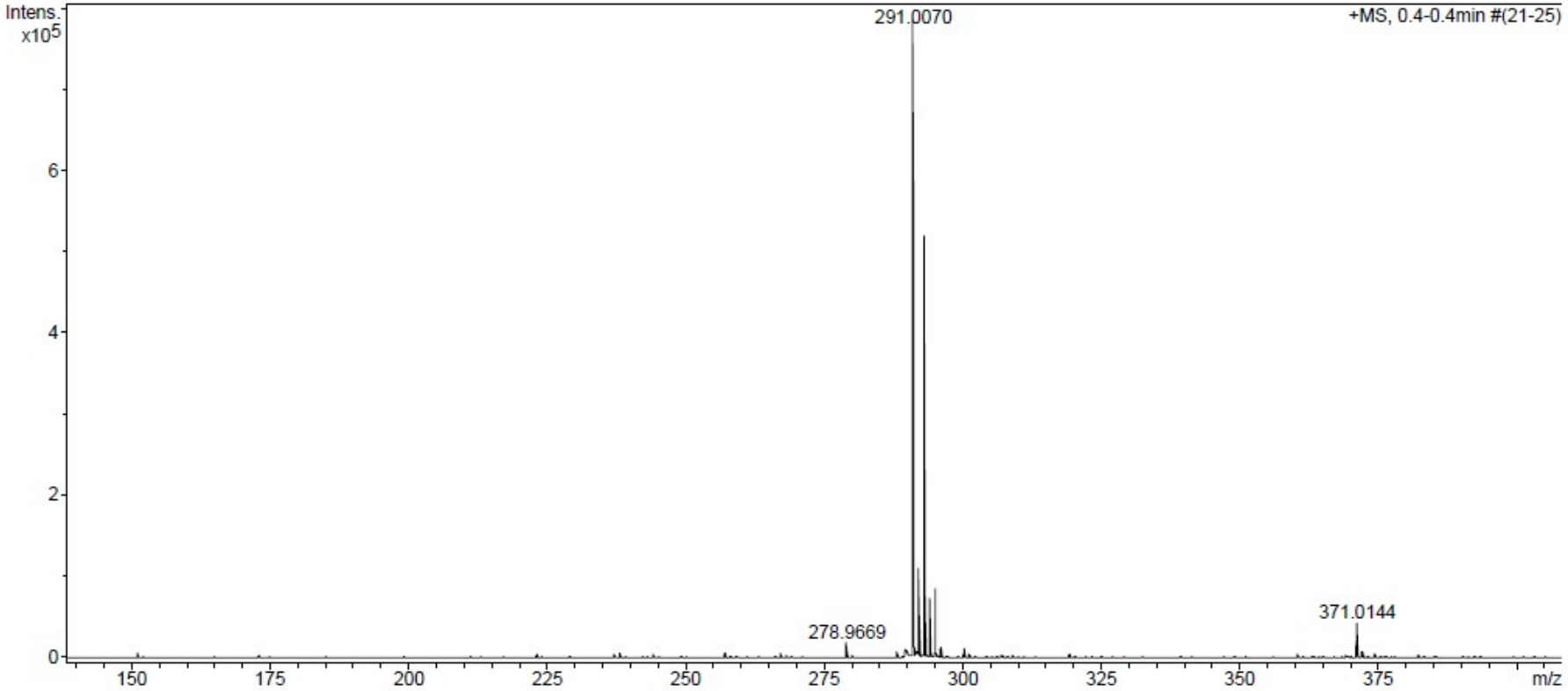

Figure 43S. HRESI^{+}-MS of **11**.

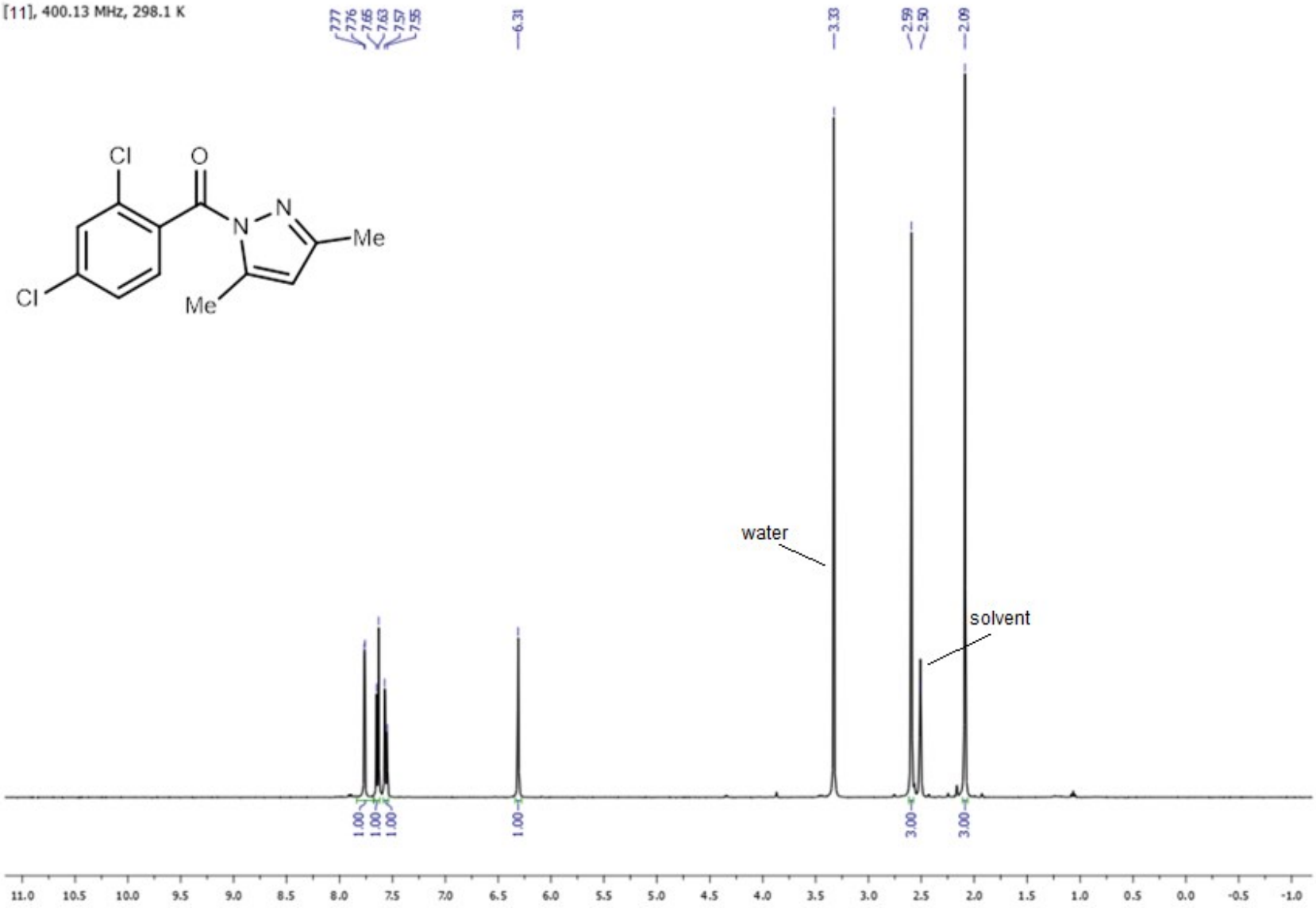

Figure 44S. ^{1}H NMR spectrum of **11**.

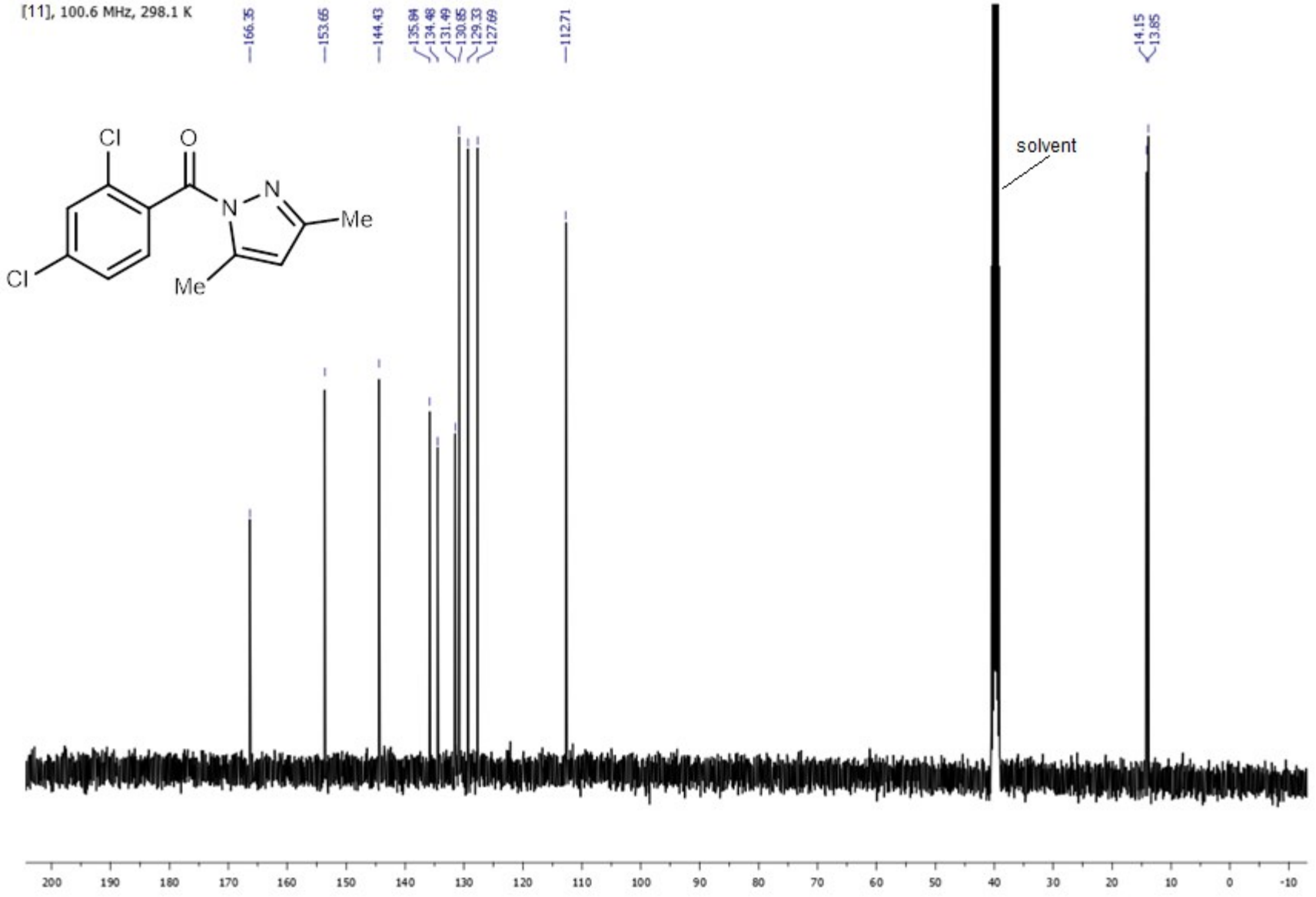

Figure 45S. $^{13}C\{^{1}H\}$ NMR spectrum of **11**.

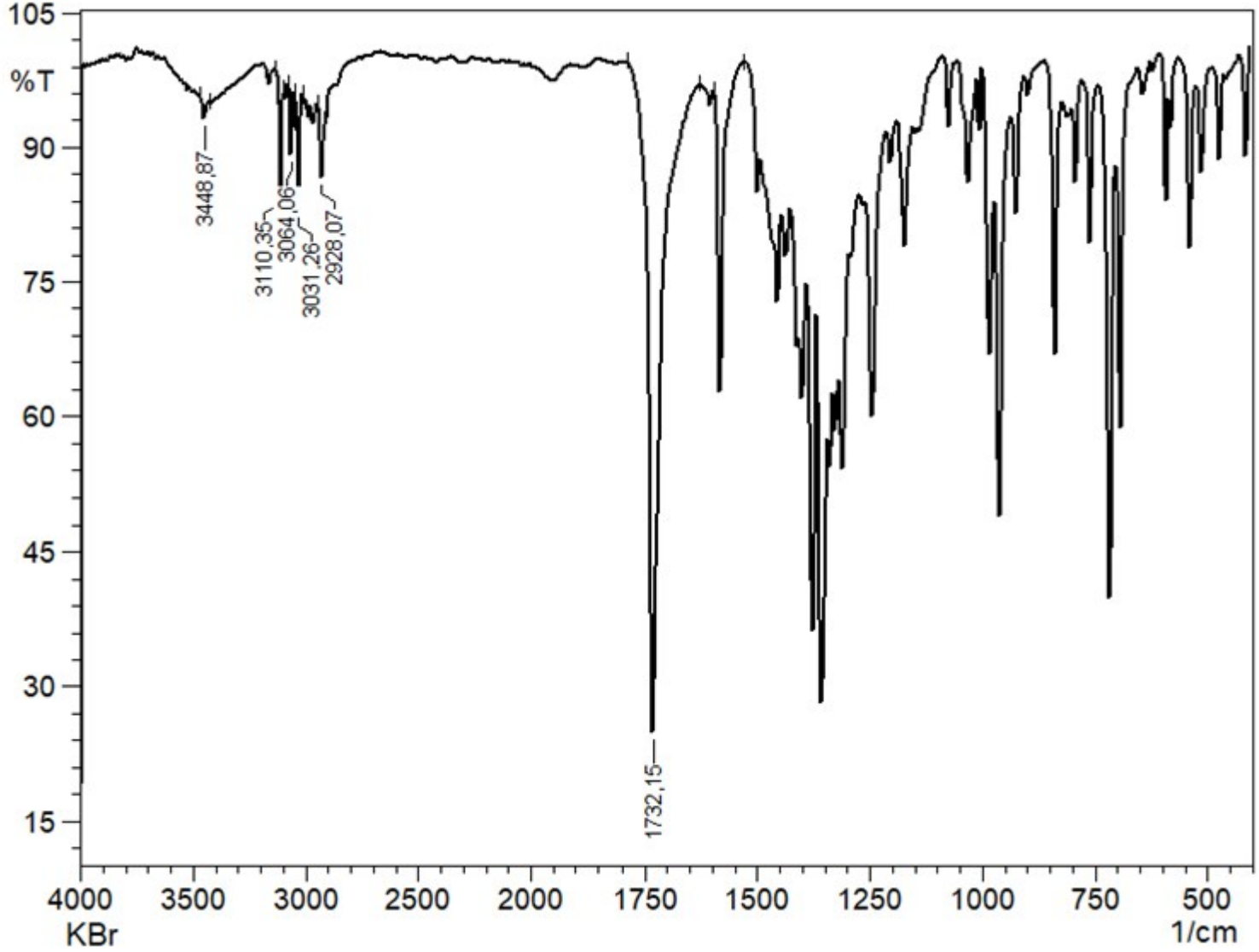

Figure 46S. IR spectrum of **12**.

Acquisition Parameter

Source Type	ESI	Ion Polarity	Positive	Set Nebulizer	0.4 Bar
Focus	Not active			Set Dry Heater	180 °C
Scan Begin	50 m/z	Set Capillary	4500 V	Set Dry Gas	4.0 l/min
Scan End	3000 m/z	Set End Plate Offset	-500 V	Set Divert Valve	Source

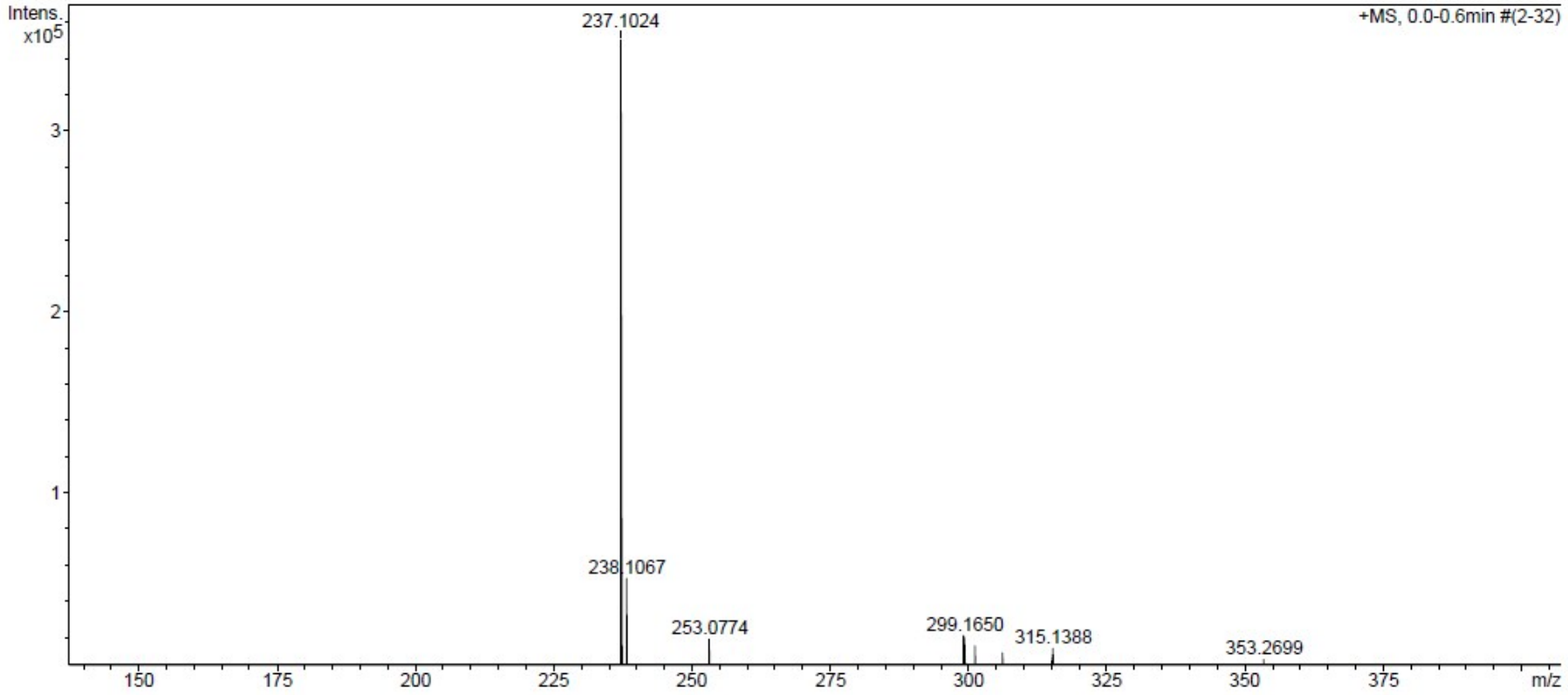

Figure 47S. HRESI^{+}-MS of **12**.

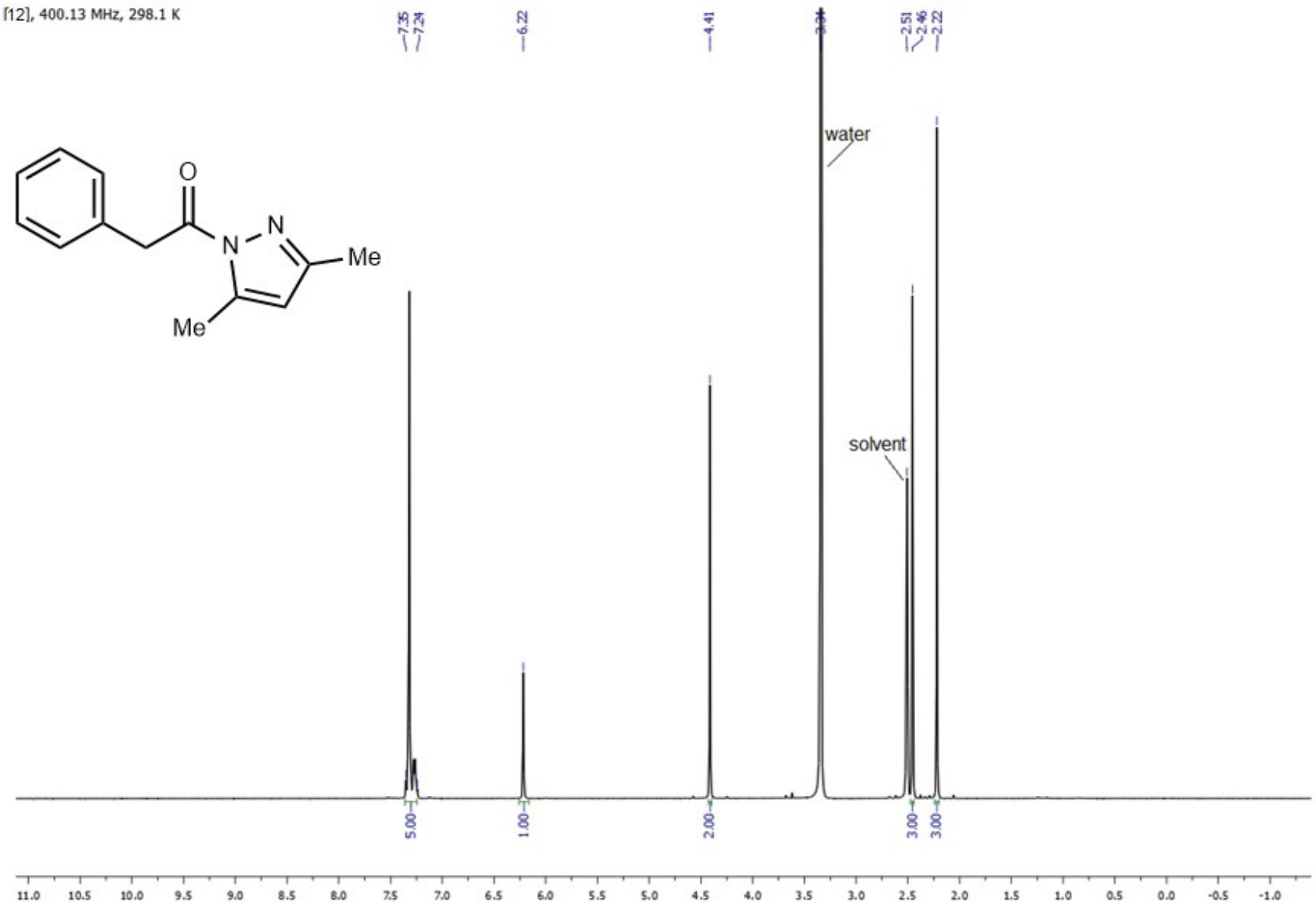

Figure 48S. ^{1}H NMR spectrum of **12**.

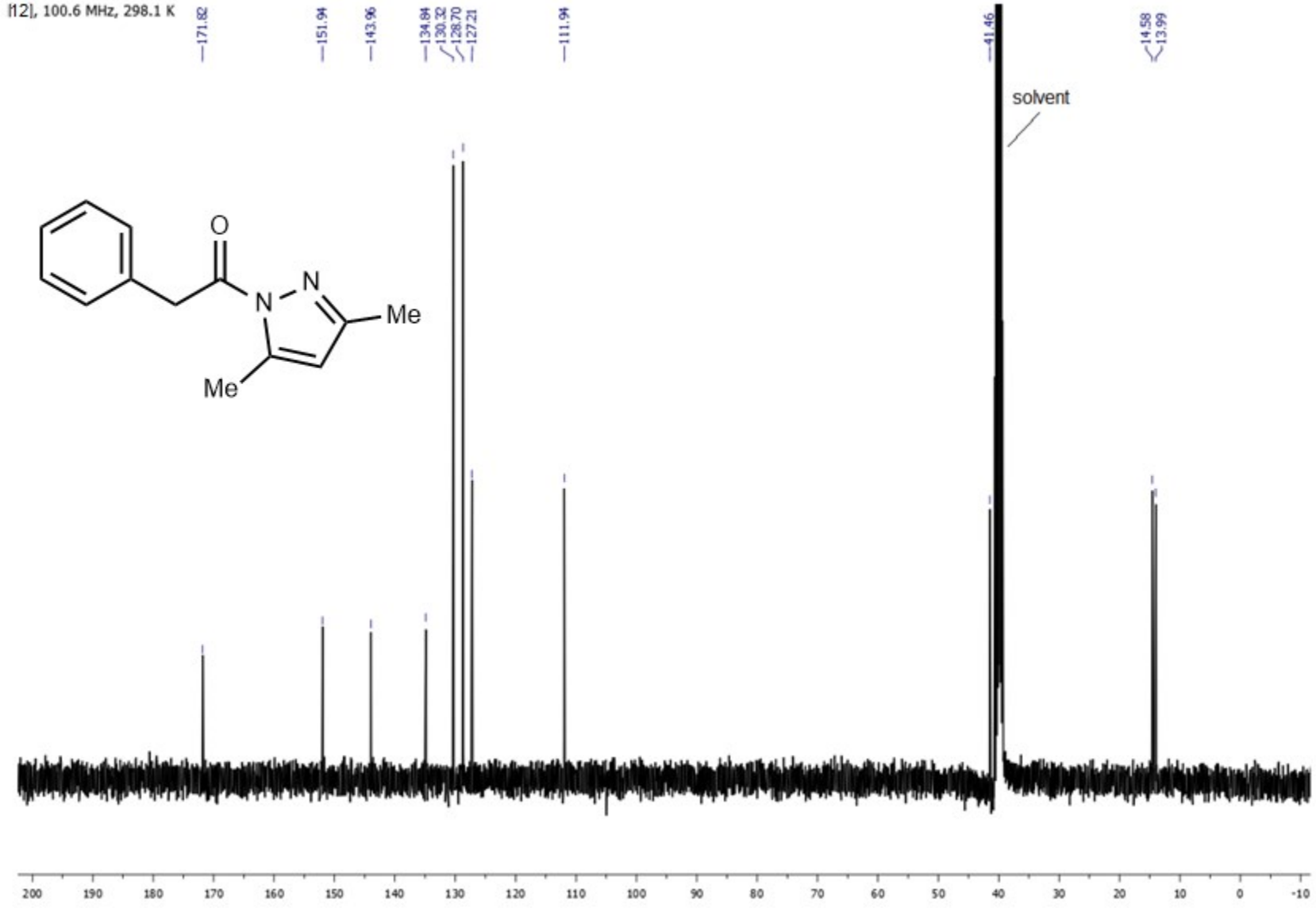

Figure 49S. $^{13}C\{^{1}H\}$ NMR spectrum of **12**.

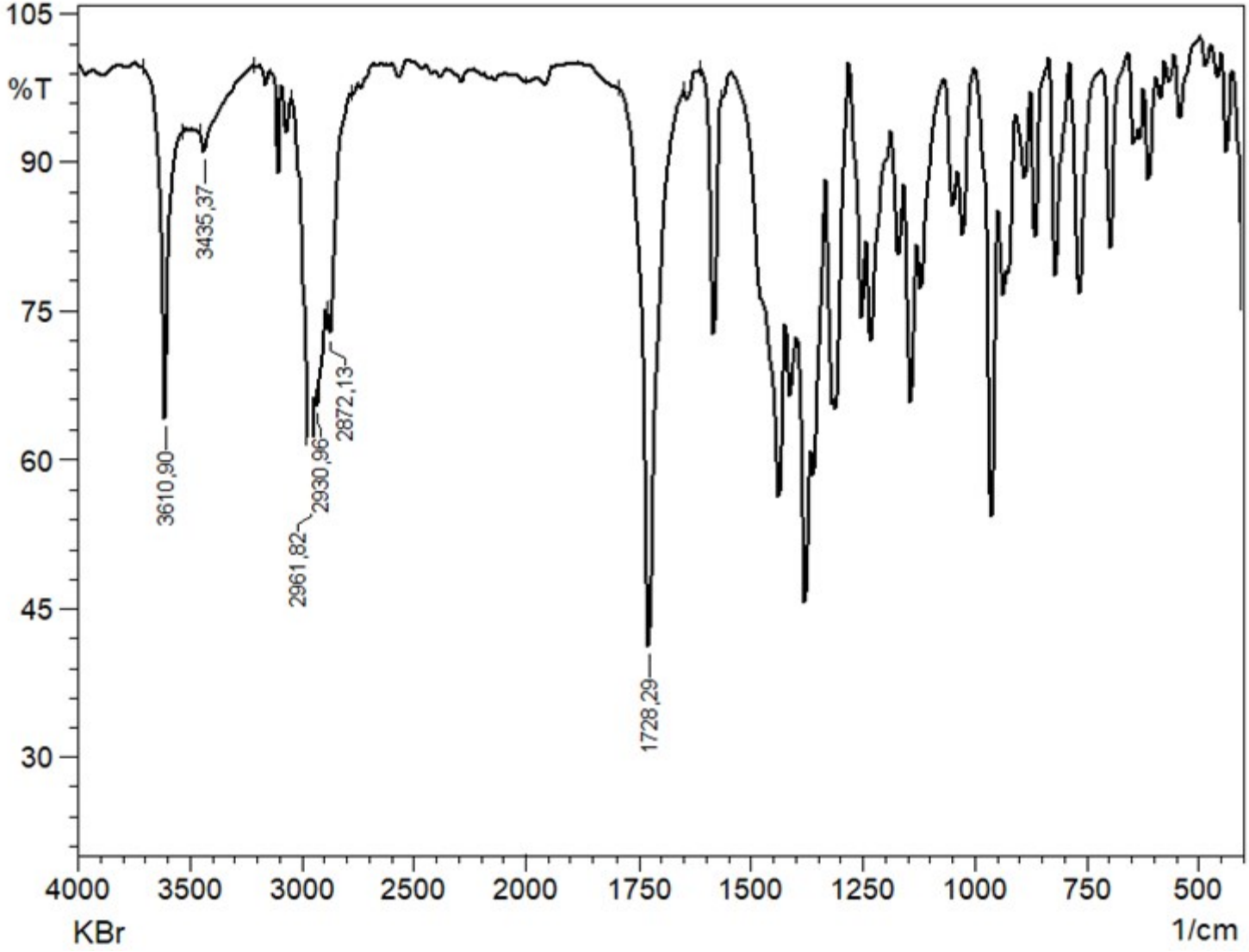

Figure 50S. IR spectrum of **13**.

Acquisition Parameter

Source Type	ESI	Ion Polarity	Positive	Set Nebulizer	0.4 Bar
Focus	Not active			Set Dry Heater	180 °C
Scan Begin	50 m/z	Set Capillary	4500 V	Set Dry Gas	4.0 l/min
Scan End	3000 m/z	Set End Plate Offset	-500 V	Set Divert Valve	Source

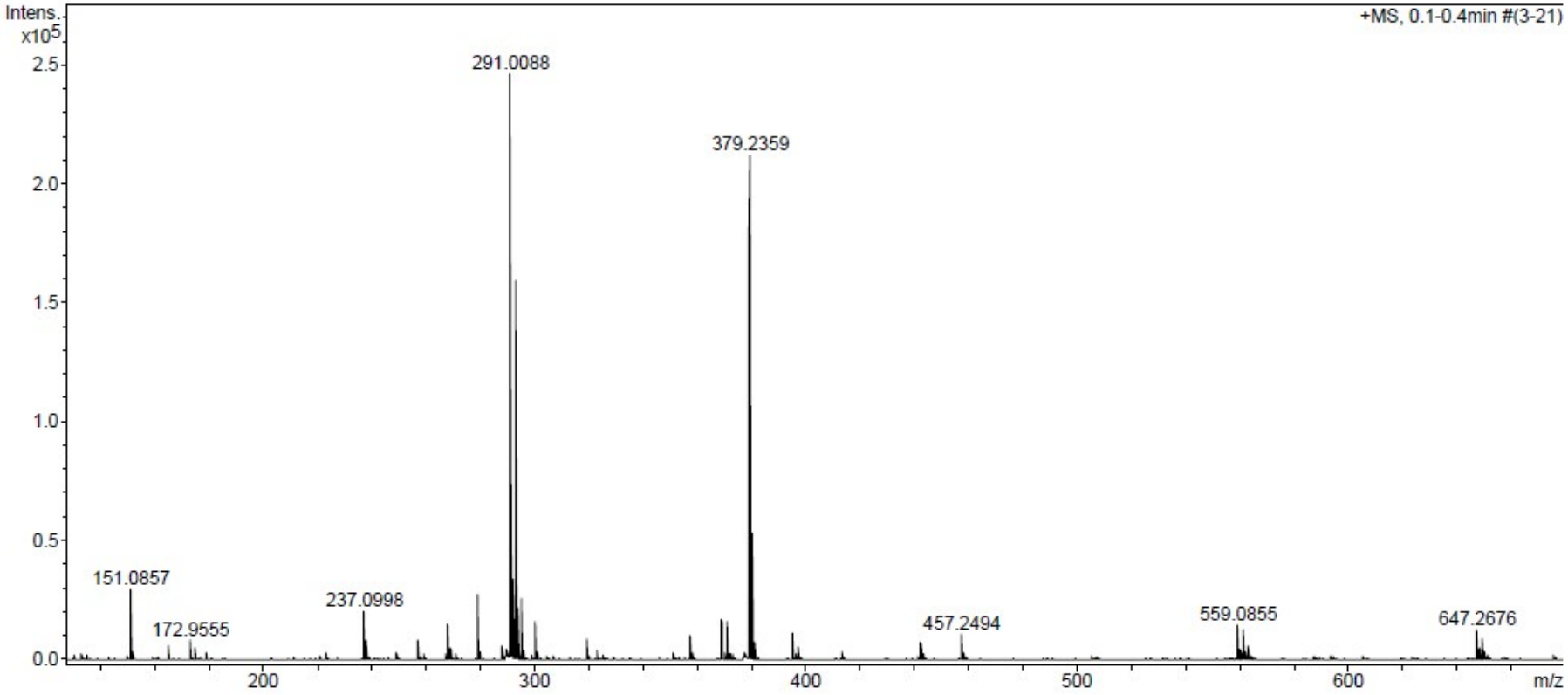

Figure 51S. HRESI^{+}-MS of **13**.

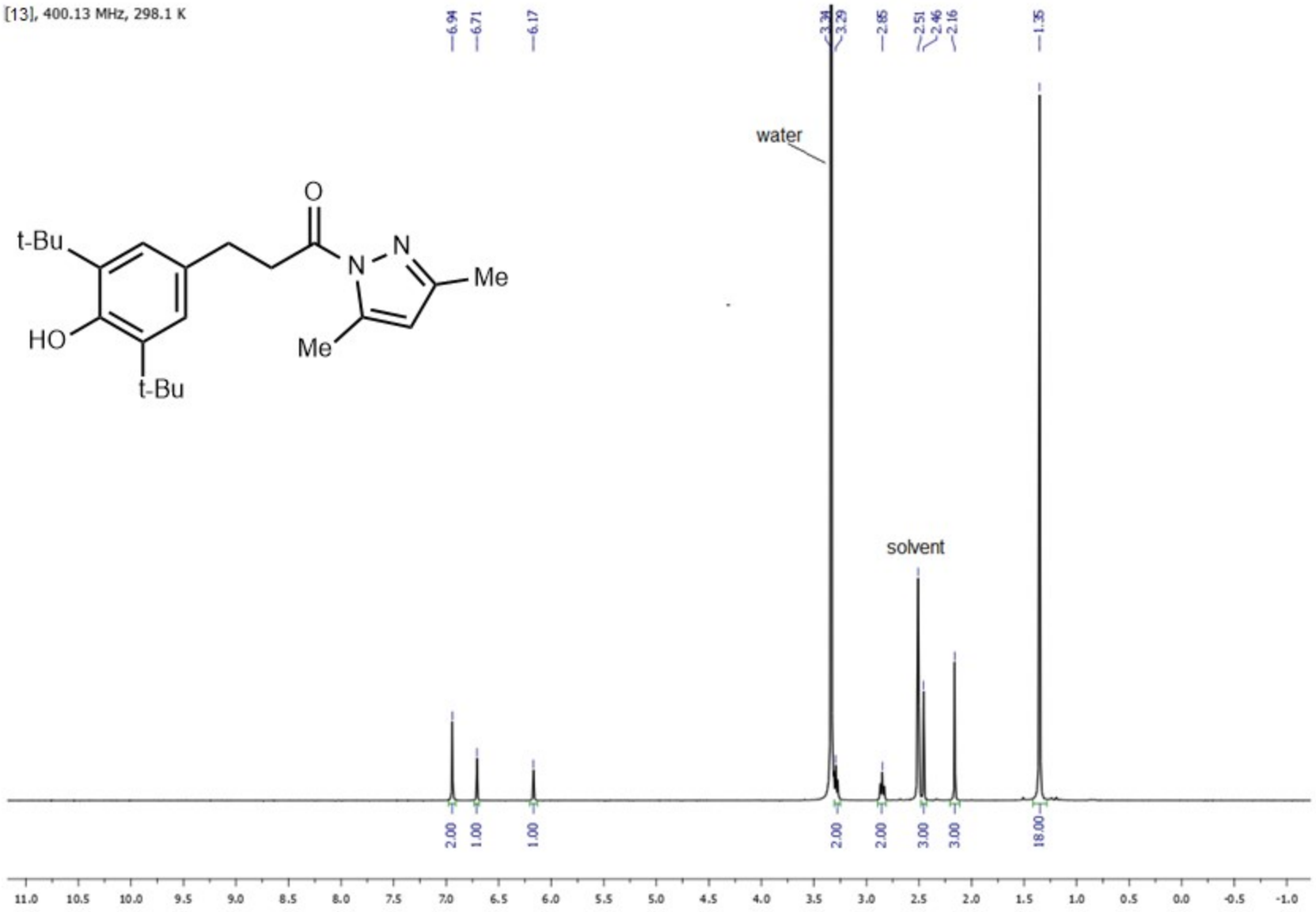

Figure 52S. ^{1}H NMR spectrum of **13**.

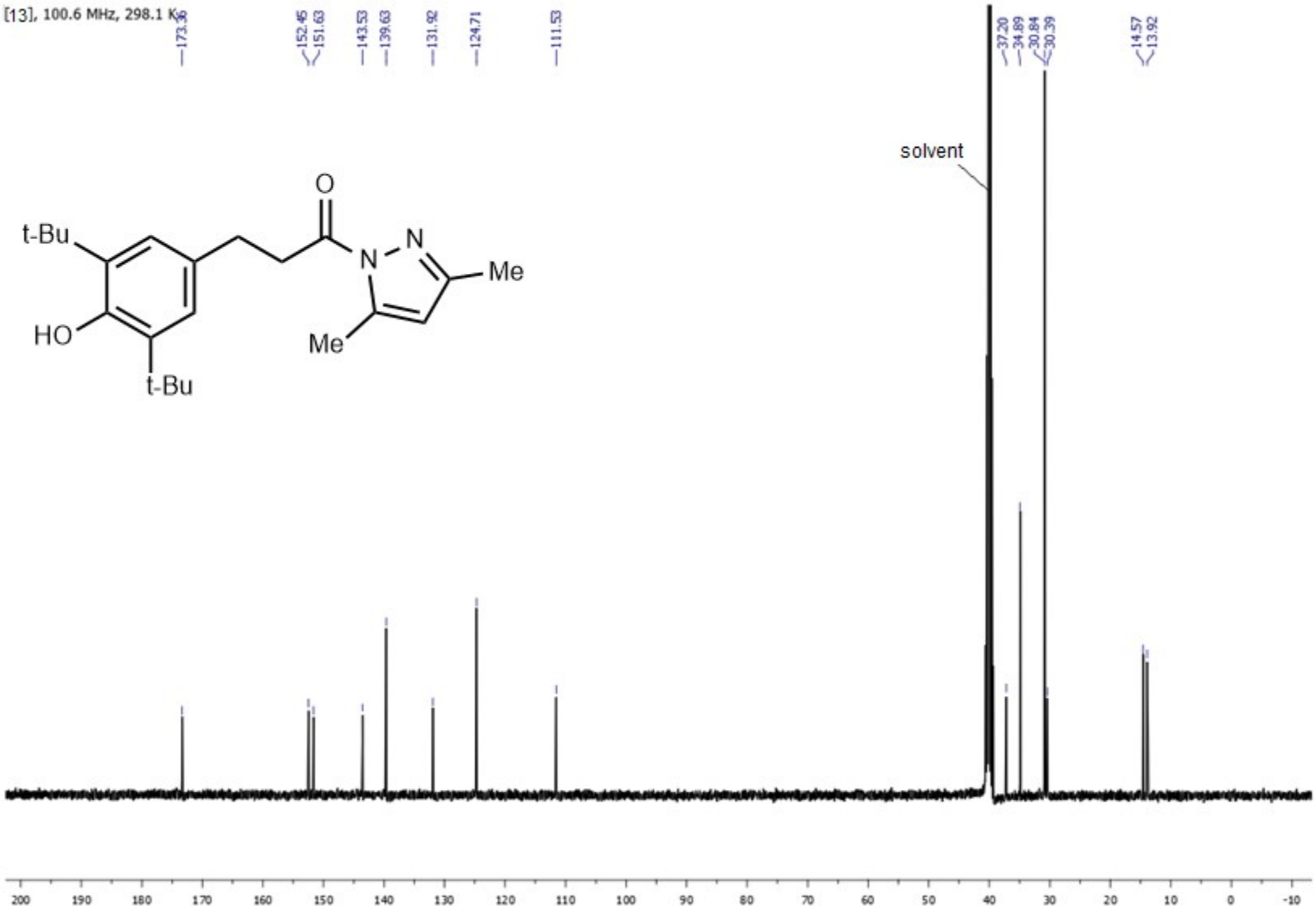

Figure 53S. $^{13}C\{^{1}H\}$ NMR spectrum of **13**.

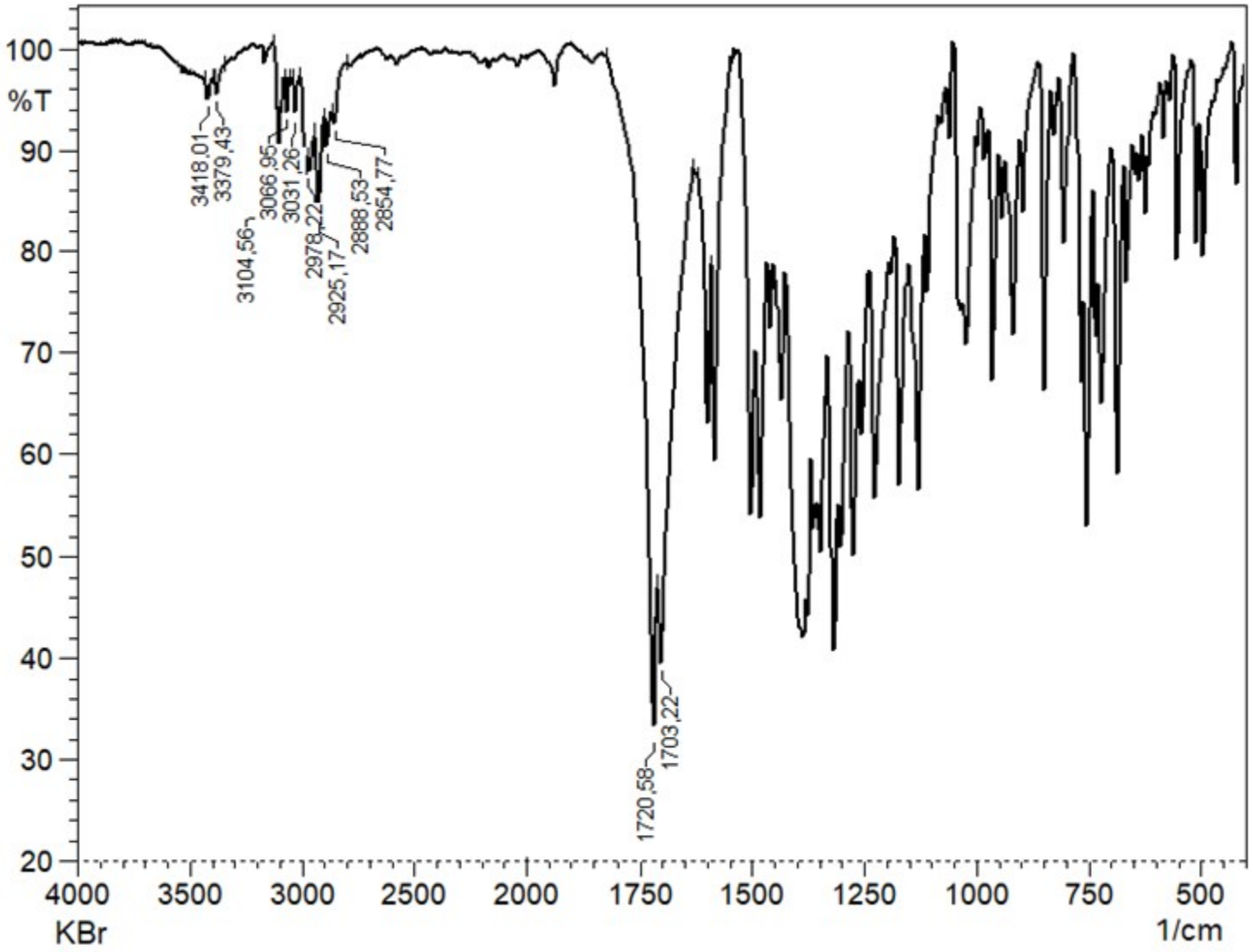

Figure 54S. IR spectrum of **14**.

Acquisition Parameter

Source Type	ESI	Ion Polarity	Positive	Set Nebulizer	0.4 Bar
Focus	Not active			Set Dry Heater	180 °C
Scan Begin	50 m/z	Set Capillary	4500 V	Set Dry Gas	4.0 l/min
Scan End	3000 m/z	Set End Plate Offset	-500 V	Set Divert Valve	Source

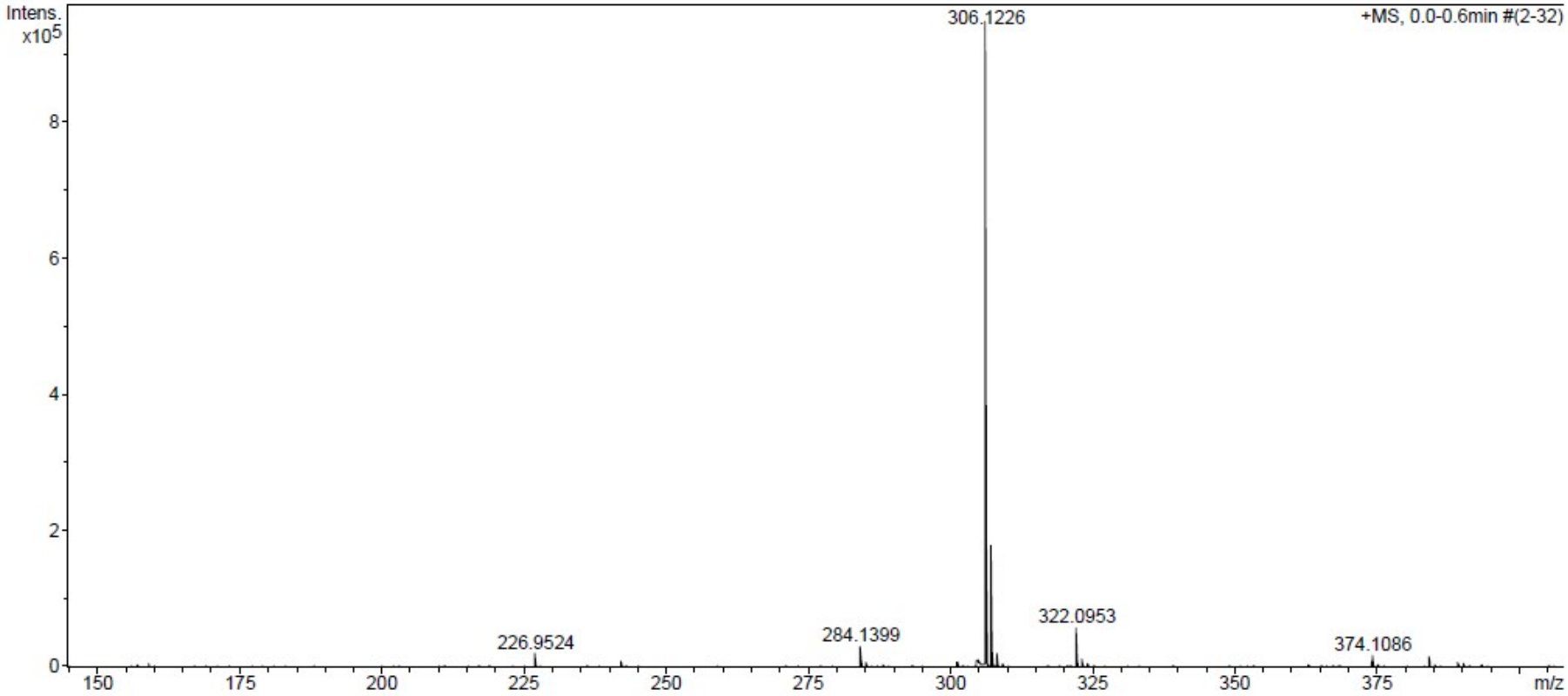

Figure 55S. HRESI^{+}-MS of **14**.

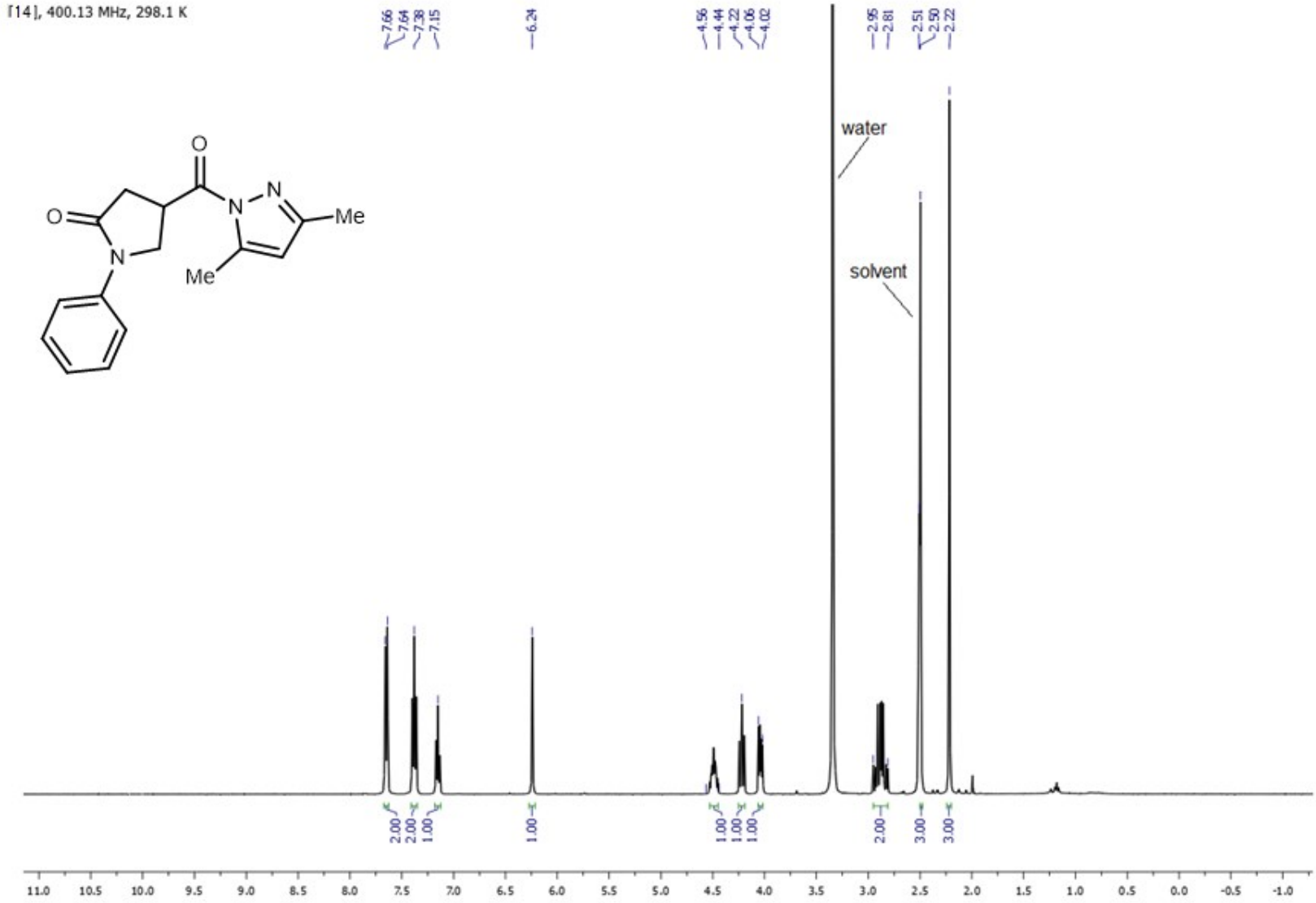

Figure 56S. ^{1}H NMR spectrum of **14**.

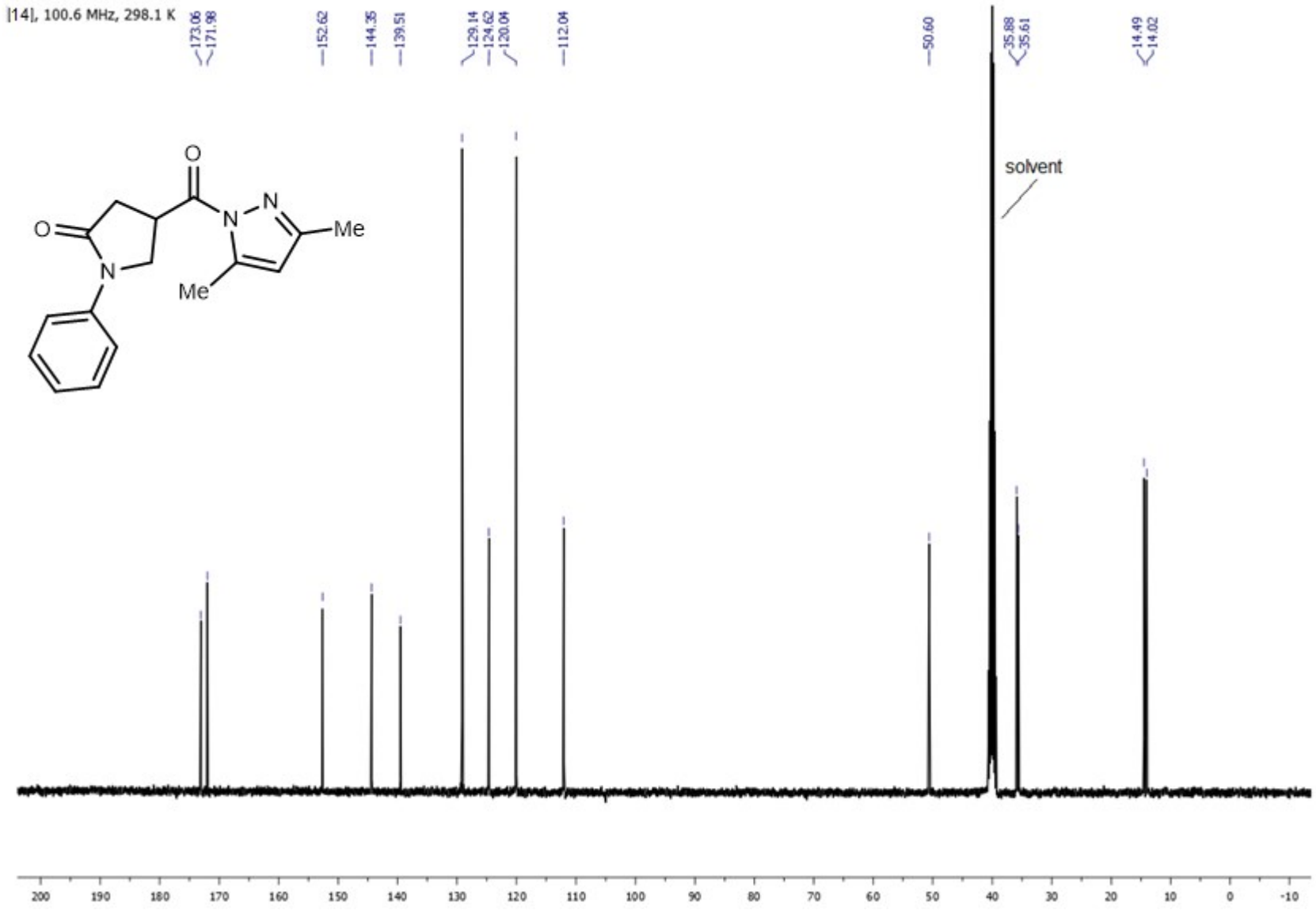

Figure 57S. $^{13}C\{^{1}H\}$ NMR spectrum of **14**.

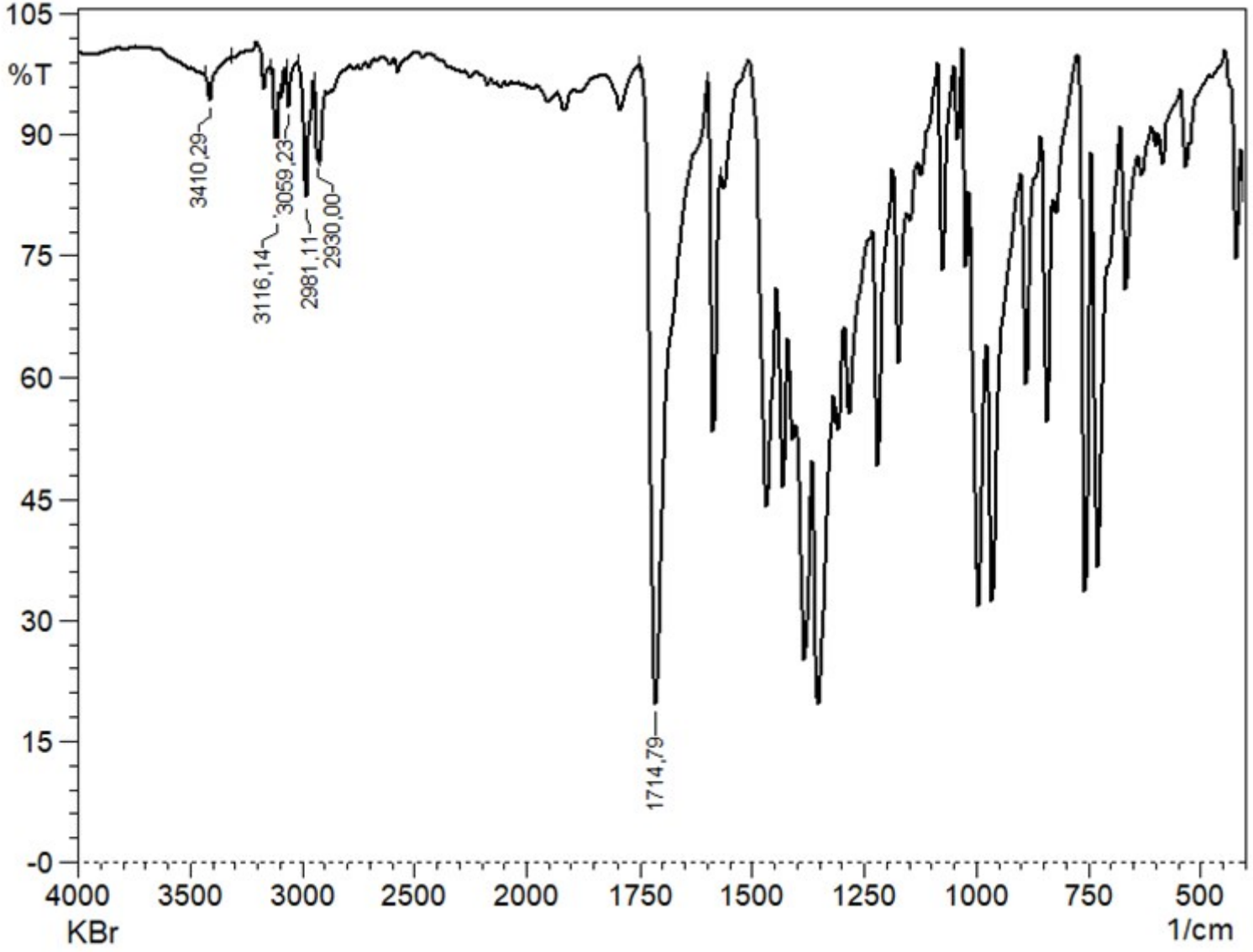

Figure 58S. IR spectrum of **15**.

Acquisition Parameter

Source Type	ESI	Ion Polarity	Positive	Set Nebulizer	0.4 Bar
Focus	Not active			Set Dry Heater	180 °C
Scan Begin	50 m/z	Set Capillary	4500 V	Set Dry Gas	4.0 l/min
Scan End	3000 m/z	Set End Plate Offset	-500 V	Set Divert Valve	Source

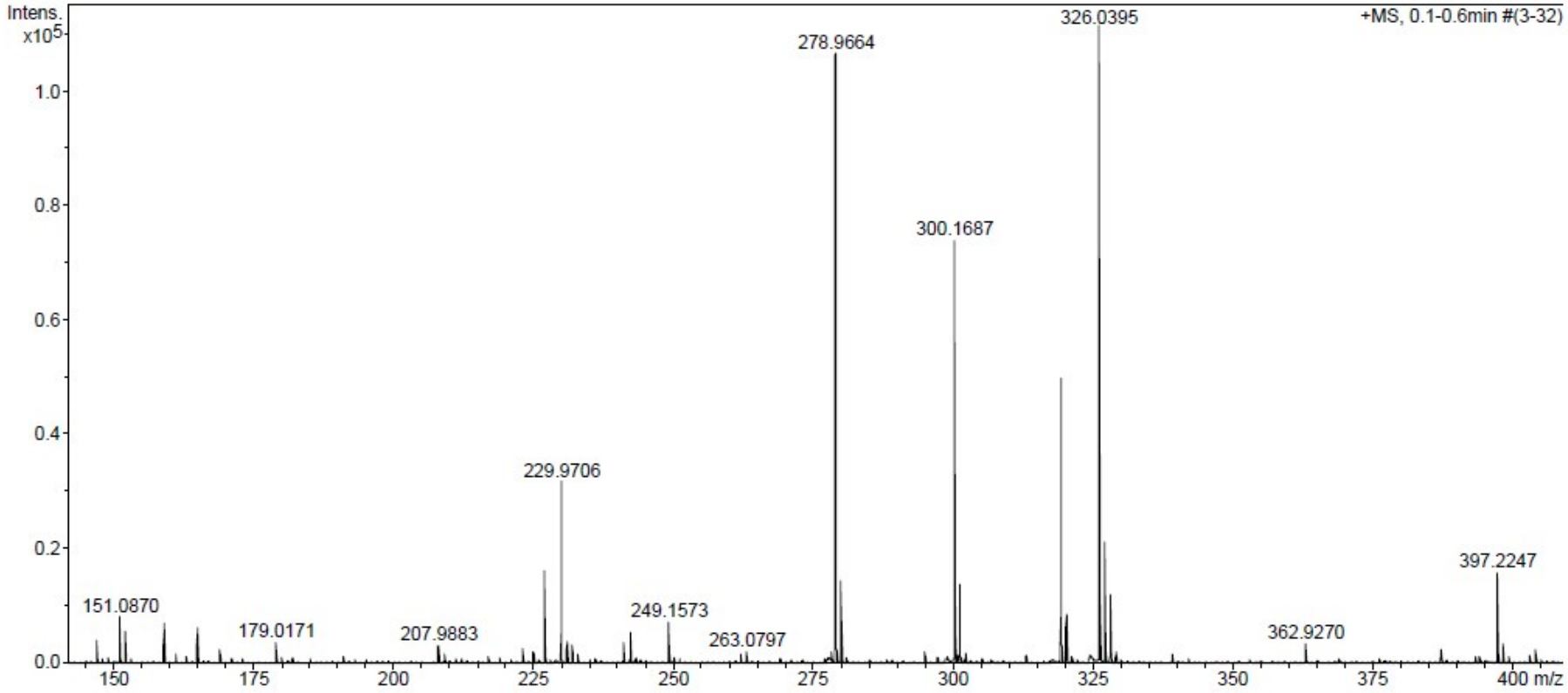

Figure 59S. HRESI^{+}-MS of **15**.

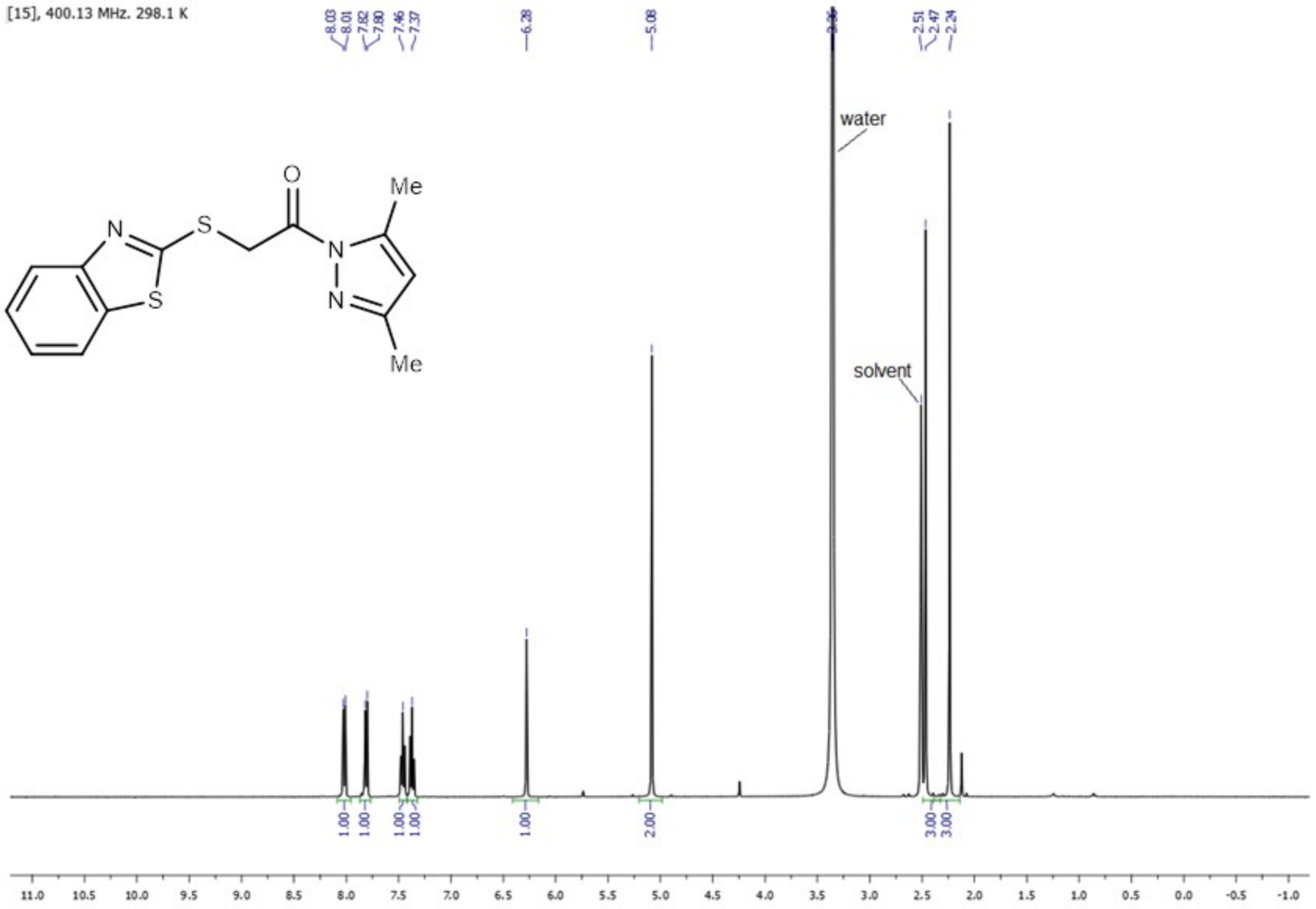

Figure 60S. ^{1}H NMR spectrum of **15**.

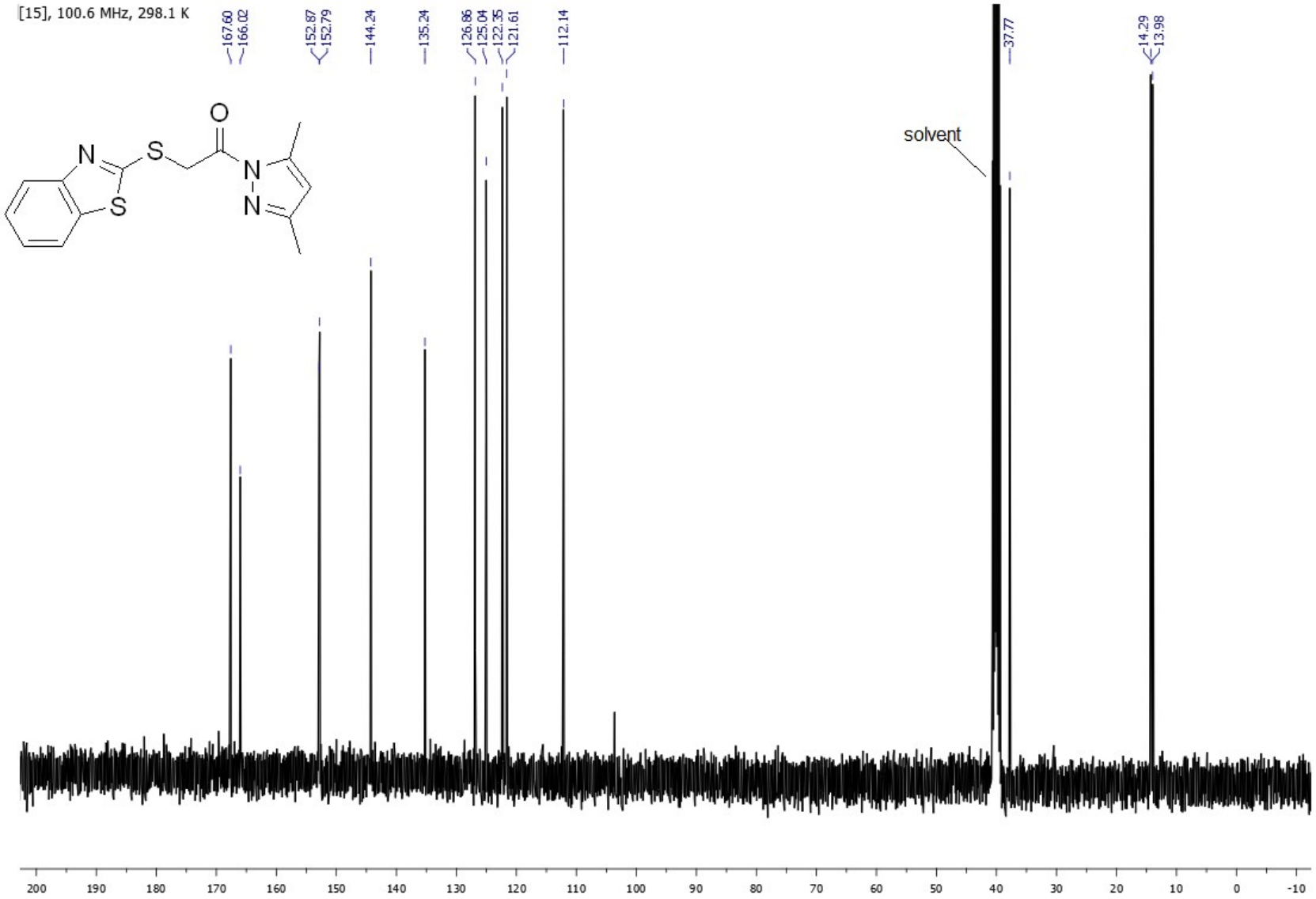

Figure 61S. $^{13}C\{^{1}H\}$ NMR spectrum of **15**.

Details of theoretical calculations

We theoretically estimated strength of hydrogen and halogen bonds in optimized equilibrium model structures ***i***, **TS4**, and **J** using the topological analysis of the electron density distribution technique (QTAIM analysis, see **Table 1S**).

Table 1S. Values of the density of all electrons – $\rho(\mathbf{r})$, Laplacian of electron density – $\nabla^2\rho(\mathbf{r})$, energy density – H_b, potential energy density – $V(\mathbf{r})$, and Lagrangian kinetic energy – $G(\mathbf{r})$ (a.u.) at the bond critical points (3, –1), corresponding to hydrogen and halogen bonds in optimized equilibrium model structures ***i***, **TS4**, and **J** as well as bond lengths – *l* (Å) and estimated energies – E_{int} (kJ/mol) for these contacts.

Contact	$\rho(\mathbf{r})$	$\nabla^2\rho(\mathbf{r})$	H_b	$V(\mathbf{r})$	$G(\mathbf{r})$	*l*	E_{int}*
i							
H36···O3	0.013	0.049	0.001	-0.010	0.011	2.298	13.1
H35···O41	0.012	0.041	0.001	-0.009	0.009	2.423	11.8
I22···O3	0.022	0.086	0.000	-0.016	0.017	2.846	28.6
I22···O41	0.022	0.083	0.000	-0.016	0.017	2.870	28.6
TS4							
H56···O9	0.013	0.046	0.001	-0.010	0.011	2.317	13.1
H57···O63	0.013	0.046	0.001	-0.010	0.011	2.329	13.1
I43···O9	0.018	0.069	0.001	-0.013	0.014	2.941	23.2
I43···O63	0.026	0.099	0.000	-0.020	0.019	2.800	35.7
J							
H56···O9	0.010	0.037	0.001	-0.007	0.008	2.445	9.2
H57···O63	0.015	0.052	0.001	-0.012	0.012	2.275	15.8
I43···O9	0.016	0.058	0.001	-0.011	0.012	3.025	19.6
I43···O63	0.027	0.103	0.000	-0.020	0.020	2.781	35.7

* $E_{int} \approx -V(\mathbf{r})/2$ for hydrogen bonds[1] and $E_{int} \approx 0.68(-V(\mathbf{r}))$ for halogen bonds involving iodine atoms as σ-hole donors.[2]

The QTAIM analysis demonstrates the presence of bond critical points (3, –1) corresponding to hydrogen and halogen bonds in optimized equilibrium model structures ***i***, **TS4**, and **J**. The low magnitude of the electron density (0.010–0.027 a.u.), positive values of the Laplacian of electron density (0.037–0.103 a.u.), and zero or very close to zero positive energy density (0.000–0.001 a.u.) in these bond critical points (3, –1) are typical for noncovalent interactions. The balance between the potential and kinetic energy densities of electrons at the bond critical points (3, –1) for studied weak contacts in optimized equilibrium model structures ***i***, **TS4**, and **J** reveals that a covalent contribution is absent in these interactions.[3]

References

1. E. Espinosa, E. Molins and C. Lecomte, *Chem. Phys. Lett.*, 1998, **285**, 170–173.
2. E. V. Bartashevich and V. G. Tsirelson, *Russ. Chem. Rev.*, 2014, **83**, 1181–1203.
3. E. Espinosa, I. Alkorta, J. Elguero and E. Molins, *J. Chem. Phys.*, 2002, **117**, 5529–5542.